

MONA OFFSHORE WIND PROJECT

Environmental Statement

Volume 6, Annex 10.1: Radar Early Warning Systems and Microwave Communication Links Technical Report

Document Number: MOCNS-J3303-RPS-10088

Document Reference: F6.10.1

APFP Regulations: 5(2)(a)

February 2024

F01



Image of an offshore wind farm

MONA OFFSHORE WIND PROJECT

| Document status | | | | | |
|------------------------|----------------------------|--------------------|--------------------|--------------------|--------------------|
| Version | Purpose of document | Authored by | Reviewed by | Approved by | Review date |

| | | | | | |
|-----|-------------|--|------------------------|------------------------|----------|
| F01 | Application | Manchester Advanced Radar Services Ltd | Mona Offshore Wind Ltd | Mona Offshore Wind Ltd | Feb 2024 |
|-----|-------------|--|------------------------|------------------------|----------|

Prepared by:

Prepared for:

Manchester Advanced Radar Services Ltd

Mona Offshore Wind Limited.

Contents

| | | |
|----------|--|----------|
| 1 | RADAR EARLY WARNING SYSTEMS AND MICROWAVE COMMUNICATION LINKS TECHNICAL REPORT | 1 |
| 1.1 | Introduction | 1 |
| 1.1.1 | Overview | 1 |
| 1.1.2 | Background | 2 |
| 1.2 | Scope of assessment | 3 |
| 1.2.1 | Target masking..... | 3 |
| 1.2.2 | Shadowing effects..... | 3 |
| 1.2.3 | Rerouted traffic..... | 5 |
| 1.2.4 | Adaptive detection threshold modelling | 5 |
| 1.2.5 | Tracker modelling..... | 6 |
| 1.2.6 | Ultra-High Frequency communication links..... | 6 |
| 1.2.7 | Other effects..... | 7 |
| 1.3 | Modelling parameters | 7 |
| 1.3.1 | Wind turbine parameters..... | 7 |
| 1.3.2 | Wind farm parameters..... | 11 |
| 1.3.3 | Mona Offshore Wind Project indicative wind turbine and offshore substations/platform layouts | 11 |
| 1.3.4 | Assessment region and study area..... | 12 |
| 1.3.5 | REWS modelling | 14 |
| 1.3.6 | Detection threshold (CFAR) | 16 |
| 1.3.7 | Target modelling..... | 16 |
| 1.3.8 | Wind turbine shadow modelling | 16 |
| 1.3.9 | Measurements and modelling of RCS of wind turbines | 17 |
| 1.4 | REWS Returns and vessel detection modelling results | 20 |
| 1.4.1 | Overview | 20 |
| 1.4.2 | Assessment of the base case scenario..... | 20 |
| 1.4.3 | Cumulative assessment | 51 |
| 1.5 | Assessment of the rerouted traffic on REWS alarm rates..... | 67 |
| 1.5.1 | Overview | 67 |
| 1.5.2 | Routes and alarms modelling..... | 68 |
| 1.5.3 | Modelling the existing traffic (pre-development of the Mona Offshore Wind Project).... | 69 |
| 1.5.4 | Modelling the predicted shipping reroutes Around the Mona Offshore Wind Project in isolation and cumulatively with other wind farms in the study area | 74 |
| 1.5.5 | Modelling results and comparison of the base case and the predicted shipping reroutes around the Mona Offshore Wind Project in isolation and around Mona Offshore Wind Project and Morgan Generation Assets cumulatively. | 77 |
| 1.5.6 | Remarks on the TCPA/CPA alarm modelling results..... | 80 |
| 1.5.7 | Assessment of the TCPA/CPA alarm modelling results | 81 |
| 1.6 | Microwave communication links assessment..... | 82 |
| 1.6.1 | Overview | 82 |
| 1.6.2 | Modelling parameters..... | 84 |
| 1.6.3 | Exclusion zone modelling results | 90 |
| 1.6.4 | Remarks on the microwave communication links modelling..... | 91 |
| 1.7 | Summary and final remarks..... | 92 |
| 1.7.1 | General REWS returns modelling summary | 92 |
| 1.7.2 | General TCPA/CPA modelling summary | 93 |
| 1.7.3 | Further considerations..... | 94 |
| 1.8 | References | 96 |

MONA OFFSHORE WIND PROJECT

Tables

| | | |
|------------|--|----|
| Table 1.1: | MDS parameters for the REWS modelling..... | 11 |
| Table 1.2: | Radar modelling parameters..... | 14 |
| Table 1.3: | Shipping routes in the region and the number of vessels travelling on each route per day..... | 69 |
| Table 1.4: | The estimated change in yearly alarm rates against the base case (green = reduced alarms / no change, white = small alarm increase, orange = elevated alarm increase)..... | 80 |
| Table 1.5: | Exclusion zones around the Spirit Energy microwave communication links..... | 91 |
| Table 1.6: | Exclusion zones around the ENI Energy microwave communication links..... | 91 |

Figures

| | | |
|--------------|--|----|
| Figure 1.1: | Illustration of radar shadowing with diffraction effects (Butler and Johnson, 2003)..... | 4 |
| Figure 1.2: | 2D CFAR cells around a given cell with wind turbine present..... | 6 |
| Figure 1.3: | Modelled turbine geometry..... | 8 |
| Figure 1.4: | Indicative Mona and Morgan MDS layout with nearby oil and gas platforms with REWS..... | 10 |
| Figure 1.5: | Mona REWS study area..... | 13 |
| Figure 1.6: | The radar antenna elevation and azimuth patterns..... | 15 |
| Figure 1.7: | Optical blockage and partial shadowing..... | 17 |
| Figure 1.8: | Wind turbine layout at Hornsea Project One array area and the location of the radar system used in the study. The red area denotes the region shown in Figure 1.9 (Terma, 2021)..... | 18 |
| Figure 1.9: | Compressed radar image in range-azimuth coordinates showing a zoomed area of the Hornsea Project One array area around a substation platform (Z13). A vessel is visible between Z13 and WTG G05. The signal level (in dB) is colour coded (Terma, 2021)..... | 19 |
| Figure 1.10: | Power received by the REWS on Spirit Energy's South Morecambe AP1 platform..... | 20 |
| Figure 1.11: | Modelled layout of the base case scenario showing the location of the existing wind farms and the coverage of the REWS in the region..... | 22 |
| Figure 1.12: | ENI Energy's Douglas platform REWS clutter map showing returns from the wind turbines and sea clutter..... | 23 |
| Figure 1.13: | ENI Energy's Douglas platform REWS detection threshold..... | 24 |
| Figure 1.14: | Modelled power received from 1000 m ² target (coverage)..... | 25 |
| Figure 1.15: | ENI Energy's Douglas platform REWS detection plot showing loss regions for a 1000 m ² target..... | 26 |
| Figure 1.16: | Enlarged portion of the detection plot showing the effect of wind turbine shadowing..... | 27 |
| Figure 1.17: | Harbour Energy's Millom West platform REWS clutter map showing returns from the wind turbines and sea clutter..... | 28 |
| Figure 1.18: | Harbour Energy's Millom West platform REWS detection threshold..... | 29 |
| Figure 1.19: | Harbour Energy's Millom West platform REWS detection plot showing loss regions for a 1000 m ² target..... | 30 |
| Figure 1.20: | ENI Energy's OSI REWS clutter map showing returns from the wind turbines and sea clutter..... | 31 |
| Figure 1.21: | ENI Energy's OSI REWS detection threshold..... | 32 |
| Figure 1.22: | ENI Energy's OSI REWS detection plot showing loss regions for a 1000 m ² target..... | 33 |
| Figure 1.23: | Spirit Energy's South Morecambe AP1 platform REWS clutter map showing returns from the wind turbines and sea clutter..... | 34 |
| Figure 1.24: | Spirit Energy's South Morecambe AP1 platform REWS detection threshold..... | 35 |
| Figure 1.25: | Spirit Energy's South Morecambe AP1 platform REWS detection plot showing loss regions for a 1000 m ² target..... | 36 |
| Figure 1.26: | Modelled layout of the Mona Offshore Wind Project showing the indicative location of the wind turbines and the location of oil and gas platforms in the region..... | 38 |
| Figure 1.27: | ENI Energy's Douglas platform REWS clutter map showing returns from the Mona wind turbines and sea clutter..... | 39 |
| Figure 1.28: | ENI Energy's Douglas platform REWS detection threshold over the Mona Array Area..... | 40 |
| Figure 1.29: | ENI Energy's Douglas platform REWS detection plot showing loss regions for a 1000 m ² target..... | 41 |
| Figure 1.30: | Harbour Energy's Millom West platform REWS clutter map showing returns from the Mona wind turbines and sea clutter..... | 42 |
| Figure 1.31: | Harbour Energy's Millom West platform REWS detection threshold over the Mona Array Area..... | 43 |

MONA OFFSHORE WIND PROJECT

| | |
|---|----|
| Figure 1.32: Harbour Energy’s Millom West platform REWS detection plot showing loss regions for a 1000 m ² target..... | 44 |
| Figure 1.33: ENI Energy’s OSI REWS detection clutter map showing returns from the Mona wind turbines and sea clutter. | 45 |
| Figure 1.34: ENI Energy’s OSI REWS detection threshold over the Mona Array Area..... | 46 |
| Figure 1.35: ENI Energy’s OSI REWS detection plot showing loss regions for a 1000 m ² target..... | 47 |
| Figure 1.36: Spirit Energy’s South Morecambe AP1 platform REWS clutter map showing returns from the Mona wind turbines and sea clutter. | 48 |
| Figure 1.37: Spirit Energy’s South Morecambe AP1 platform REWS detection threshold over the Mona Array Area. | 49 |
| Figure 1.38: Spirit Energy’s South Morecambe AP1 platform REWS detection plot showing loss regions for a 1000 m ² target. | 50 |
| Figure 1.39: REWS cumulative wind farms. | 52 |
| Figure 1.40: Modelled cumulative layout of the Mona Offshore Wind Project and Morgan Generation Assets showing the indicative location of the wind turbines and the location of oil and gas platforms in the region. | 54 |
| Figure 1.41: ENI Energy’s Douglas platform REWS clutter map showing returns from the wind turbines and sea clutter. | 55 |
| Figure 1.42: ENI Energy’s Douglas platform REWS detection threshold. | 56 |
| Figure 1.43: ENI Energy’s Douglas platform REWS detection plot showing loss regions for a 1000 m ² target..... | 57 |
| Figure 1.44: Harbour Energy’s Millom West platform REWS clutter map showing returns from the wind turbines and sea clutter. | 58 |
| Figure 1.45: Harbour Energy’s Millom West platform REWS detection threshold. | 59 |
| Figure 1.46: Harbour Energy’s Millom West platform REWS detection plot showing loss regions for a 1000 m ² target..... | 60 |
| Figure 1.47: ENI Energy’s OSI REWS detection clutter map showing returns from the wind turbines and sea clutter. | 61 |
| Figure 1.48: ENI Energy’s OSI REWS detection threshold. | 62 |
| Figure 1.49: ENI Energy’s OSI REWS detection plot showing loss regions for a 1000 m ² target..... | 63 |
| Figure 1.50: Spirit Energy’s South Morecambe AP1 platform REWS clutter map showing returns from the wind turbines and sea clutter. | 64 |
| Figure 1.51: Spirit Energy’s South Morecambe AP1 platform REWS detection threshold..... | 65 |
| Figure 1.52: Spirit Energy’s South Morecambe AP1 platform REWS detection plot showing loss regions for a 1000 m ² target. | 66 |
| Figure 1.53: Existing ferry routes within and around the Mona Array Area..... | 71 |
| Figure 1.54: Existing commercial routes within and around the Mona Array Area..... | 72 |
| Figure 1.55: Modelled existing shipping routes (1,000 variations each route). | 73 |
| Figure 1.56: Modelled shipping routes post-construction of the Mona Offshore Wind Project. | 75 |
| Figure 1.57: Modelled shipping routes post-construction of the Mona and Morgan Generation Assets cumulatively. | 76 |
| Figure 1.58: Modelled yearly alarm rates for the Conway platform..... | 77 |
| Figure 1.59: Modelled yearly alarm rates for the Douglas Complex..... | 77 |
| Figure 1.60: Modelled yearly alarm rates for the Hamilton platform..... | 77 |
| Figure 1.61: Modelled yearly alarm rates for the Hamilton North platform..... | 77 |
| Figure 1.63: Modelled yearly alarm rates for the Lennox platform. | 78 |
| Figure 1.64: Modelled yearly alarm rates for the OSI. | 78 |
| Figure 1.65: Modelled yearly alarm rates for the Calder platform. | 78 |
| Figure 1.66: Modelled yearly alarm rates for the Millom West platform. | 78 |
| Figure 1.67: Modelled yearly alarm rates for the South Morecambe DP4 platform. | 78 |
| Figure 1.68: Modelled yearly alarm rates for the South Morecambe DP3 platform. | 78 |
| Figure 1.69: Modelled yearly alarm rates for the North Morecambe platform. | 79 |
| Figure 1.70: Modelled yearly alarm rates for the South Morecambe AP1 platform..... | 79 |
| Figure 1.71: Modelled yearly alarm rates for the South Morecambe DP6 platform. | 79 |
| Figure 1.72: Modelled yearly alarm rates for the South Morecambe DP8 platform. | 79 |
| Figure 1.73: Layout of the modelled platforms and the communication links considered..... | 83 |
| Figure 1.74: Geometry and parameters used in the wind turbine bistatic RCS modelling. | 85 |

MONA OFFSHORE WIND PROJECT

| | |
|--|----|
| Figure 1.75: Bistatic RCS modelling results of the proposed MDS wind turbine..... | 86 |
| Figure 1.76: Illustration of the nearfield and diffraction exclusion zones. | 87 |
| Figure 1.77: The signal to noise ratio around the Douglas – Hamilton link. | 89 |
| Figure 1.78: Illustration of the refraction exclusion zone resulting in C/I less than 33 dB. | 90 |
| Figure 1.79: Simplified illustration of all exclusion zones around the Douglas – Hamilton link. | 90 |

MONA OFFSHORE WIND PROJECT

Glossary

| Term | Meaning |
|---------------------------|---|
| Allision | The act of striking or collision of a moving vessel against a stationary object. |
| Clutter | Clutter is the term used for unwanted echoes in electronic systems, particularly in reference to radars. Such echoes are typically returned from ground, sea, rain, animals/insects, chaff and atmospheric turbulences, and can cause serious performance issues with radar systems. |
| Doppler signature | Doppler signature is the parameter used by Doppler enabled radars to produce velocity data about objects at a distance. It does this by bouncing a microwave signal off a desired target and analysing how the object's motion has altered the frequency of the returned signal. This variation gives direct and highly accurate measurements of the radial component of a target's velocity relative to the radar. |
| Hops | In relation to microwave communication links, hops refer to the number of transient stations that a communication signal needs to travel to (to be amplified, redirected and retransmitted) before reaching its final receiver location |
| Radar Cross-Section (RCS) | RCS is the measure of a target's ability to reflect radar signals in the direction of the radar receiver. An object reflects a limited amount of radar energy back to the source. A larger RCS indicates that an object is more easily detected. |
| Radar returns | The electromagnetic signal that has been reflected back to the radar antenna. Such reflections contain information about the location and distance of the reflecting object. |
| Radar shadow | Radar shadow is the region whereby the radar beam is unable to fully illuminate a region due to blockage from terrain or structures within the area of coverage. Radar shadowing causes objects within the shadow region to produce reduced radar returns which can affect the radar's ability to detect such objects. |
| Target detection | A radar's ability to distinguish between radar returns from wanted targets and returns from clutter and/or the system's noise level. |

Acronyms

| Acronym | Description |
|---------|---------------------------------------|
| AD | Air Defence |
| AIS | Automatic Identification System |
| AMSL | Above Mean Sea Level |
| ATC | Air Traffic Control |
| C/I | Carrier-to-interference ratio |
| CA | Constant Averaging |
| CAD | Computer Aided Design |
| CFAR | Constant False-Alarm Rate |
| CPA | Closest Point of Approach |
| ERRV | Emergency Response and Rescue Vessels |

MONA OFFSHORE WIND PROJECT

| Acronym | Description |
|---------|---|
| IALA | International Association of Marine Aids to Navigation and Lighthouse Authorities |
| LoS | Line of Sight |
| MDS | Maximum Design Scenario |
| MTI | Moving Target Indicator |
| NUI | Normally Unmanned Installation |
| OSI | Offshore Storage Installation |
| RCS | Radar Cross Section |
| REWS | Radar Early Warning System |
| TCPA | Time to the Closest Point of Approach |
| UHF | Ultra-High Frequency |
| VTS | Vessel Traffic Services |

Units

| Unit | Description |
|------------------|-----------------------|
| % | Percentage |
| ° | Degrees |
| dB | Decibel |
| dBm ² | Decibel square metres |
| ft | Feet |
| GHz | Gigahertz |
| GT | Gross tons |
| hr | Hours |
| kHz | Kilohertz |
| m | Metre |
| m ² | Square metres |
| km | Kilometre |
| kt | Knot |
| kW | Kilowatt |
| mm | Millimetres |
| ms ⁻¹ | Metres per second |
| MW | Megawatt |
| nm | Nautical miles |
| ns | Nanoseconds |
| RPM | Rotations per minute |

1 Radar early warning systems and microwave communication links technical report

1.1 Introduction

1.1.1 Overview

1.1.1.1 This document is an annex to Volume 2, Chapter 10: Other sea users of the Environmental Statement and considers the potential effect of the Mona Offshore Wind Project during the operations and maintenance phase on Radar Early Warning Systems (REWS) and Line of Sight (LoS) microwave communication links located on offshore oil and gas platforms. Specifically, this annex considers the effects of the Mona Offshore Wind Project on the ability of REWS to detect vessels within the vicinity of the wind farm and the effect of rerouted traffic on the REWS alarm rates. There may be effects associated with the construction and decommissioning phase of the Mona Offshore Wind Project in regard to increased vessel movement within the Mona Array Area. This is not within the scope of this study as it needs detailed data regarding vessel movement during the construction and decommissioning phases, which might be governed by separate agreements between the REWS operators and the Applicant. As such, this assessment considers the Maximum Design Scenario (MDS) for the operations and maintenance phase of the project.

1.1.1.2 REWS uses the radar returns to monitor and track vessels within the detection region and alert the operator when a proximity violation or an allision threat is detected. The modelling work presented within this report considers a REWS configuration, which was based on technical information provided by the REWS operators (see section 1.3.5). It addresses the effects of the Mona Offshore Wind Project (assessed in isolation and cumulatively) on vessel detection due to raised thresholds, clutter returns and radar shadowing effects generated from the wind turbines. The REWS also uses a defined set of rules to identify a breach of the Closest Point of Approach (CPA) and Time to Closest Point of Approach (TCPA) alarms. This report will present modelling work and analysis results that aims to predict the effect of traffic rerouted as a result of the presence of the operational Mona Offshore Wind Project on the CPA/TCPA alarm rates.

1.1.1.3 The report considers four platforms where REWS are installed that are in proximity to the Mona Array Area. The four identified platforms are operated by Harbour Energy (Millom West platform), ENI UK Ltd. (Douglas platform and the Offshore Storage Installation (OSI)) and Spirit Energy (South Morecambe AP1 platform). These four REWS installations provide radar coverage and protection for a number of other nearby offshore platforms (i.e. Conwy, Douglas DA, Douglas DW, Hamilton, Hamilton North, Lennox, Calder, North Morecambe DPPA, South Morecambe CPP1, South Morecambe DP1, South Morecambe DP6 and South Morecambe DP8).

1.1.1.4 This report also provides the technical information and modelling results considering the potential cumulative impact of the Mona Offshore Wind Project in combination with other projects currently present in the region.

1.1.1.5 Additionally, offshore oil and gas platforms often use microwave communications links to transmit operational data and communicate status and other critical information regarding the operation and maintenance of these platforms. However, offshore wind farms may be located within the same regions of the oil and gas platforms and may interfere with the performance of the link and may reduce the effectiveness and efficiency of communication protocol.

1.1.1.6 This assessment considers the potential impact of the proposed Mona Offshore Wind Project on the existing microwave communications links onboard the ENI Energy platforms and the Spirit Energy Platforms operating in the Irish Sea.

1.1.2 Background

1.1.2.1 Wind turbines and associated offshore structures (such as Offshore Substation Platforms (OSPs)) located within the LoS of radars, may interfere with the radar performance and degrade its ability to distinguish between wind turbines and associated offshore structures, and returns from targets of interest.

1.1.2.2 REWS are primarily used to detect and track vessels navigating in the vicinity of offshore oil and gas assets and provide allision warning when vessels are in breach of defined CPA and TCPA parameters. The impact of offshore wind farms on REWS may arise from a number of factors such as high radar returns from the wind turbines and associated offshore structures, increased number of detections and false alarm/track generation.

1.1.2.3 Offshore wind turbines are large structures with geometries and materials that may cause them to have a high radar cross-section (RCS). Furthermore, the rotation of the wind turbine blades produces a time-variable RCS fluctuation and a Doppler frequency shift that can confuse radars that rely on moving target indicator (MTI) filters to distinguish between static objects and moving targets of interest. The interference to Doppler based Air Traffic Control (ATC) and Air Defence (AD) radars due to the rotating blades and the large reflection of the radar signal has been well reported and explained (Jago and Taylor, 2002; Poupart, 2003; Wind Energy, Defence & Civil Aviation Interests Working Group, 2002). However, this technical report discusses and models the potential impact of the Mona Offshore Wind Project on the REWS used on oil and gas platforms which have been identified as potentially being affected by the Mona Offshore Wind Project due to their location. Typically, REWS does not employ Doppler processing and MTI filters as it operates in naval environments whereby the returns from the sea surface (and the movement of the waves) may generate radar returns with Doppler signatures similar to that of surface vessels. REWS can be integrated with newer radar transceivers that are capable of Doppler processing if deemed necessary.

1.1.2.4 For non-Doppler based radars such as the REWS, the potential impact from offshore wind farms may arise due to the large radar returns. The large RCS of wind turbines may cause target spreading at extended ranges and potential detections through the sidelobes at close ranges. This will cause smearing and cluttering of the radar screen and potentially mask other targets in the area. In addition, depending on the thresholding techniques used within a radar system, the presence of wind turbines and associated offshore structures may increase the threshold over parts of Mona Array Areas, which potentially may cause smaller targets to be lost.

1.1.2.5 Degradation of the radar performance may also be caused by the radar shadow due to the presence of wind turbines within the LoS of the radar, as shown in Figure 1.1. Shadowing may cause smaller targets to temporarily disappear from the radar display as it moves in and out of the shadow regions. The extent of the impact caused by shadowing depends on the size and height of the wind turbine and the target of interest (i.e. different effects may be observed if looking at surface targets or air targets). However, previous studies and trials showed that the effect of shadowing can be considered to be an effect of secondary importance that may have little impact on the REWS performance due to the size of vessels that the REWS is typically interested in detecting (Butler and Johnson, 2003; Greenwell, 2016).

1.1.2.6 This report uses a number of modelling techniques developed at the University of Manchester to model and predict the impact of wind turbines and associated offshore structures on radar systems. These models have been verified and were compared against real-life radar and RCS measurements and it is noted that the modelling results showed very good correlation with measurements. The models used within this report allow the radar returns coming both from the wanted target and the Mona Offshore Wind Project to be simulated so that the effects on radar detection can be evaluated. The results from the models can then be used to indicate the regions within which vessels can be detected and tracked. Section 1.2 below describes the different modelling techniques utilised in the assessments.

1.2 Scope of assessment

1.2.1 Target masking

1.2.1.1 The size, geometry and construction materials of wind turbines cause them to have a very large radar return. This may cause target spreading (smearing) at extended ranges and potential detections through the sidelobes at close ranges. Such effects will add clutter to the radar screen and potentially mask other targets in the area. This may also affect the tracking software performance when vessels are travelling within the Mona Array Area causing the radar tracks of vessels to be seduced and merged into the larger returns generated from the wind turbines. This report addresses the impact of target masking and compares the levels of the wind turbine radar returns against that of a typical vessel within the radar detection range. This report does not consider the effects of varying wind turbine returns on the tracker as this requires a detailed knowledge of the employed tracking software, which is proprietary information (discussed further in paragraph 1.2.5.1). Despite this, it remains possible to draw robust conclusions.

1.2.2 Shadowing effects

1.2.2.1 The extent and length of the shadow region cast by a wind turbine depends on the size of the wind turbine, the distance to the radar antenna, the height of the radar and the height of the target of interest. The severity of the shadow will also depend on the distance of the target from the wind turbine. This is illustrated in Figure 1.1.

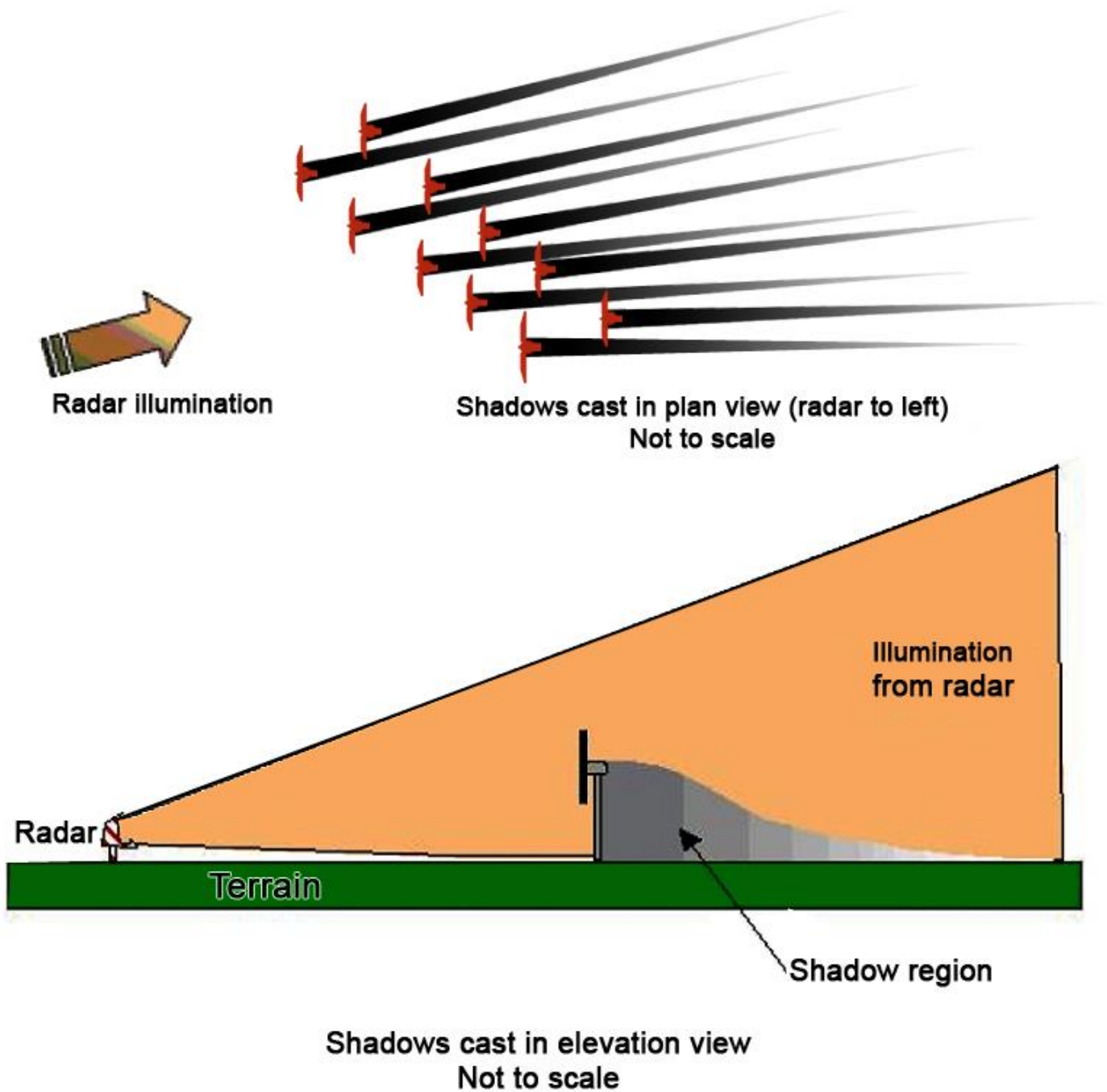


Figure 1.1: Illustration of radar shadowing with diffraction effects (Butler and Johnson, 2003).

1.2.2.2

Due to the diffraction of the radar waves around the wind turbine, increasing the range between the target and the wind turbine will reduce the severity of the attenuation to the target's returns. It has been reported that a target 1 km behind the wind turbine will experience 6 dB reduction in the returned power while targets that are significantly further suffer only 2 dB reduction in the received radar echo (Butler and Johnson, 2003). This is an important characteristic of the radar shadow and is illustrated in Figure 1.1. This is in good agreement with the recent measurement campaign carried out by Ultra Electronics to assess the effects of wind farms on the REWS performance located in the east Irish Sea (Greenwell, 2016). The measurement campaign and the work presented in Danoon and Brown (2014) indicate that shadowing may not have a significant effect on the performance of the REWS due to the diffraction effects and the size of the vessel, which might be larger than the shadow region generated from individual wind turbines.

1.2.2.3 For completeness, a shadowing assessment has been undertaken within this assessment and is used in conjunction with the study of the rerouting of traffic around the Mona Offshore Wind Project (see section 1.2.3). Within this assessment the radar shadows were modelled based on optical shadowing. Optical shadows conservatively assume no diffraction effects and therefore ignore the improvement in the shadow region at extended ranges. Depending on the wind turbine size and radar height, the optical shadows may extend all the way to the radar horizon. The use of optical shadows is used to assess scenarios which might have an impact on the radar's performance.

1.2.3 Rerouted traffic

1.2.3.1 Some of the existing shipping routes will be altered by the physical presence of the Mona Offshore Wind Project, and vessels may be rerouted nearer to existing platforms covered by the REWS as they deviate around either project (as shown in Figure 1.30 and described in detail within Volume 6, Annex 7.1: Navigational Risk Assessment of the Environmental Statement). This may cause an increase in the CPA/TCPA alarm rates. The effects of the rerouting of traffic on the alarm rates are discussed in section 1.6.

1.2.4 Adaptive detection threshold modelling

1.2.4.1 A REWS deploys a number of techniques for clutter thresholding, target extraction and tracking. The use of adaptive thresholding algorithms such as Constant False Alarm Rate (CFAR) is very common within offshore REWS installations. A variety of CFAR algorithms can be used to adjust the threshold around noisy/cluttered areas to avoid unwanted and false detections depending on the clutter within the local environment. REWS uses CFAR techniques to dynamically adjust the detection threshold over sea and rain clutter. Digital signal processing is applied to calculate a constant false alarm rate for plot-extraction by generating a radar threshold below which all radar samples are ignored as they are considered to be noise or clutter. The threshold is calculated individually for each radar cell using a two-dimensional sliding window area technique whereby surrounding cells in both range and azimuth are considered. Typically, the mean and standard deviation of samples is calculated, and the threshold is set to the mean value plus a factor derived from the standard deviation of the sample.

1.2.4.2 Finally, it is worth noting that as CFAR uses multiple adjacent range and azimuth cells (see Figure 1.2) to derive the detection threshold, the presence of a single turbine will affect the threshold of multiple cells around it as shown in Figure 1.2.

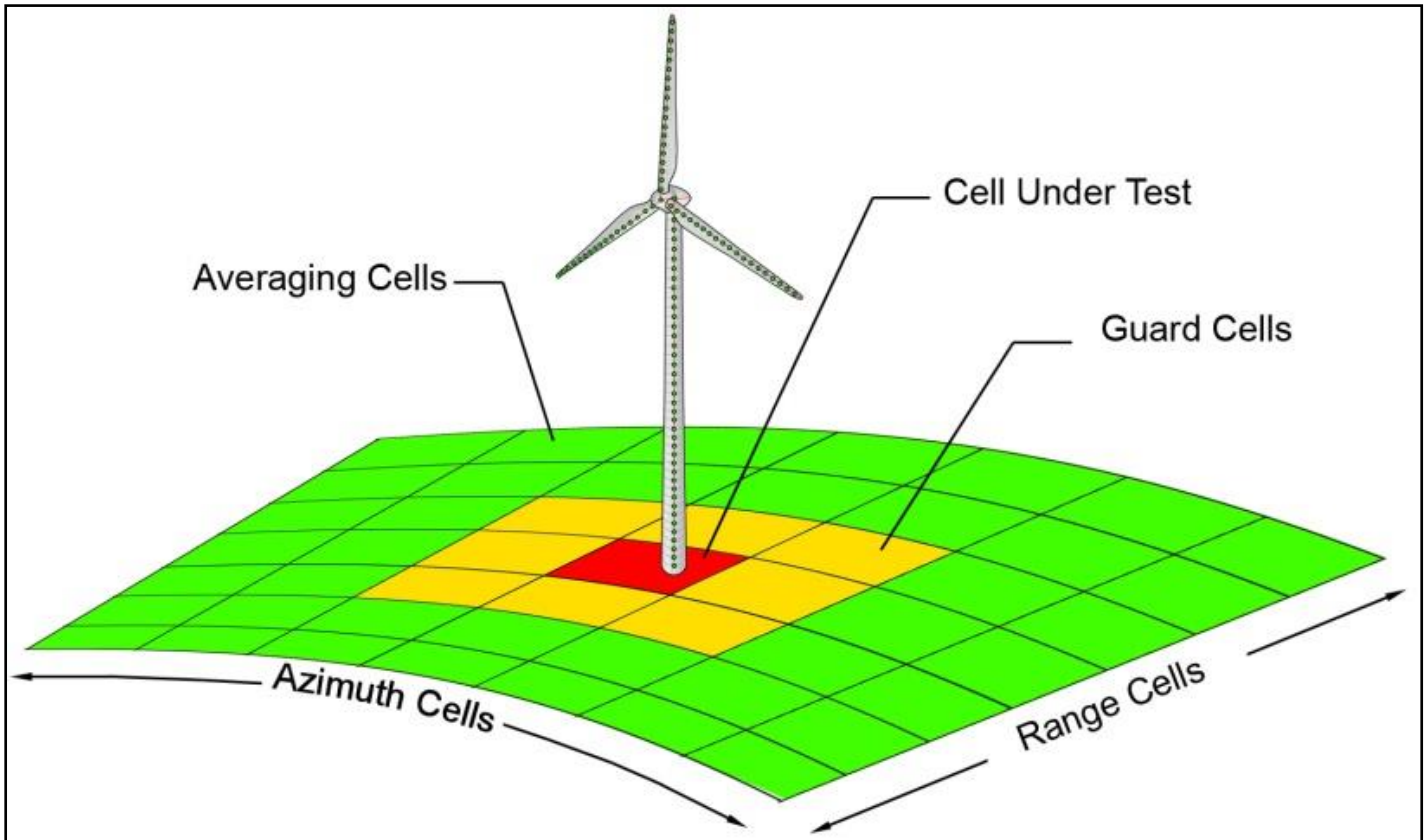


Figure 1.2: 2D CFAR cells around a given cell with wind turbine present.

1.2.5 Tracker modelling

1.2.5.1 Radar trackers provide the radar operator with a processed and clear image of the location and bearing of moving targets in the area of interest. It is also very common for currently used radar trackers to compensate for momentary loss of detection of a target over multiple radar rotations and maintain an active track. The presence of advanced tracking within REWS can greatly benefit and enhance the operator's ability to maintain radar visibility of moving targets near or within a wind farm. REWS deploy proprietary tracker algorithms, which may vary depending on the system supplier. The impact of the wind farm on the tracker performance cannot be accurately modelled without detailed knowledge of the tracker and the proprietary tracking algorithms - which are not available for this assessment and so were not included in this assessment. However, it is expected that the tracker software along with integration of Automatic Identification System (AIS) within the REWS data will enhance the detection and tracking of vessels within the Mona Offshore Wind Project.

1.2.6 Ultra-High Frequency communication links

1.2.6.1 Depending on the REWS system and the tracker software, it is possible that returns from the wind turbines will add new target detections to the track-table. The track-tables are shared with Emergency Response and Rescue Vessels (ERRVs) via ultra-high frequency (UHF) radio links. UHF links use a low-bandwidth telemetry system and have a limit on the total number of tracks that can be transmitted. The maximum size of the track-table is a system limitation that depends largely on the hardware used and hence cannot be modelled. A typical number for the maximum track-table size is

assumed to be between 400 and 600 tracked targets. Depending on the tracking software, the number of tracks within the track-table can be reduced by applying non-acquire zones over the wind farm area or by applying filters to track moving targets only. UHF communications are different and separate systems than the radar. They operate at different frequencies than the radar frequency and use different modulation techniques to transmit and receive data. Therefore, the potential impact of wind farms on the performance of UHF communication systems cannot be modelled and assessed using the radar models used within this assessment. As such, the effects of the Mona Offshore Wind Project on UHF communication links are considered outside the scope of this work.

1.2.7 Other effects

- 1.2.7.1 False tracks may be initiated due to the variation of the wind turbines' radar returns over multiple range-cells. However, the radar tracker requires consecutive detections over a number of radar rotations, which will reduce the likelihood of false track initiation. Furthermore, to raise a TCPA alarm, the track vector must continue to breach the TCPA condition for multiple radar rotations. Thus, raising false alarms due to range-cell spreading is considered very unlikely and was not included in this assessment.
- 1.2.7.2 It is also possible to model the effects of multiple reflections of the radar signal within the Mona Array Area, and between the wind turbines and nearby large targets, using the radar and WinR (Wind Turbine RCS) models developed at the University of Manchester. However, as the closest modelled turbine in the Mona Array Area is more than 3 km away from any REWS, the effects of the multiple reflections were considered to be of second order (not a primary cause or concern) and were not included in the models (QinetiQ, 2005; Baker, 2007).
- 1.2.7.3 Depending on the detailed structure of the REWS host platform, the presence of external fittings near the radar antenna such as masts, wires and other structural elements may cause distortion of the antenna pattern and possibly the appearance of false reflection if a flat surface is near the antenna. The inclusion of such structures will greatly increase the modelling complexity and is not expected to affect the overall findings of the assessment. Therefore, these effects were not modelled.

1.3 Modelling parameters

1.3.1 Wind turbine parameters

- 1.3.1.1 The maximum dimensions of the wind turbines proposed for Mona Offshore Wind Project have been defined in the MDS in Volume 1, Chapter 3: Project description of the Environmental Statement, and are shown in Table 1.1.
- 1.3.1.2 In order to accurately predict the RCS of wind turbines at different orientations and ranges, the wind turbines need to be modelled as continuous curved surfaces that represent the geometry of the wind turbine. This includes the shape of the tower, the nacelle and the airfoil profile of the blades. However, the MDS only provides the main features and dimensions of the wind turbines, and it does not provide details of the tower, blades, nacelle and hub geometries. Therefore, to undertake this study and to better model the RCS of the wind turbines, a realistic model of pre-existing turbine surfaces was used. This was achieved by using a realistic blade shape and airfoil profile of a 5 MW turbine that was scaled up to match the MDS parameters. The shape of the nacelle, hub and tower were also scaled to match the MDS turbines. The

MONA OFFSHORE WIND PROJECT

resultant scaled turbine matches the MDS parameters and has a realistic geometry that can then be used to model the RCS and radar returns.

1.3.1.3 The scaled Computer Aided Design (CAD) geometries for the modelled turbines (i.e. 96 turbines with a rotor diameter of 250 m and a hub height of 163 m) used to compute the RCS of the wind turbines are shown in Figure 1.3 below. Details such as ladders, warning lights, wind measurement/lightning protection equipment etc. were removed from the wind turbine CAD for RCS modelling as these will not have a significant effect on the scattering profile which is dominated by the larger components (i.e. tower, blades and nacelle), and will greatly increase the computational complexity.

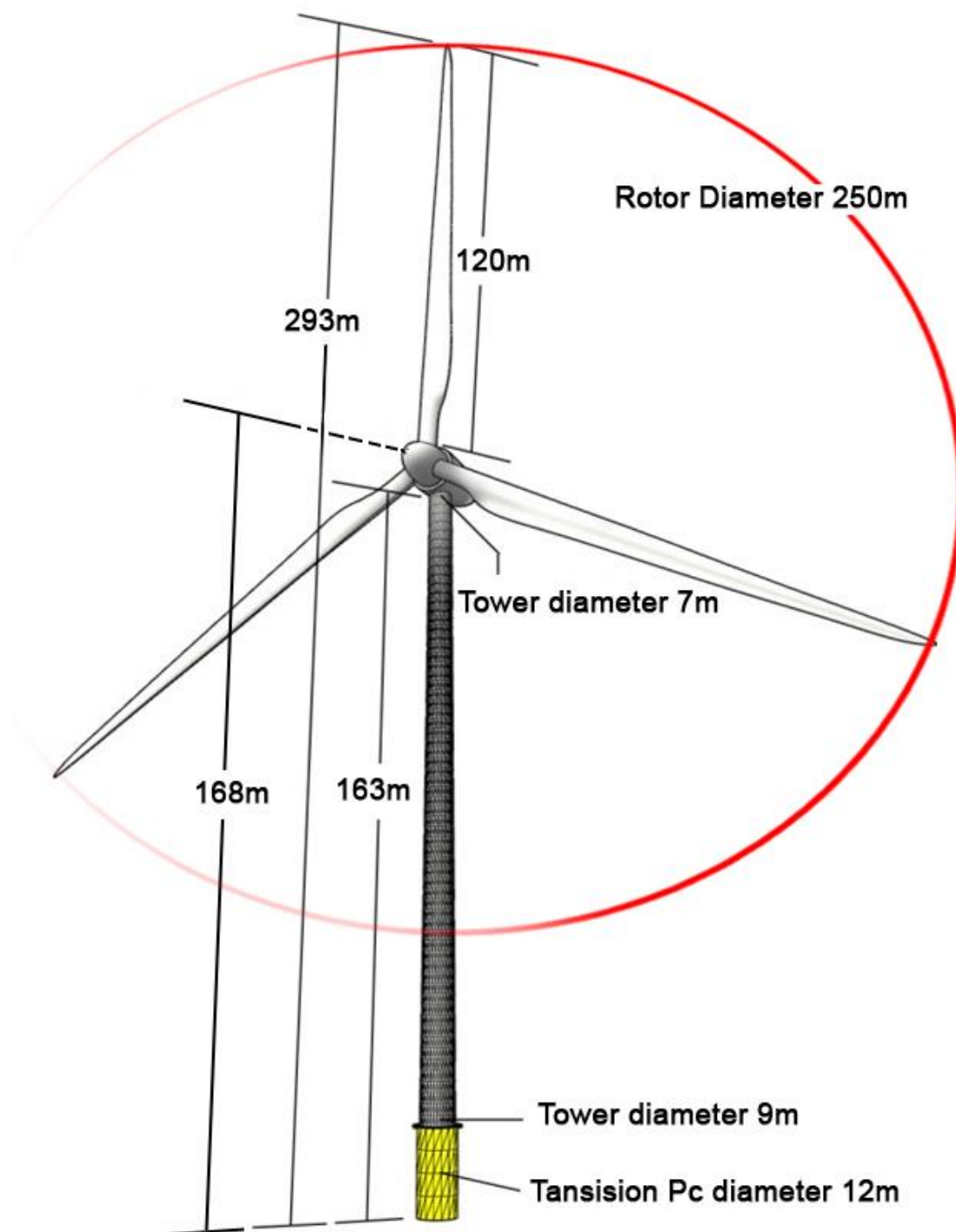


Figure 1.3: Modelled turbine geometry.

MONA OFFSHORE WIND PROJECT

- 1.3.1.4 Within this assessment, it has been assumed that the wind turbines are mounted on a monopile foundation with a transition piece leading to the tower. Traditionally, a monopile with the transition piece design gives a very large radar return, which in some cases might dominate the wind turbine RCS. This is due to the shape and construction materials of the transition piece which makes it highly reflective to the radar. The upright cylindrical and parallel, metallic sides of the transition piece will reflect the radar energy directly to the radar which may make up to 80% of the total radar signature generated from the wind turbine. Other supporting structures, such as jacket foundations are expected to have tapered sides and smaller reflective areas which will not be as prominent as a monopile foundation. Monopile foundations therefore have been modelled to provide a worst case modelling scenario. The indicative MDS layout of the wind turbines is presented in Figure 1.4, which shows the indicative layout of both Mona Offshore Wind Project and Morgan Generation Assets. These indicative layouts will be used for the assessment of the proposed project in isolation and cumulatively with Morgan Generation Assets.
- 1.3.1.5 When assessing the potential impact of the Mona Offshore Wind Project in isolation, and in combination with other projects in the assessment area, the wind is conservatively assumed to be coming from the radar site in the direction of the centre of the Morgan and Mona Array Areas. This results in the majority of the wind turbines facing the radar, which will then give the maximum RCS value. As the RCS of each wind turbine is individually computed, the blades' rotation angle on each wind turbine is generated randomly as a value between 0° and 119°. This results in a different RCS for each wind turbine rather than an unrealistic unified rotation angle across all turbines.

MONA OFFSHORE WIND PROJECT

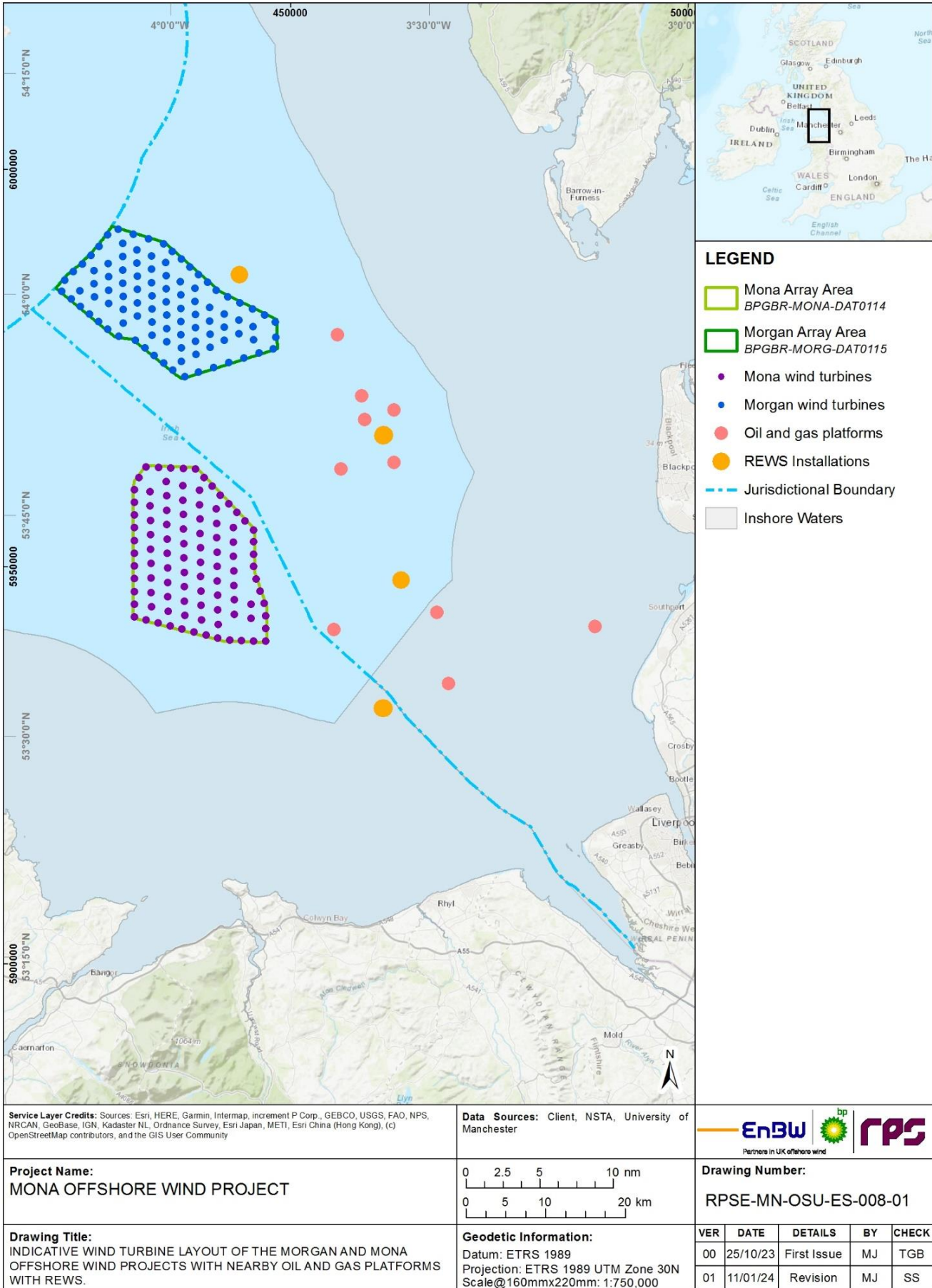


Figure 1.4: Indicative Mona and Morgan MDS layout with nearby oil and gas platforms with REWS.

1.3.2 Wind farm parameters

1.3.2.1 A summary of the MDS parameters for the REWS modelling for the Mona Offshore Wind Project is presented in Table 1.1.

Table 1.1: MDS parameters for the REWS modelling.

| Mona Offshore Wind Project parameter | Value |
|--|--|
| Maximum number of wind turbines | 96 |
| Rotor diameter | 250 m |
| Hub height (centre point) | 168 m above mean sea level (AMSL) |
| Hub height (lowest point) | 163 m AMSL |
| Maximum blade tip height | 293 m |
| Blade length | 120 m |
| Turbine tower upper diameter | 7 m |
| Turbine tower lower diameter | 9 m |
| Transition piece diameter | 12 m |
| Maximum number of offshore substations within the array area | 4 |
| Maximum dimensions of small offshore substations | 60 m (length) x 80 m (width) x 70 m (height) |
| Total RCS of offshore substations and platforms | 4,000 m ² |

1.3.3 Mona Offshore Wind Project indicative wind turbine and offshore substations/platform layouts

1.3.3.1 The indicative layout of the Mona Offshore Wind Project was imported into the models using proposed coordinates for each wind turbine and offshore substation platform. The locations of the offshore substations/platforms and the imported turbine locations are shown in Figure 1.4.

1.3.3.2 Four offshore substations/platforms are allocated within the envelope proposed wind farms. The exact geometry and location profile of the substations is not defined at this stage and is not considered to be of significant importance to the radar modelling results. However, when considering offshore substations, it is important to include an approximated source of radar echoes and a structure that will cast a radar shadow. Therefore, the modelling results that are shown within this report assume that the offshore substations/platforms are large offshore structures. The radar scattering from the substations was estimated by modelling a number of scattering points distributed within a rectangular box. The dimensions of the offshore substations/platforms are presented in Table 1.1. The total RCS of each substation was set to be 4,000 m². This is an approximate value used to assess the impact of the substation on the shadowing and the radar detection threshold. The exact scattering characteristic will depend on the substation's geometry and construction material as well as its range from the radar antenna.

1.3.3.3 Once the locations of the wind turbines and the offshore substations/platforms were defined, a desk-based review of charts was undertaken alongside consultation with oil and gas operators in order to identify the location of nearby offshore oil and gas

platforms and any REWS installations that might be affected by the presence of Mona Offshore Wind Project. The location of offshore oil and gas platforms and the identified REWS host platforms are also shown in Figure 1.4.

- 1.3.3.4 Typically, a 30 km (16 nm) detection range is assumed to be the minimum requirement for REWS to detect and track smaller vessels (100 m² RCS). This indicates that some of the identified REWS installations will have a direct LoS with the Mona Array Area. The four REWS installations are located on Harbour Energy's Millom West platform, ENI Energy's Douglas platform and the OSI, and Spirit Energy's South Morecambe AP1 platform. These REWS installations provide a good overlapping radar coverage in the area to protect other oil and gas assets in the region (see Figure 1.11).

1.3.4 Assessment region and study area

- 1.3.4.1 Typically, a 30 km (16 nm) detection range is assumed to be the minimum requirement for REWS to detect and track smaller vessels (100 m² RCS). This indicates that some of the identified REWS installations will have a direct LoS with the Mona Array Area. The four REWS installations are located on Harbour Energy's Millom West platform, ENI Energy's Douglas platform and the OSI, and Spirit Energy's South Morecambe AP1 platform. These REWS installations provide a good overlapping radar coverage in the area to protect other oil and gas assets in the region (see Figure 1.11) Figure 1.5.

MONA OFFSHORE WIND PROJECT

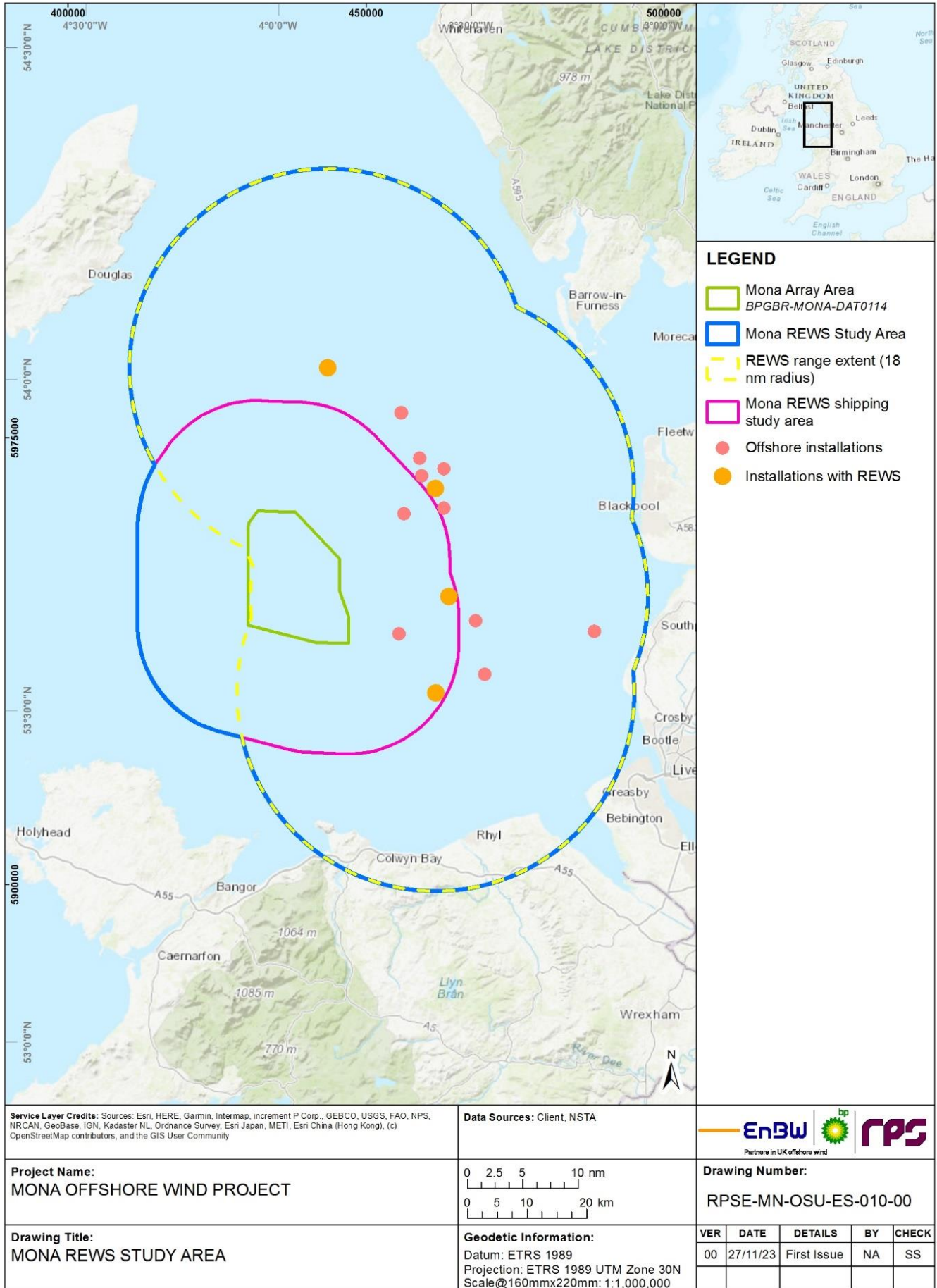


Figure 1.5: Mona REWS study area.

1.3.5 REWS modelling

- 1.3.5.1 REWS provides coverage over offshore oil and gas installations and provides early warning to the operators' when vessels breach the alarm settings. REWS use pre-set allision alarm rules. Typically, for both manned and normally un-manned installations (NUI) an Amber alarm is raised if a vessel is within CPA of 0.6 nm and a Red alarm is raised if the CPA is 0.27 nm. For manned installations an Amber TCPA alarm is raised if a vessel is 40 minutes away and a Red alarm is raised if the vessel is 30 minutes away. For NUI an Amber TCPA alarm is raised if a vessel is 25 minutes away and a Red alarm is raised if the vessel is 15 minutes away. Should a vessel breach these rules an automatic alarm is raised to alert the operator. It is worth noting that TCPA alarms are only triggered if the vessel's vector remains in breach of the TCPA condition for a set number of radar rotations. For assessed REWS, it was assumed that there is a delay of 90 seconds (or 36 radar rotations) before an alarm is triggered. This setting is included to avoid alarms due to temporary vector breach of the TCPA while vessels are turning.
- 1.3.5.2 In addition to radar data, REWS are often integrated with AIS fitted onboard ships. If a vessel is fitted with an AIS transponder and is detected by the radar, the REWS will include the AIS data into the track data. AIS is a very useful source of vessel information and location data that can complement the radar data when temporary losses are experienced.
- 1.3.5.3 Within this assessment, the performance of the REWS is based on the specification of Raytheon's Pathfinder/ST MK2 X-band transceiver with Mariners Pathfinder X-band 12 ft antenna system. The details of the modelling parameters used are shown in Table 1.2 and the antenna pattern used in the modelling is shown in Figure 1.6.

Table 1.2: Radar modelling parameters.

| Modelling parameter | Value |
|---------------------------|-------------------------------|
| Gain | 30 dB |
| Transmitter power | 25 kW |
| Frequency | 9.411 GHz |
| Pulse width | 250 ns |
| Rotation rate | 25 rotations per minute (RPM) |
| Pulse repletion frequency | 2.0 kHz |
| Noise figure | 5.5 dB |
| Dissipative losses | 1.0 dB |
| Beam-shape losses | 0.6 dB |
| Azimuth beam width | 0.7° |
| Elevation beam width | 23.0° |
| Antenna height | 55 m AMSL |

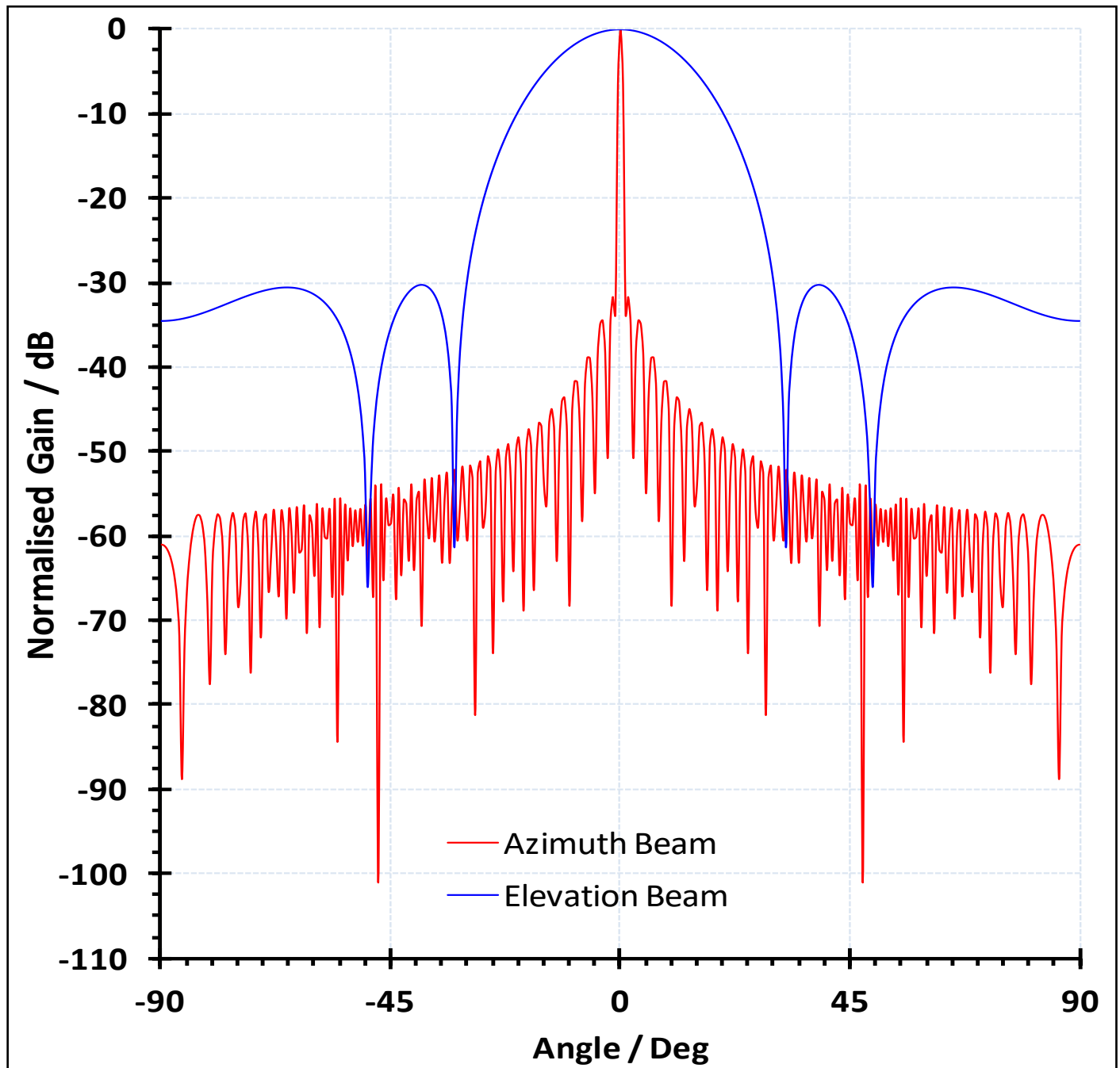


Figure 1.6: The radar antenna elevation and azimuth patterns.

- 1.3.5.4 The modelling is conducted at a rainfall rate of 0 mm/hr and sea-state 3 (wind speeds 9.6 ms⁻¹ and average wave height of 1.3 m). When computing returns from the sea surface and the rain clutter the models provide the mean levels of returns.
- 1.3.5.5 REWS processing deploys scan-to-scan correlation, which improves the noise and clutter suppression. However, this is not considered in depth as part of this study as it requires detailed knowledge of the proprietary software used within the system’s signal processing.
- 1.3.5.6 It is worth noting that only the medium pulse width of 250 ns was used throughout the assessment. This gives an approximated range resolution of 37.5 m which is then equated to the range-cell length. As the wind turbine rotor diameter is much larger than the range cell length (depending on the yaw angle with respect to the radar), parts of the blades will fall into adjacent range-cells as the wind turbine blades rotate. This phenomenon will be referred to as ‘range-cell spreading’ within this document.

1.3.6 Detection threshold (CFAR)

1.3.6.1 There are multiple variations of CFAR that can be used where different weights can be applied to each cell prior to the final averaging. However, within this document and to examine the effect of the Mona Offshore Wind Project on the threshold levels, a Constant Averaging (CA) CFAR is applied over the clutter map. The CA-CFAR modelled within this assessment uses two range cells on both sides of the cell under test as the guard region while the averaging considers six range cells on both sides of the guard region. In Azimuth the modelled CA-CFAR uses one guard cell and two averaging cells on both sides in azimuth. The overall resultant threshold was set to provide a constant 10^{-5} probability of false alarm.

1.3.7 Target modelling

1.3.7.1 REWS are mainly interested in detecting and tracking surface targets such as large fishing boats, maintenance vessels and larger ships and tankers. The role of the REWS is to alert the operator when a vessel is on an allision course with the platform. Although air targets may also appear on the radar display, the management and trafficking of air targets is controlled by other radar systems such as ATC primary and secondary radars or AD radar systems. Thus, the analysis of the potential impact of the Mona Offshore Wind Project on REWS is limited to surface targets only.

1.3.7.2 Large vessels in excess of 1,000 gross tons (GT) are the primary concern when it comes to managing the safety of offshore platforms (Love, 2014). However, within this report, the test target was set to represent a large sized maintenance vessel with a steel/metallic hull. The test vessel is assumed to have an RCS of 1000 m² and a height of 6 m. These parameters are typically used for REWS performance analysis and system acceptance testing and they comply with the International Association of Marine Aids to Navigation and Lighthouse Authorities (IALA) Vessel Traffic Services (VTS) guidelines for radar modelling of different vessel types. The test vessel was set to have an average speed of 17 knots (31.5 km/hr).

1.3.8 Wind turbine shadow modelling

1.3.8.1 As discussed in section 1.2.2, when turbines are placed within the LoS of radar systems, radar shadowing will occur behind the structure. The extent and length of the shadow region depends on the size of the wind turbine, the distance to the radar antenna, the height of the radar and the height of the target of interest. Shadowing produced by turbines may cause targets to be lost as they move in and out of the shadow region. Depending on the size of the shadow region, this may cause existing tracks to be lost or discontinued.

1.3.8.2 As REWS are mainly used to detect and track surface moving targets (ships, boats etc.), only surface or near-surface shadowing is considered. This can be approximated by using the optical shadowing/blockage cast by the wind turbine over the sea surface. The use of optical blockage to estimate the radar shadowing will give pessimistic results but is deemed acceptable for objects that are much larger than the radar wavelength at relatively short ranges (such as offshore wind turbines). Optical blockage does not account for diffraction effects around the structure which would normally reduce the shadow length. Diffraction and partial shadowing of an object has been shown to significantly improve the radar detection. Practical measurements and other studies show that the shadowing effects from the wind turbines may reduce the overall detection range of the radar but may not severely affect the detection of objects within the shadow regions.

MONA OFFSHORE WIND PROJECT

1.3.8.3 One thousand GT plus vessels (which are the main safety concern to offshore platforms) vary in size and typical vessel lengths are between 15 m and 60 m. However, the shadows from the wind turbines are relatively narrow and are typically between 4 m and 20 m in width. This indicates that a large 1,000 GT vessel will be partially shadowed by the wind turbine as it moves through the shadow regions (as shown in Figure 1.7. Partial shadowing will allow some of the radar energy to be reflected back to the radar and it might be possible for this energy to be detected by the REWS. Hence, smaller vessels can be assumed as point scatterers while larger vessels can be assessed for partial shadowing.

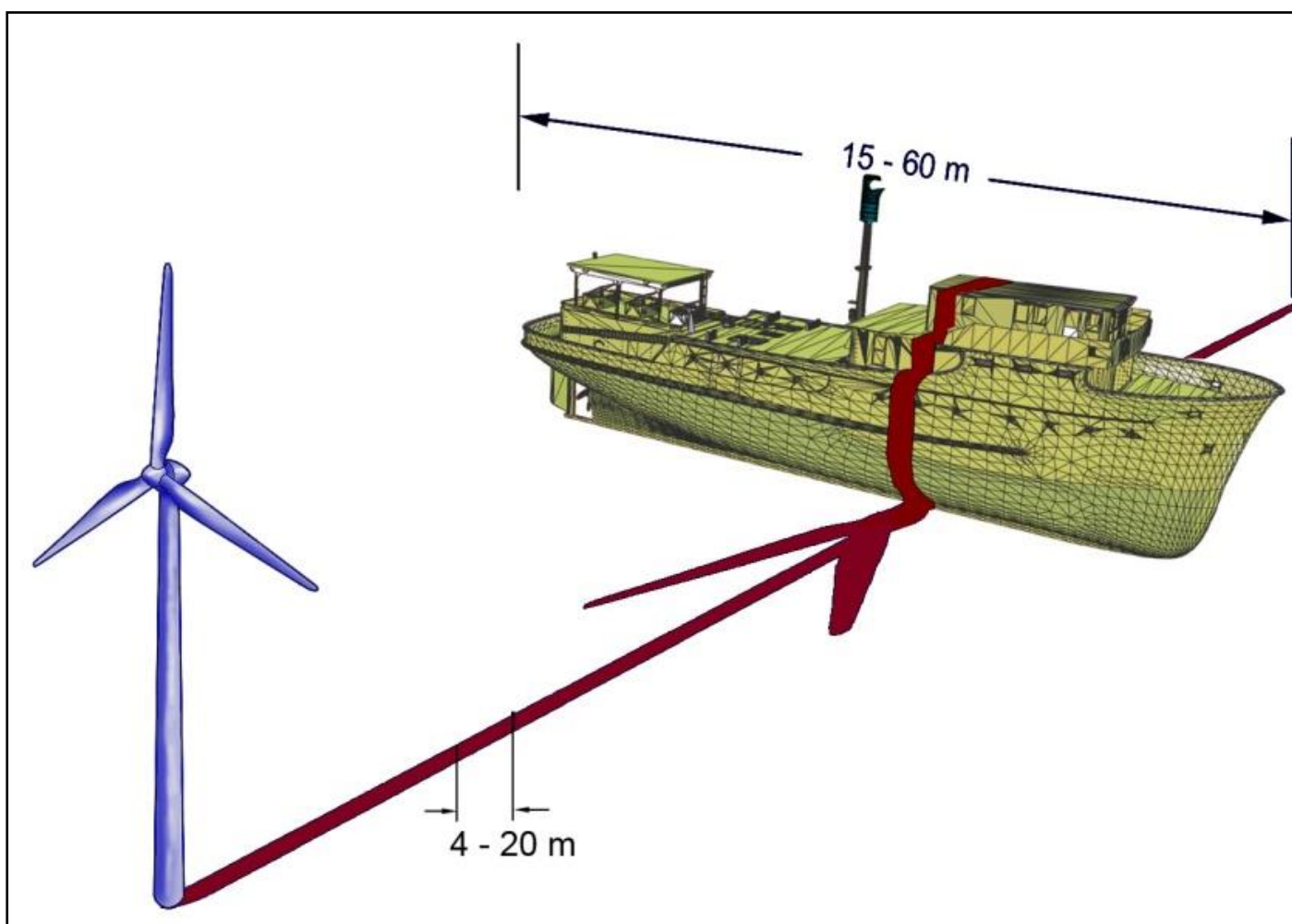


Figure 1.7: Optical blockage and partial shadowing.

1.3.9 Measurements and modelling of RCS of wind turbines

1.3.9.1 A number of studies have attempted to determine the RCS of wind turbines through measurements of the power received by a radar in the region. A study undertaken by Terma within Hornsea Project One (Terma, 2021) highlights the difference between measured and theoretical RCS values of wind turbines obtained from computational modelling. The wind turbines deployed at Hornsea Project One have a rotor diameter of 154 m and a hub height of 117.9 m AMSL. Although these turbines are smaller than the MDS turbines considered for the Mona Offshore Wind Project, they are still considered to be very large structures for radars. The results of the field study show that the power received from turbines within Hornsea Project One are within reasonable levels and the radar is able to detect a vessel travelling within the array area. The layout showing the location of the radar within the wind farm is shown in

MONA OFFSHORE WIND PROJECT

Figure 1.8. The power received by the radar is shown in Figure 1.9 and shows that the radar, which is using pulse compression to improve resolution and power levels, can detect a service vessel travelling within the array area.

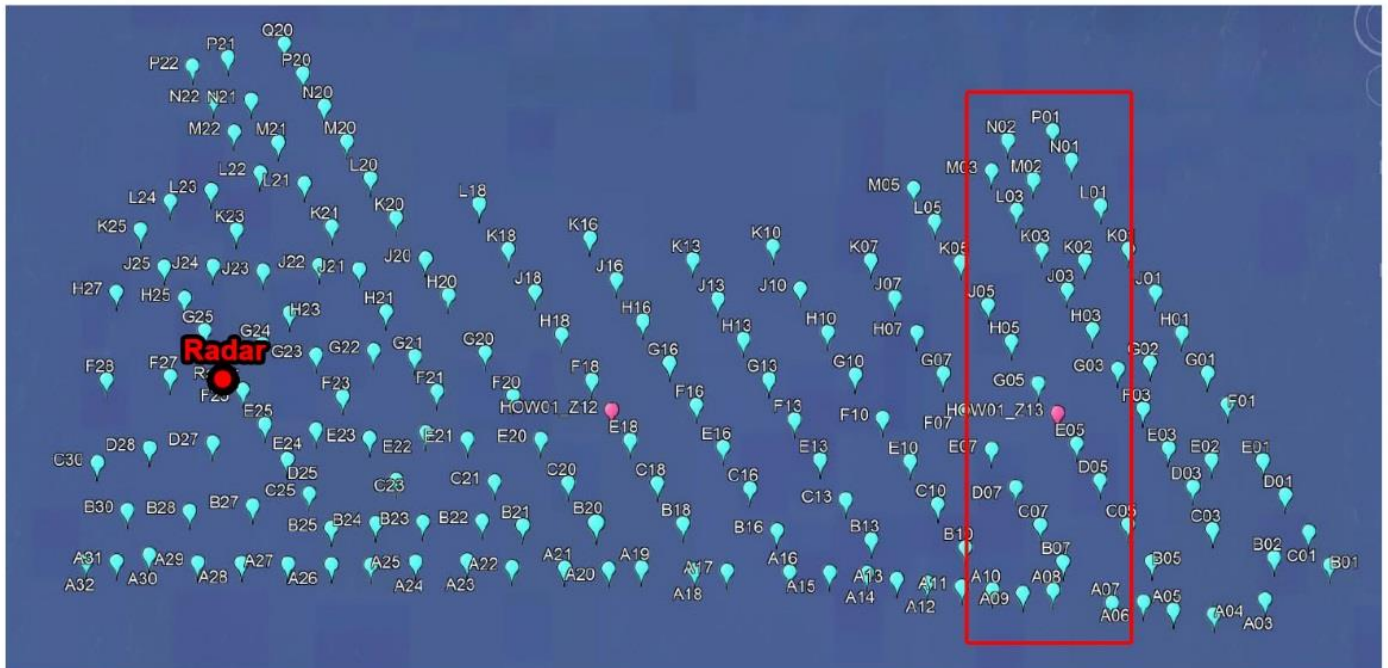


Figure 1.8: Wind turbine layout at Hornsea Project One array area and the location of the radar system used in the study. The red area denotes the region shown in Figure 1.9 (Terma, 2021).

MONA OFFSHORE WIND PROJECT

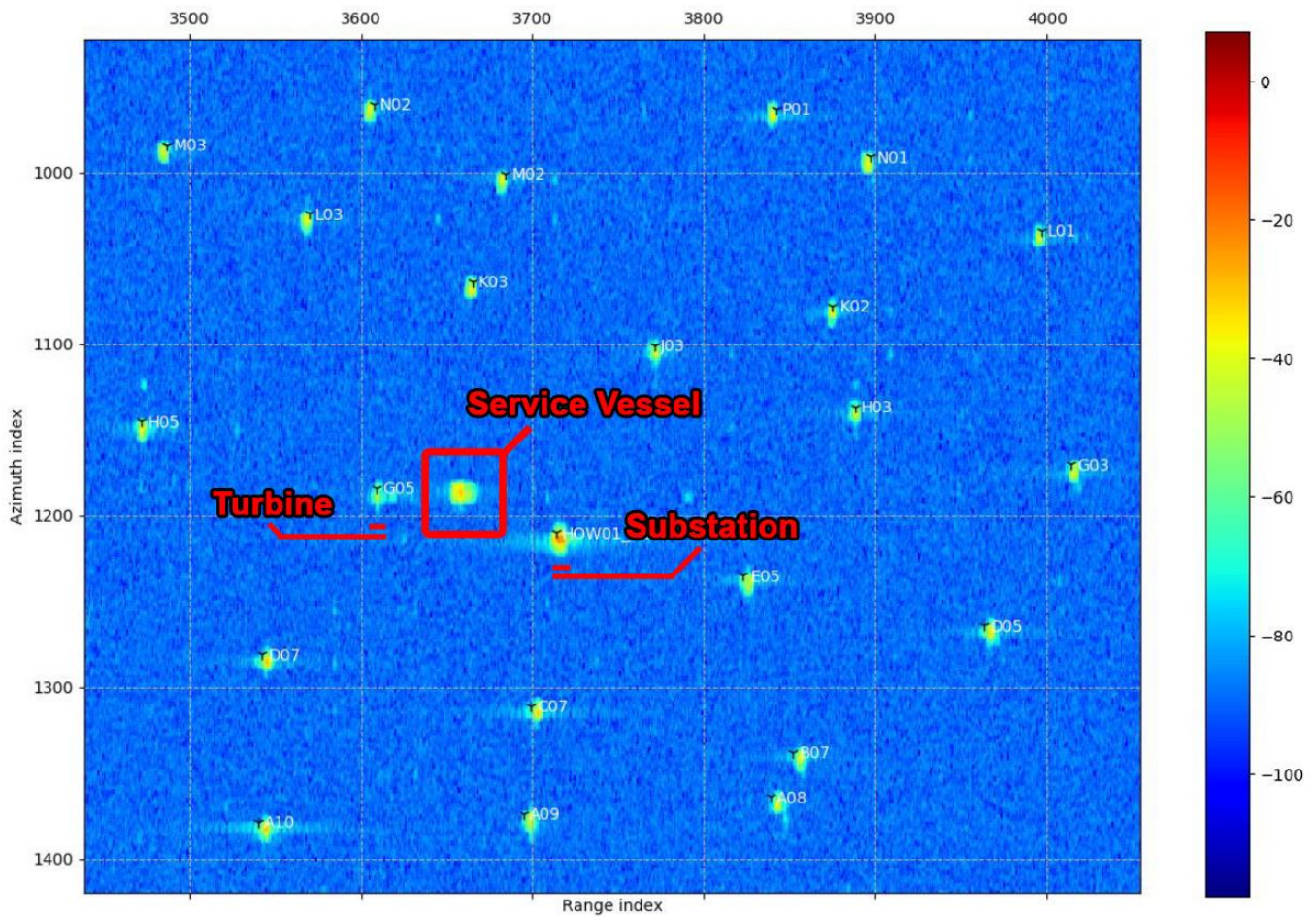


Figure 1.9: Compressed radar image in range-azimuth coordinates showing a zoomed area of the Hornsea Project One array area around a substation platform (Z13). A vessel is visible between Z13 and WTG G05. The signal level (in dB) is colour coded (Terma, 2021).

1.3.9.2 A key finding of the Terma study was that turbines located within 10 km of the radar had a lower RCS than traditional RCS models would suggest. Traditional RCS modelling methods would often need to utilise a number of assumptions in order to reduce the complexity of the RCS modelling and computational efforts needed. Many of these assumptions are related to the effect of the range (distance from the radar) on the radar signature from these large objects. Objects within close range to the radar (within the near-field) often have a lower RCS value.

1.3.9.3 Although the models used within this technical annex address many of these assumptions and account for the effect of range on the scattering profile and signal levels from the wind turbines, the utilised models still need to make certain assumptions regarding the exact geometry of the wind turbine, the materials used, and the exact blade profile under wind loading (as blades bend due to wind loading). Some of these assumptions would result in higher-than-expected RCS values but are still considered within acceptable limits and produce similar results to the measurements shown in the Terma study as illustrated in Figure 1.10.

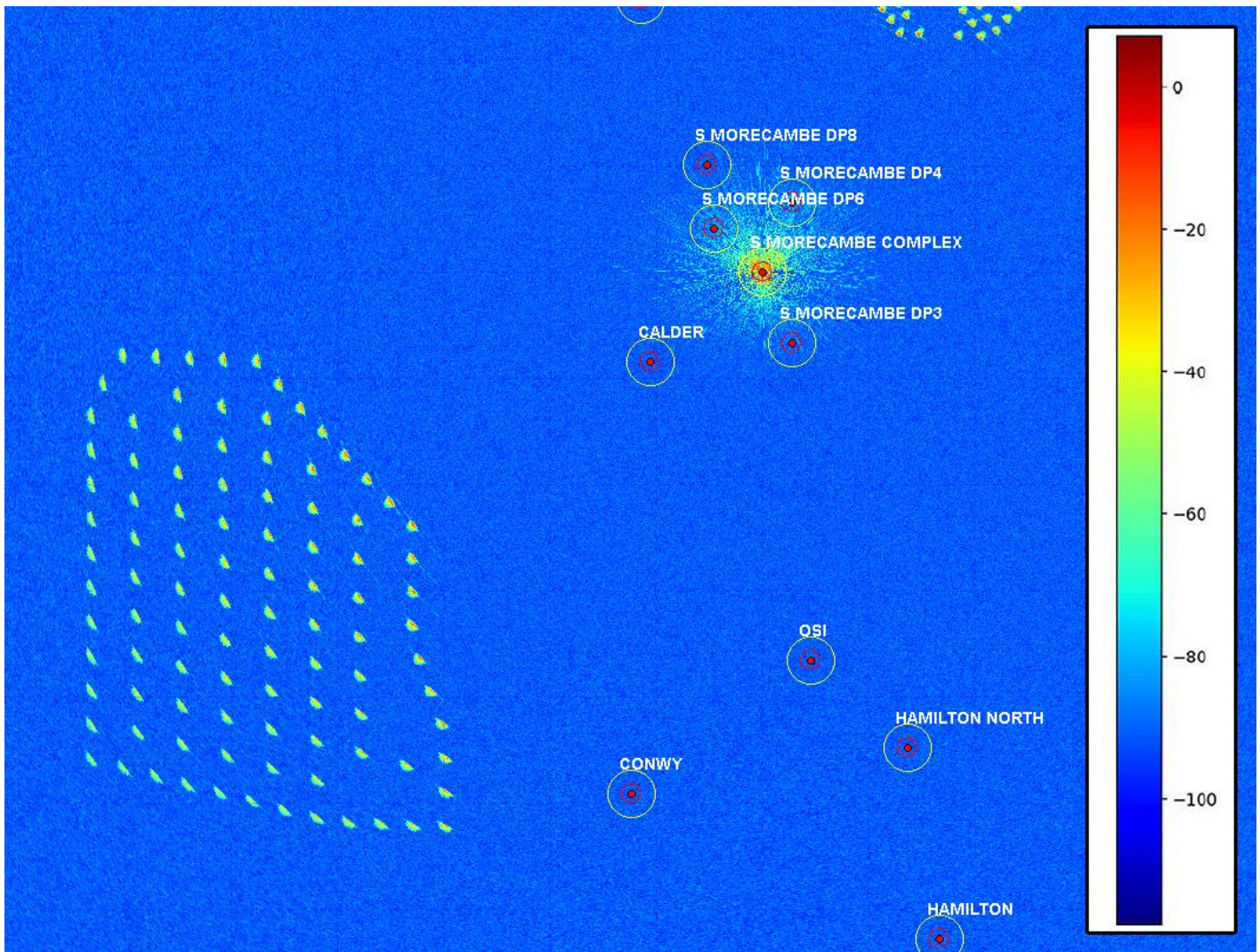


Figure 1.10: Power received by the REWS on Spirit Energy’s South Morecambe AP1 platform.

1.4 REWS Returns and vessel detection modelling results

1.4.1 Overview

1.4.1.1 There are a number of REWS installations near the Mona Array Area. Currently this region has a number of regular vessels travelling along routes passing through the area. Therefore, ENI Energy, Harbour Energy and Spirit Energy have multiple REWS installations in the region to monitor and protect their assets (Figure 1.4).

1.4.2 Assessment of the base case scenario

1.4.2.1 In order to establish the potential effect of the Mona Offshore Wind Project on REWS installation in the region, the assessment starts by looking at the base case scenario where only the existing wind farms are modelled. The location of the existing wind farms and the locations of the oil and gas platforms are shown in Figure 1.11. The REWS installations are also shown in Figure 1.11 with their coverage area denoted by the large red circles, which illustrate the 16 nm range. The red circle around each platform denotes the 0.27 nm Red CPA alarm while the yellow circle denotes the 0.6 nm Amber CPA alarm.

MONA OFFSHORE WIND PROJECT

- 1.4.2.2 For platforms with REWS installations the presence of wind farms may have potential effects on the REWS' ability to detect and track vessels travelling through wind farm areas. If the REWS is unable to detect and track the vessel within the wind farm, it may cause the REWS to issue delayed TCPA alarms, resulting in insufficient response times to deal with potential collision threats. The assessment modelled the returns and target detection at the REWS installations on ENI Energy's Douglas platform, Harbour Energy's Millom West platform, ENI Energy's OSI and Spirit Energy's South Morecambe AP1 platform (in that order). The assessment starts by considering the power received at the radar, then it establishes the expected threshold levels, followed by a comparison between the threshold level to the expected vessel returns to determine the detection regions.
- 1.4.2.3 Starting with ENI Energy's Douglas platform, Figure 1.12 shows the power received (radar returns) from the existing turbines along with the assumed clutter generated from the sea surface. The green regions represent areas where radar returns are being detected. Brighter shades of green indicate higher returns while darker green regions indicate low returns.
- 1.4.2.4 To further assess the REWS' ability to detect vessels within the wind farm areas, a CFAR threshold over the detection region was modelled using a 2D CA CFAR (as highlighted in section 1.3.6). The modelling results for ENI Energy's Douglas REWS are shown in Figure 1.13. The figure shows the regions with higher detection threshold as brighter shades of green. The strong returns from the wind turbines will significantly alter the threshold levels. It can be noted that the threshold is raised over multiple cells around each wind turbine since the CFAR threshold averages the returns over a 2D sliding window of multiple cells in azimuth and range.

MONA OFFSHORE WIND PROJECT



Figure 1.11: Modelled layout of the base case scenario showing the location of the existing wind farms and the coverage of the REWS in the region.

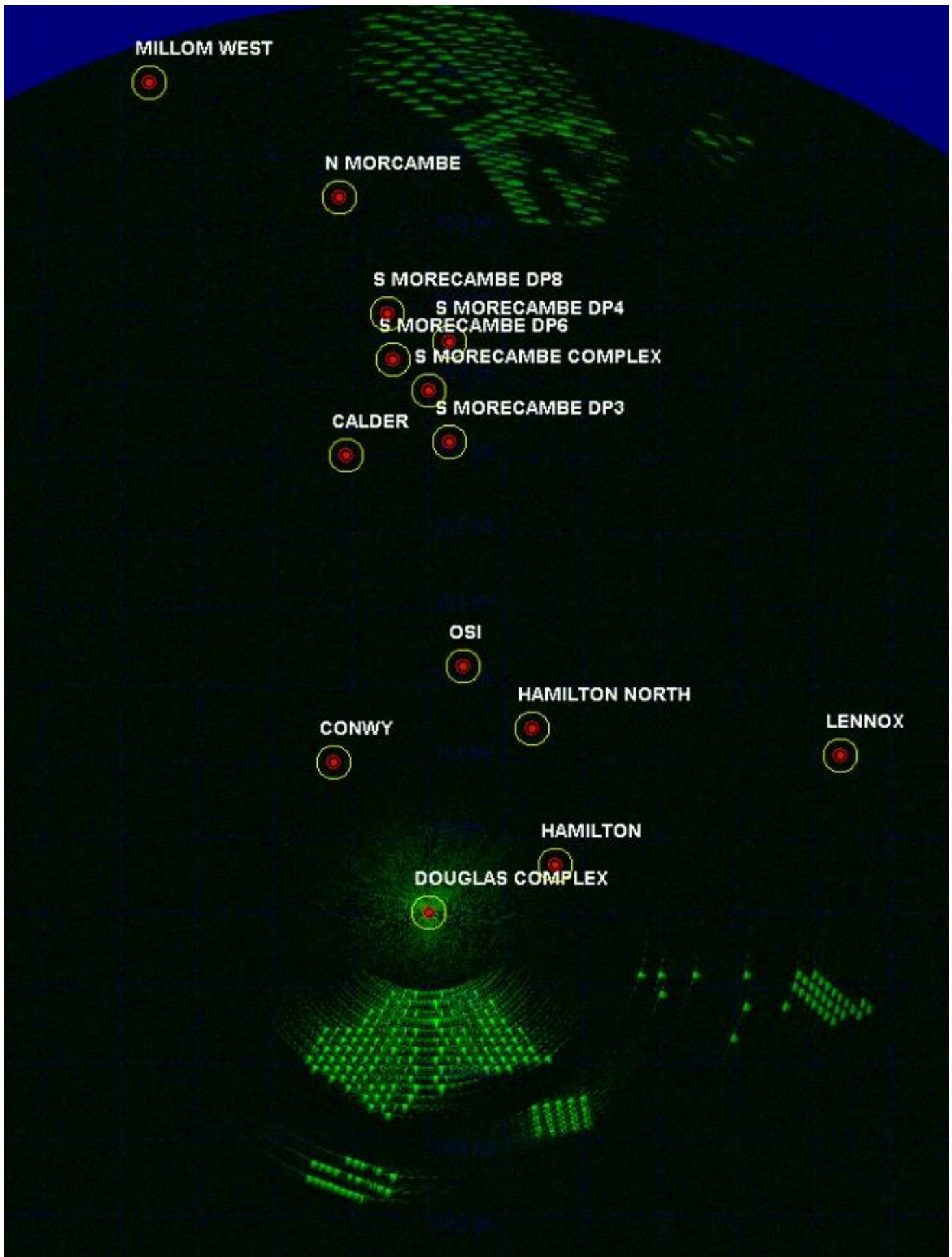


Figure 1.12: ENI Energy's Douglas platform REWS clutter map showing returns from the wind turbines and sea clutter.

MONA OFFSHORE WIND PROJECT

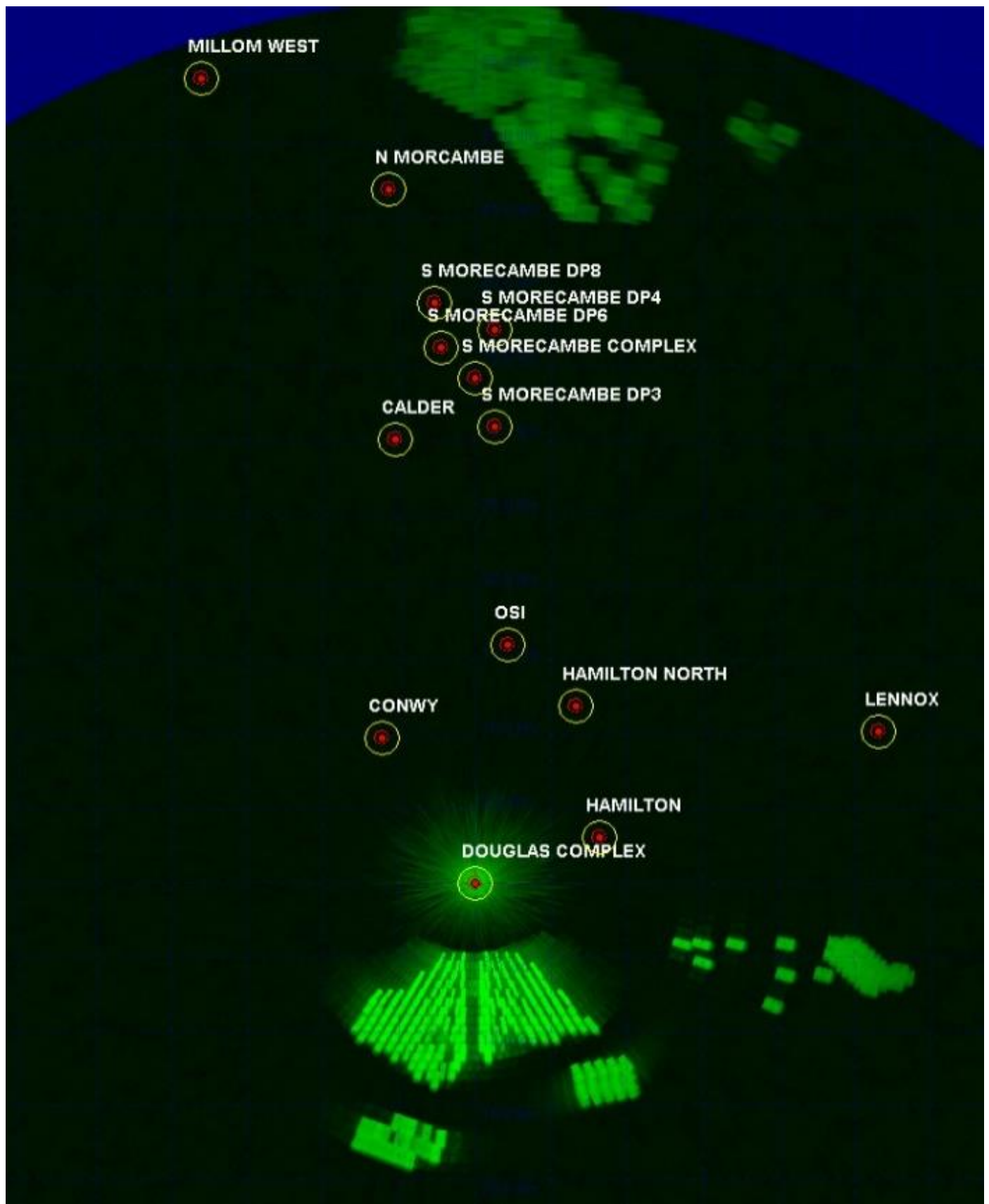


Figure 1.13: ENI Energy's Douglas platform REWS detection threshold.

MONA OFFSHORE WIND PROJECT

1.4.2.5 In order to establish the detection regions for a given vessel, the returns from the 1000 m² RCS test vessel are modelled with respect to range and plotted around the REWS as shown in Figure 1.14. Figure 1.14 shows that the vessel has high returns at close ranges which then reduces as range increases up to approximately 21 nm (39 km). The blue region in the figure represents the region beyond the radar detection range (21 nm) that has not been modelled. Higher returns are illustrated by brighter shades of green.

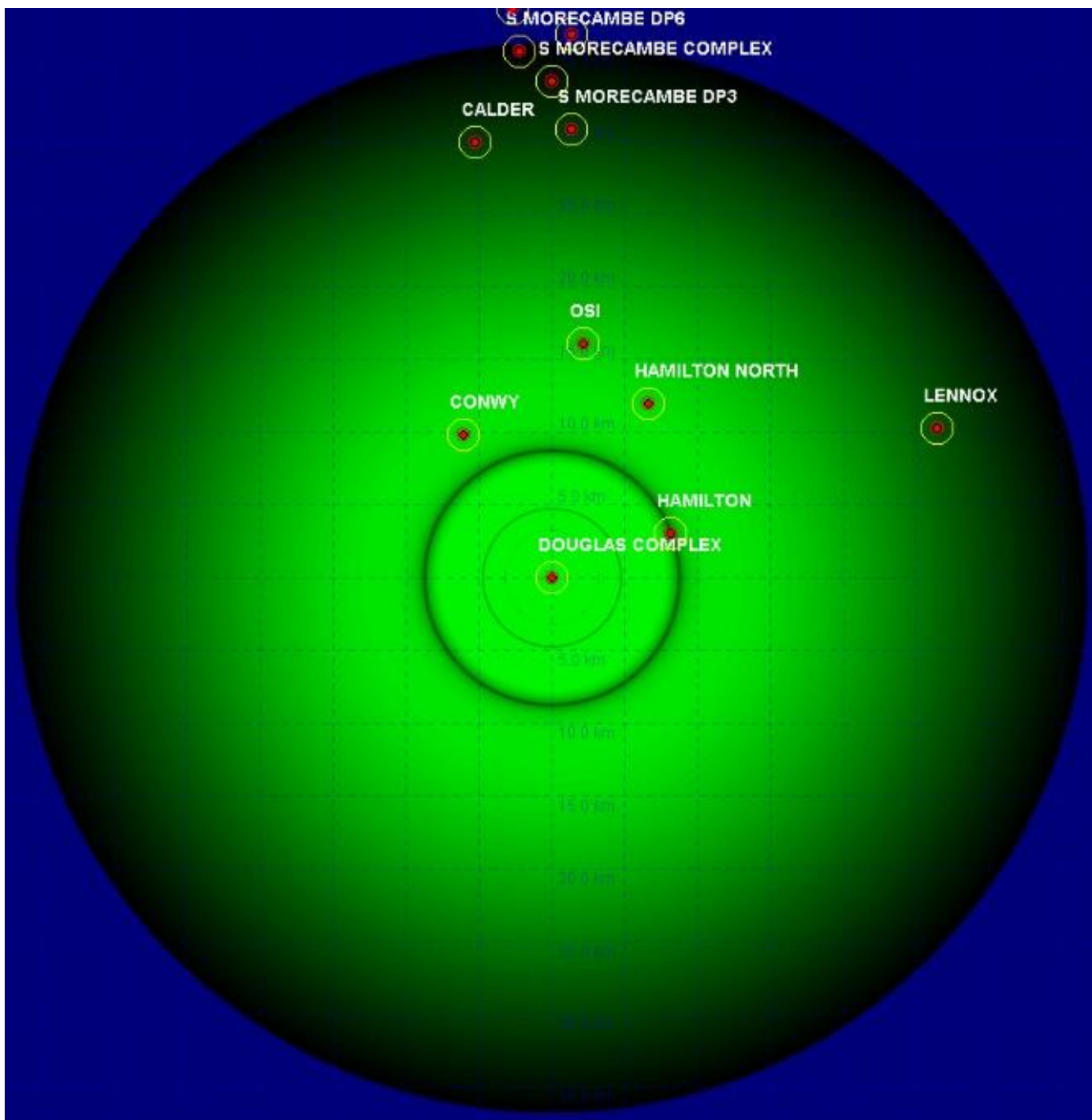


Figure 1.14: Modelled power received from 1000 m² target (coverage).

MONA OFFSHORE WIND PROJECT

- 1.4.2.6 The returns from the vessel are then compared against the CFAR detection threshold shown in Figure 1.2 to establish the detection regions. If the vessel returns are above the CFAR threshold, then the vessel is detected, however, if the returns are below the threshold, the target is assumed to be undetected within that region. Figure 1.15 shows the detection plot for the 1000 m² test vessel. Dark areas within the plot denote regions where the vessels will not be detected. The shadow regions are very narrow and are not visible within the figures due to the scale. The effects of the shadow regions are illustrated in Figure 1.16, which shows the effect of shadowing on the returns from the vessel. The narrow lines illustrate the shadow generated from each wind turbine.
- 1.4.2.7 The results show that at close ranges, the REWS easily detects the test vessel as the returns are above the detection threshold. Once the vessel is travelling within the nearby wind farm, the raised threshold over the cells around each wind turbine can cause loss of detection. This effect, in combination with the shadowing effects, may cause the REWS to lose tracks of the vessels and fail in raising TCPA alarms in a timely manner as stated for the CPA/TCPA alarm requirements.
- 1.4.2.8 The same modelling process was followed for Harbour Energy’s Millom West platform, ENI Energy’s OSI, Spirit Energy’s South Morecambe AP1 platform. The results for the base case on these REWS installations are shown in Figure 1.17 to Figure 1.25.

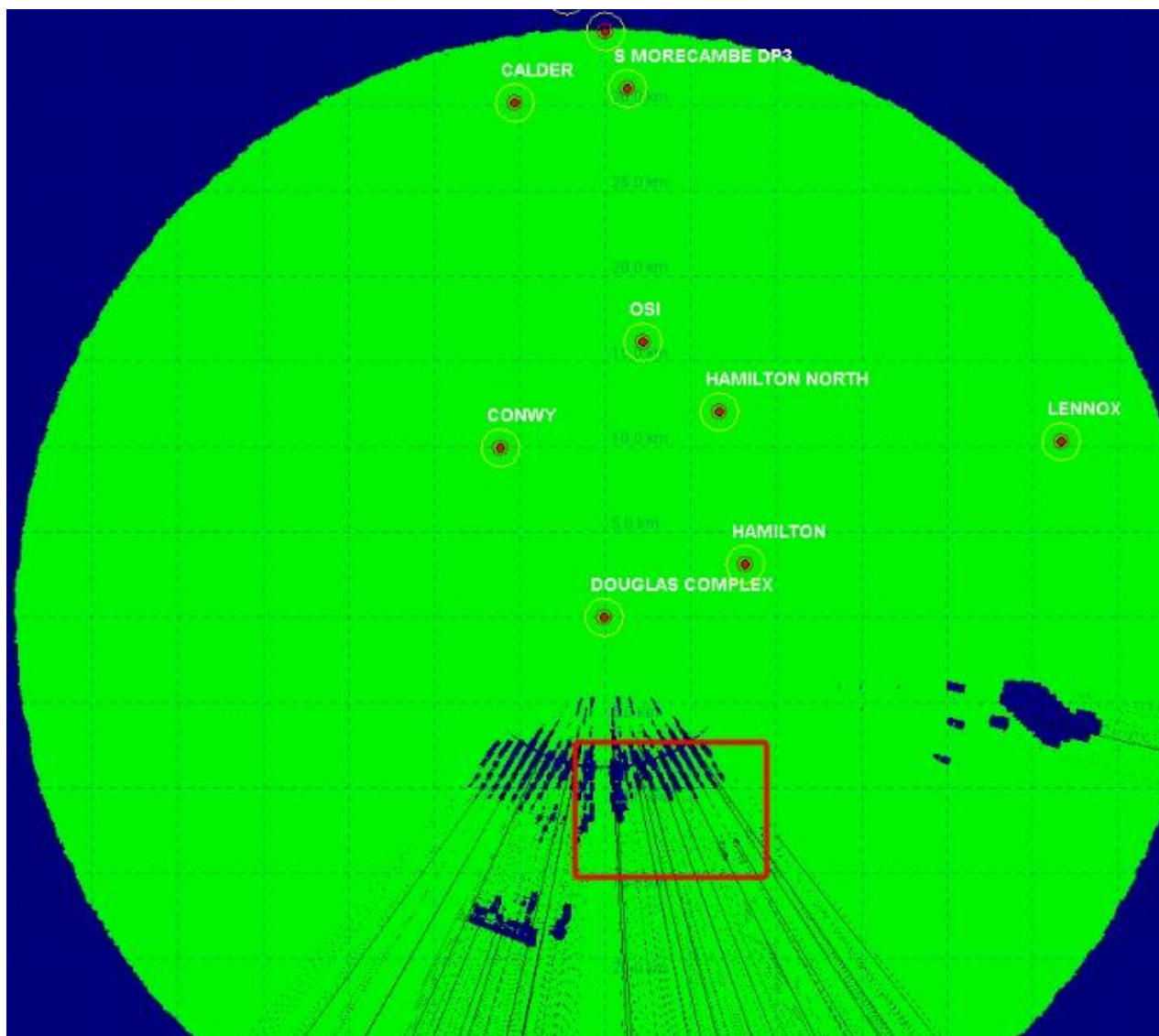


Figure 1.15: ENI Energy’s Douglas platform REWS detection plot showing loss regions for a 1000 m² target.

MONA OFFSHORE WIND PROJECT

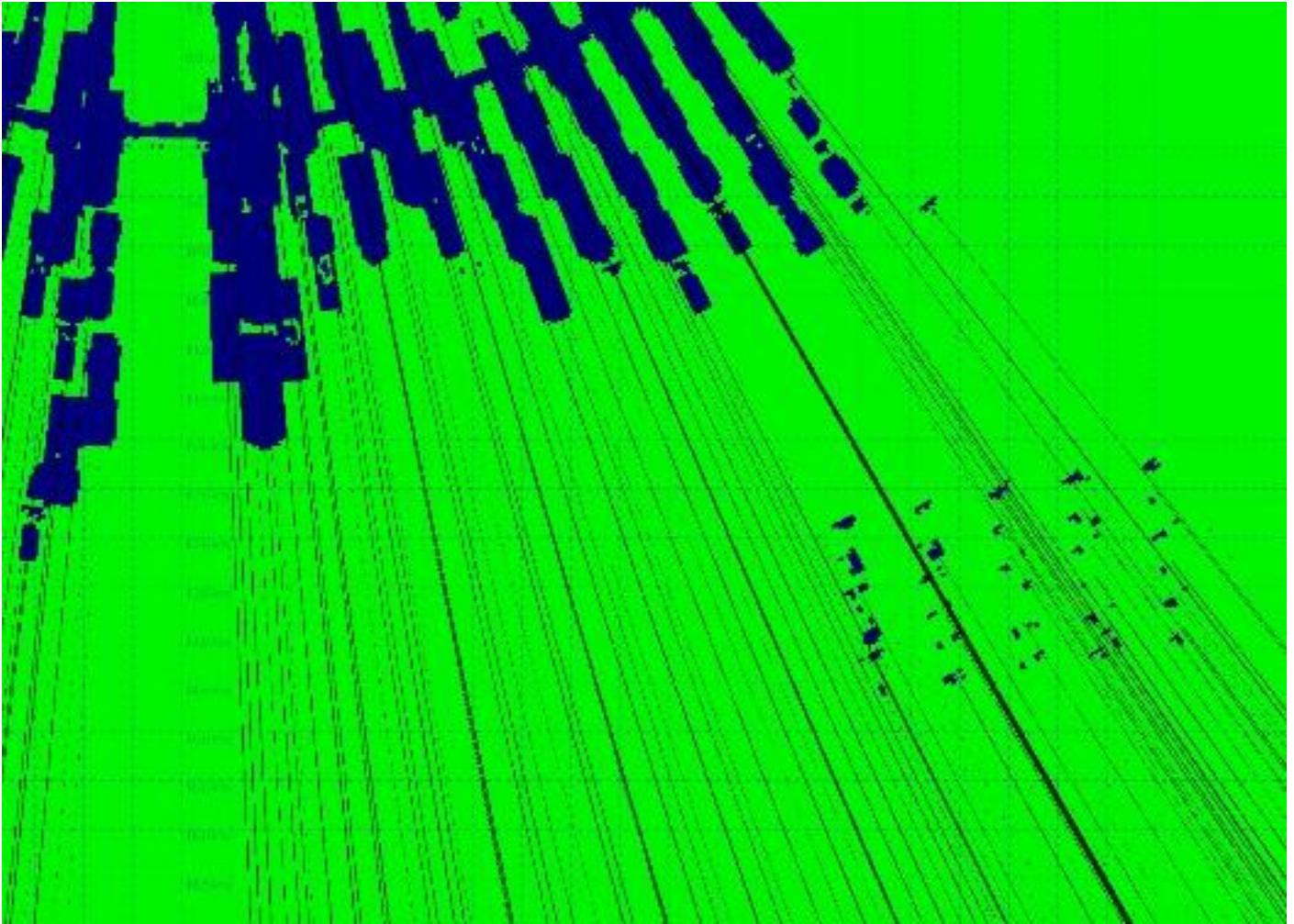


Figure 1.16: Enlarged portion of the detection plot showing the effect of wind turbine shadowing.

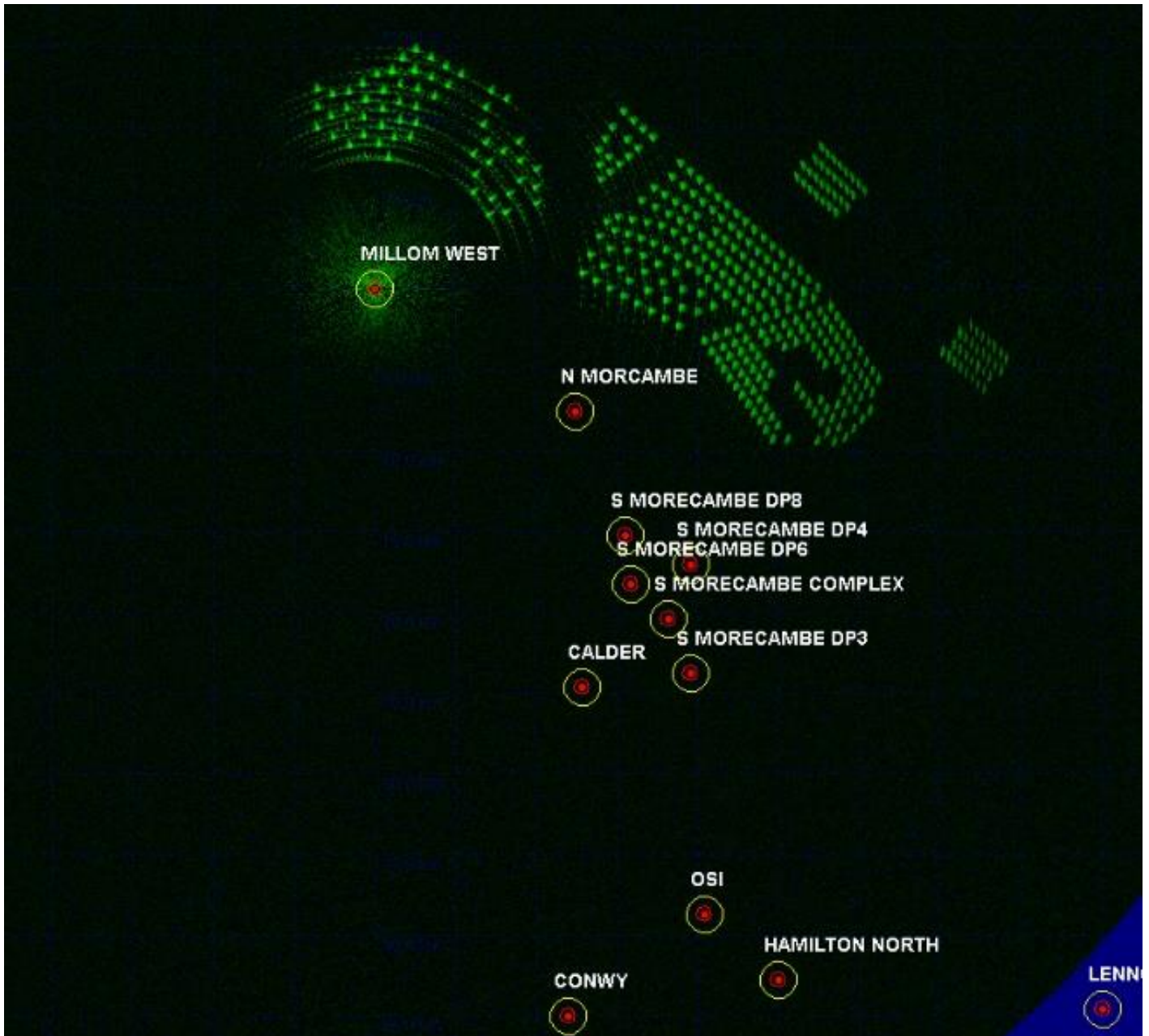


Figure 1.17: Harbour Energy's Millom West platform REWS clutter map showing returns from the wind turbines and sea clutter.

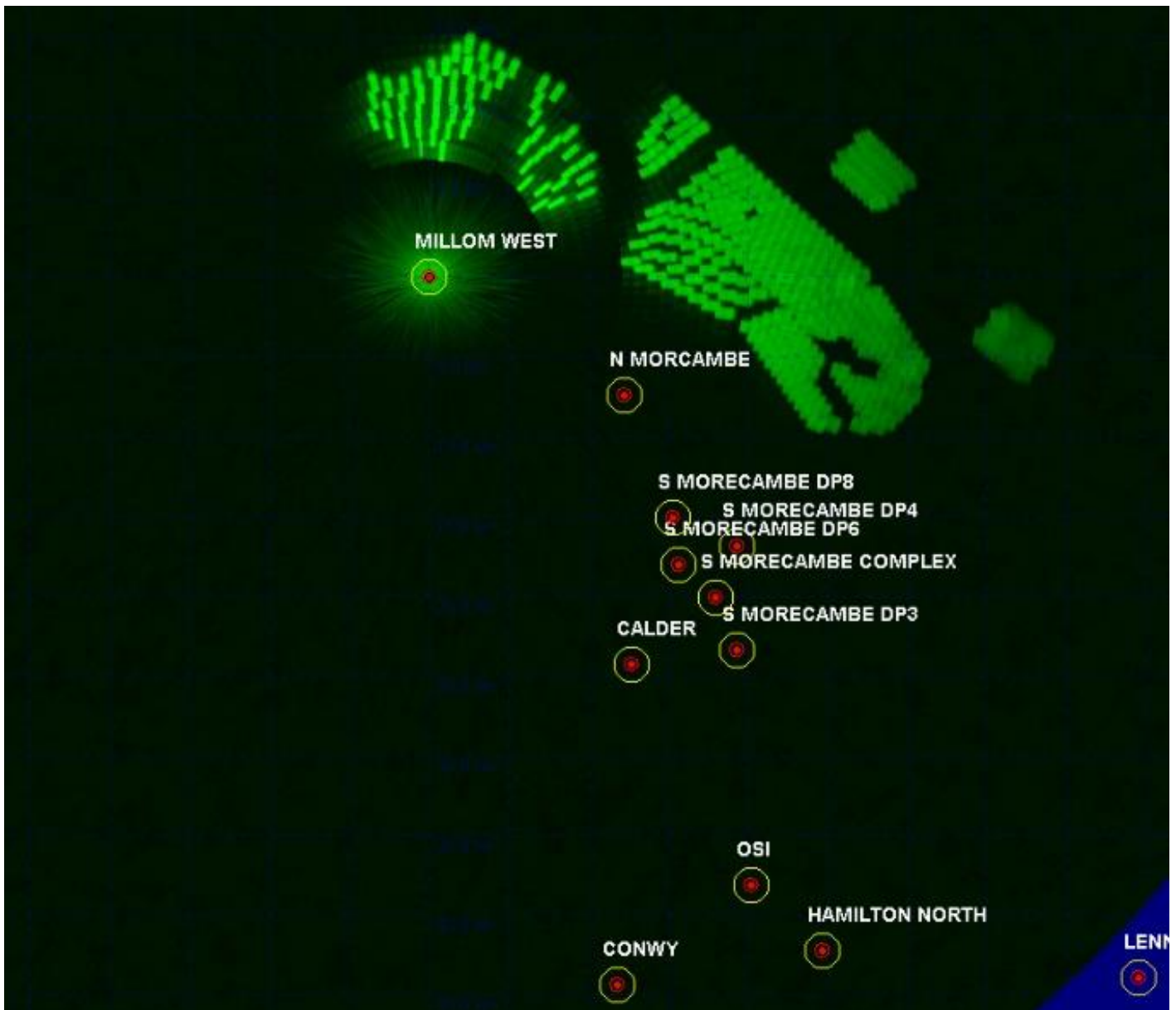


Figure 1.18: Harbour Energy's Millom West platform REWS detection threshold.

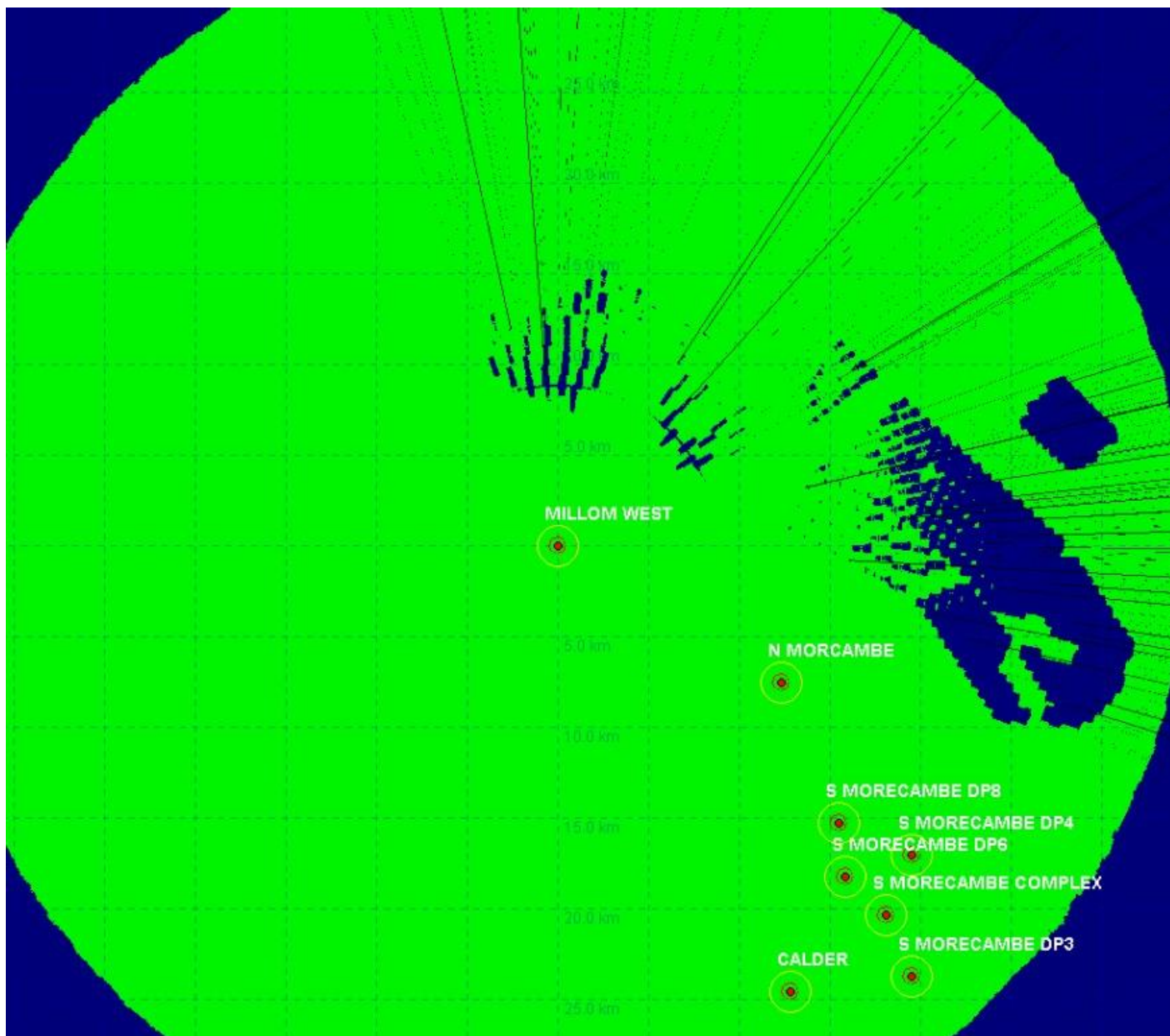


Figure 1.19: Harbour Energy’s Millom West platform REWS detection plot showing loss regions for a 1000 m² target.

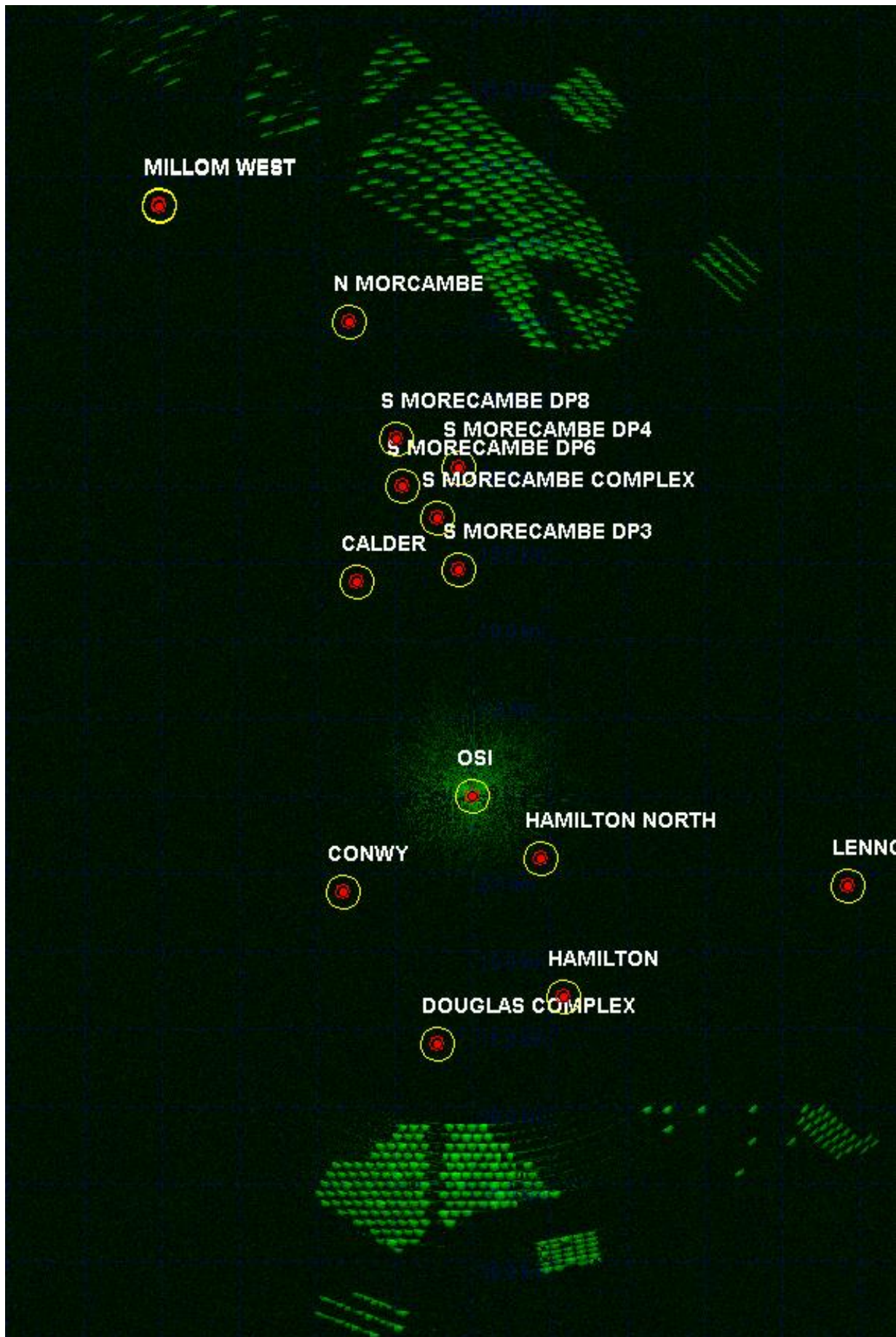


Figure 1.20: ENI Energy's OSI REWS clutter map showing returns from the wind turbines and sea clutter.

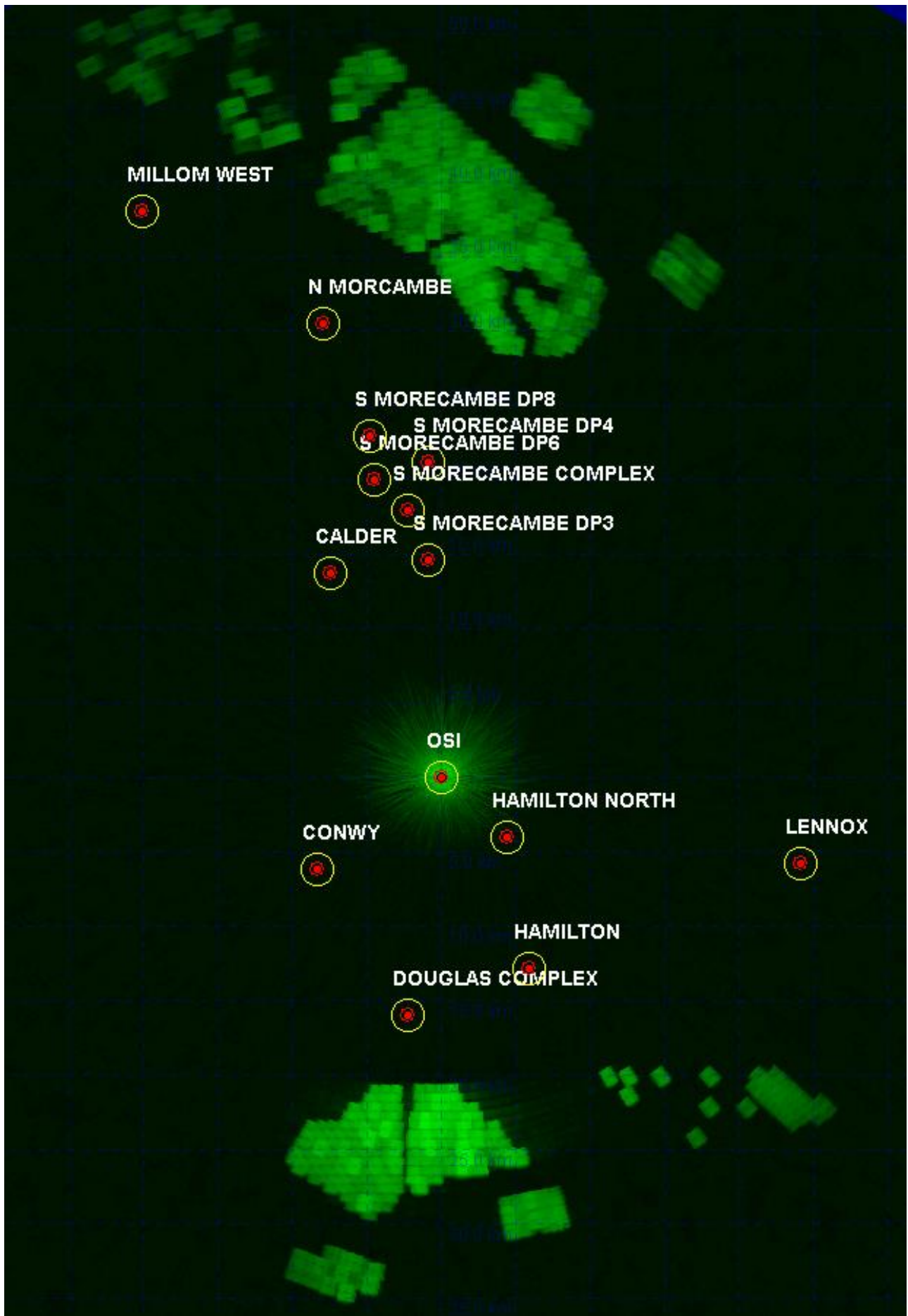


Figure 1.21: ENI Energy's OSI REWS detection threshold.

MONA OFFSHORE WIND PROJECT

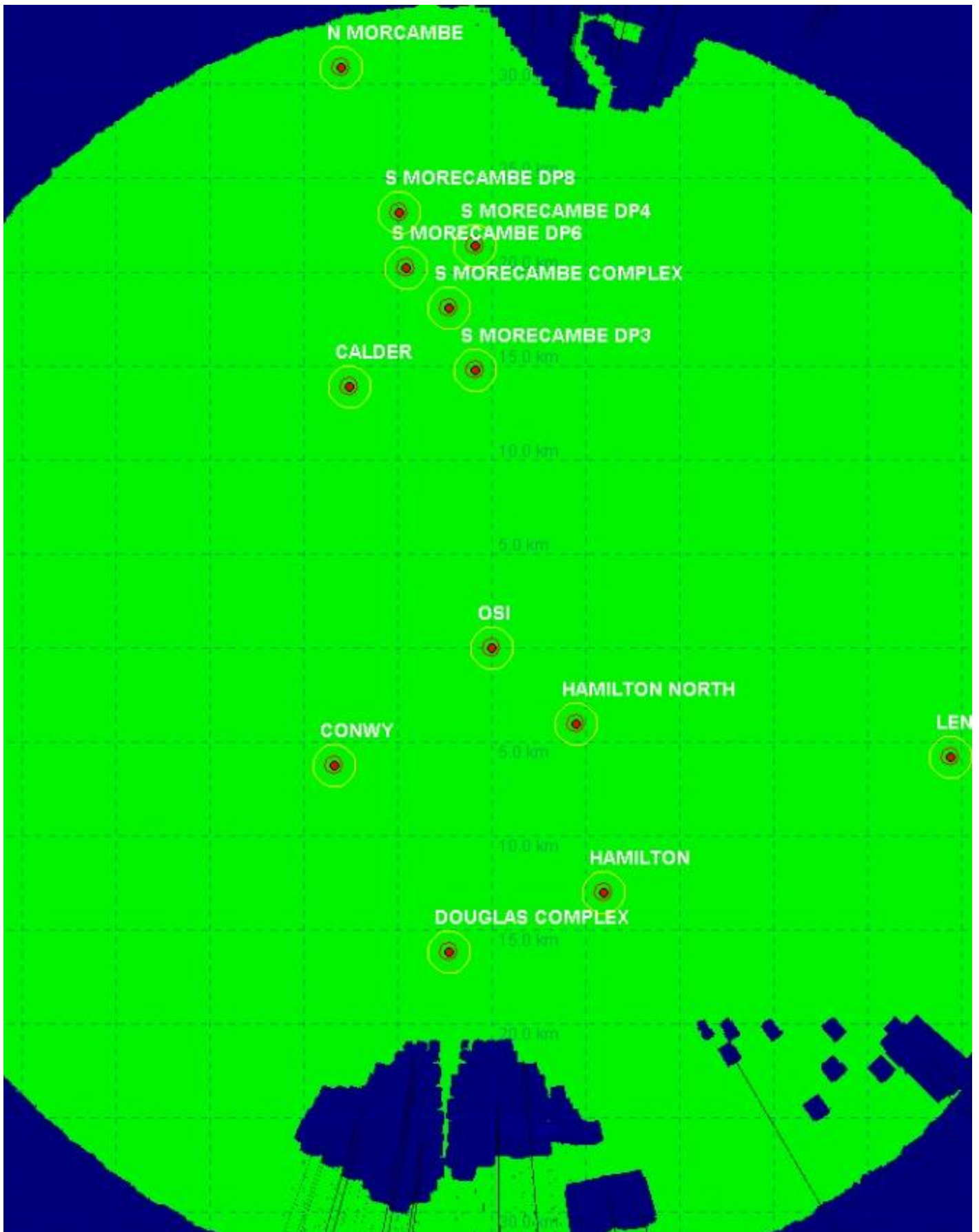


Figure 1.22: ENI Energy's OSI REWS detection plot showing loss regions for a 1000 m² target.

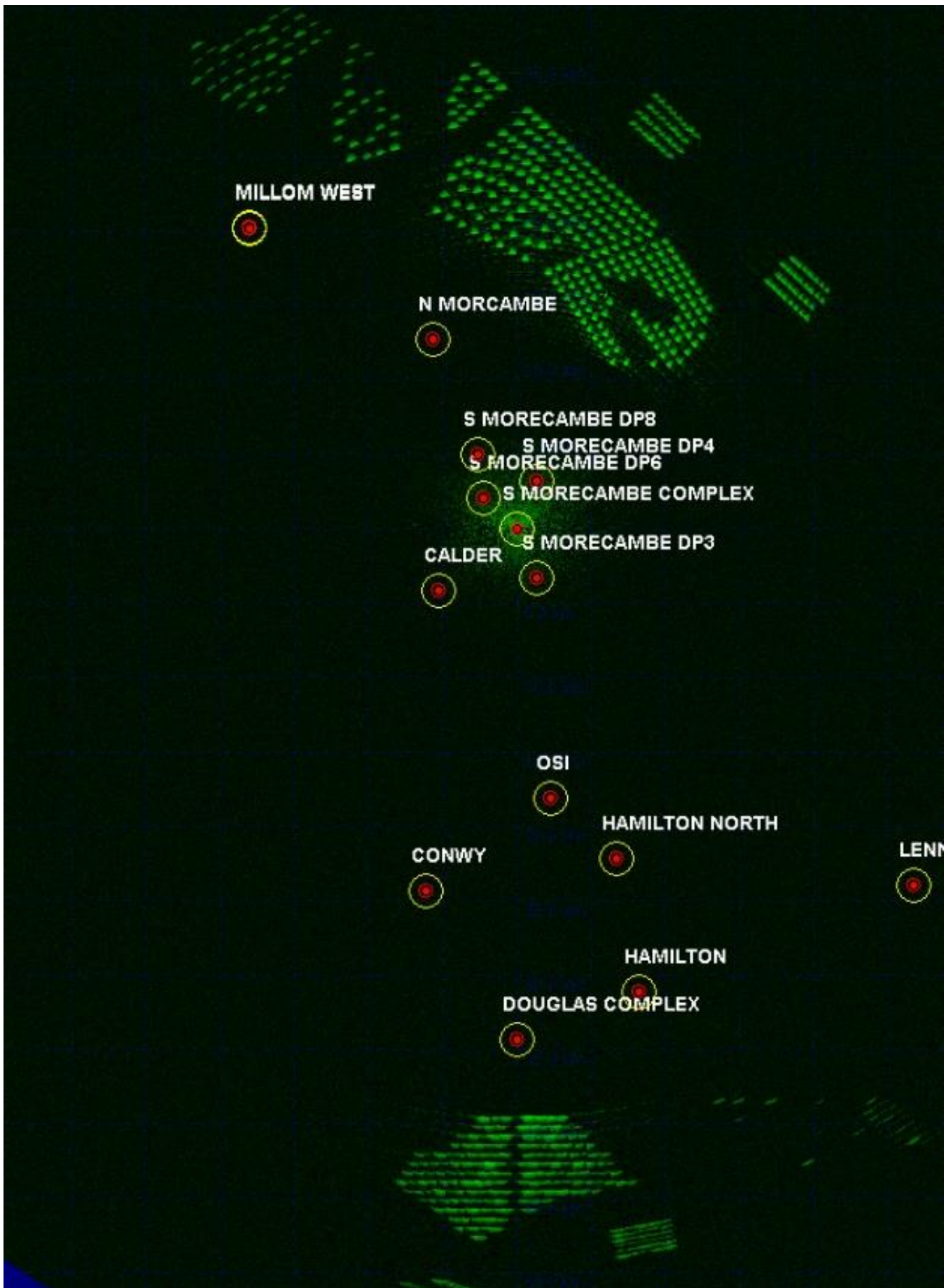


Figure 1.23: Spirit Energy’s South Morecambe AP1 platform REWS clutter map showing returns from the wind turbines and sea clutter.



Figure 1.24: Spirit Energy's South Morecambe AP1 platform REWS detection threshold.

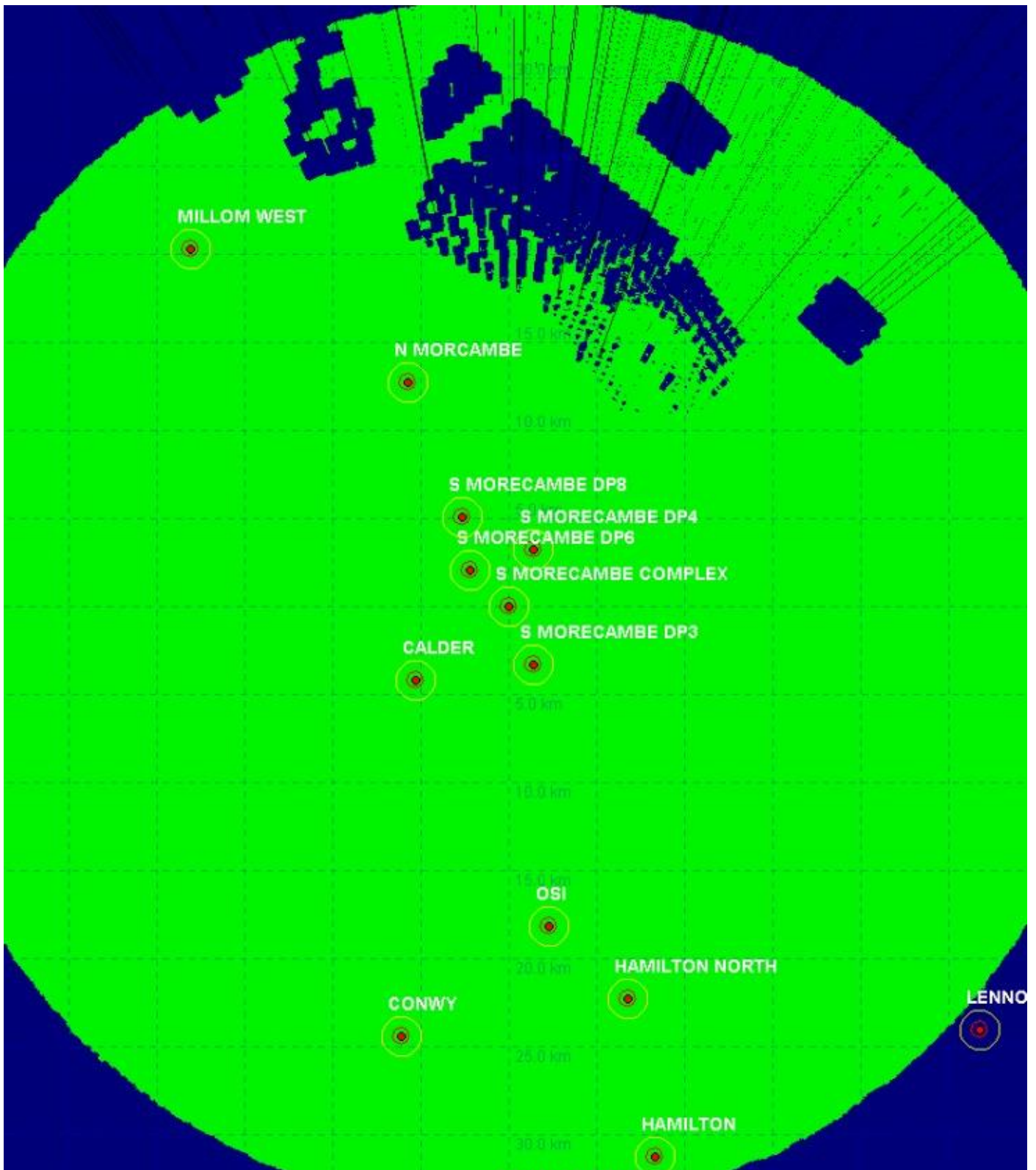


Figure 1.25: Spirit Energy's South Morecambe AP1 platform REWS detection plot showing loss regions for a 1000 m² target.

1.4.2.9

The overall results show that the REWS can easily detect the test vessel as the returns are above the detection threshold over majority of the coverage region. However, once a vessel is travelling within a wind farm, the raised threshold over the cells around each wind turbine can cause loss of detection. This can be seen in all the assessed platforms with line-of-sight coverage to nearby wind farms. In some cases, such as

MONA OFFSHORE WIND PROJECT

Sprit Energy's South Morecambe AP1 REWS, the effects on the detection region are more pronounced due to its proximity to the Walney Phase 1, Walney Phase 2 and West of Duddon Sands wind farms, which has relatively small separation distances between its turbines.

Assessment of the Mona Offshore Wind Project

1.4.2.10 In a similar manner as the base case modelling, the potential impact of the Mona Offshore Wind Project on the REWS is assessed. The modelled layout is shown in Figure 1.26 while the REWS returns, expected threshold levels and the detection regions are illustrated in Figure 1.27 to Figure 1.38.

MONA OFFSHORE WIND PROJECT

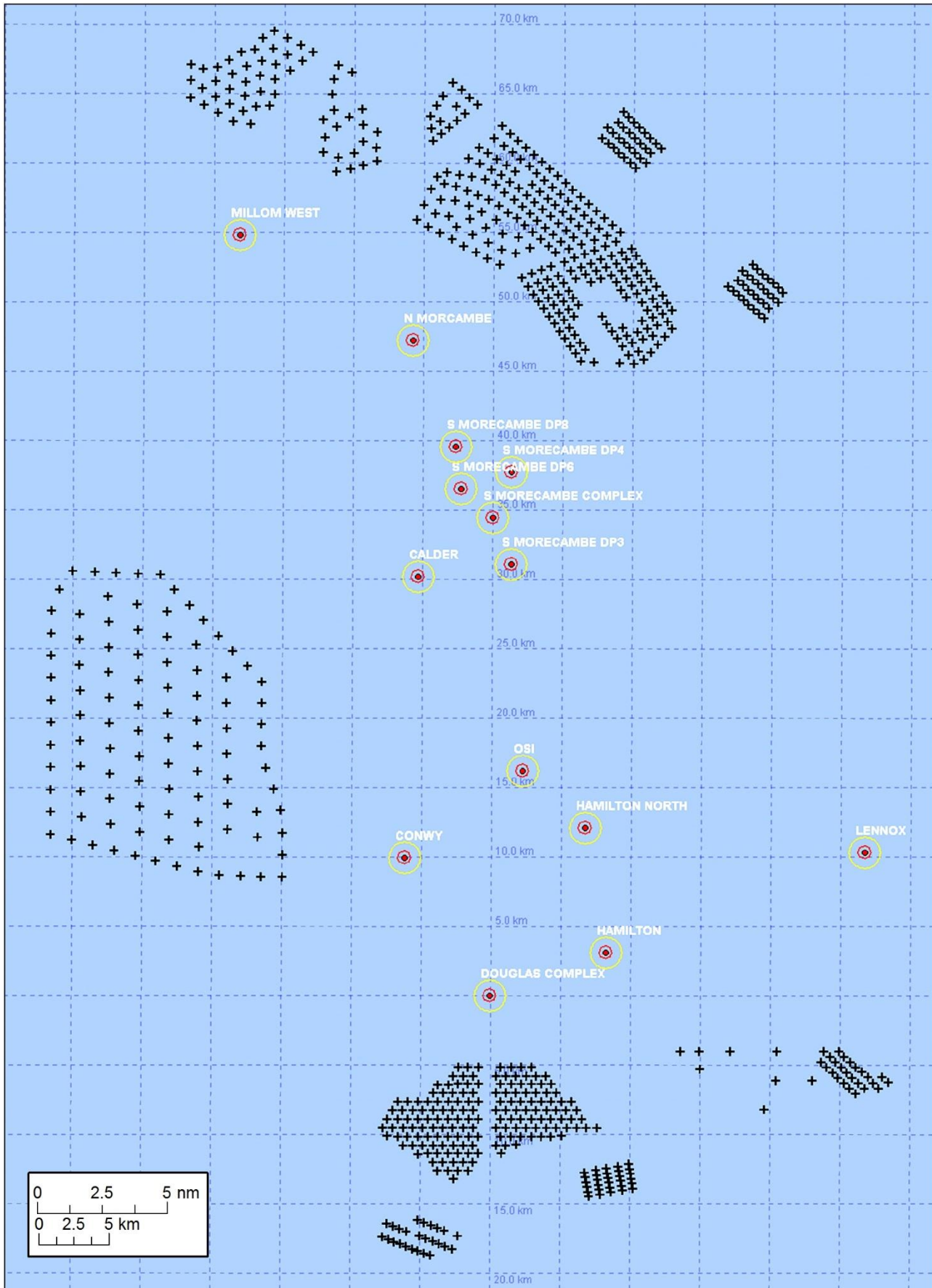


Figure 1.26: Modelled layout of the Mona Offshore Wind Project showing the indicative location of the wind turbines and the location of oil and gas platforms in the region.

MONA OFFSHORE WIND PROJECT

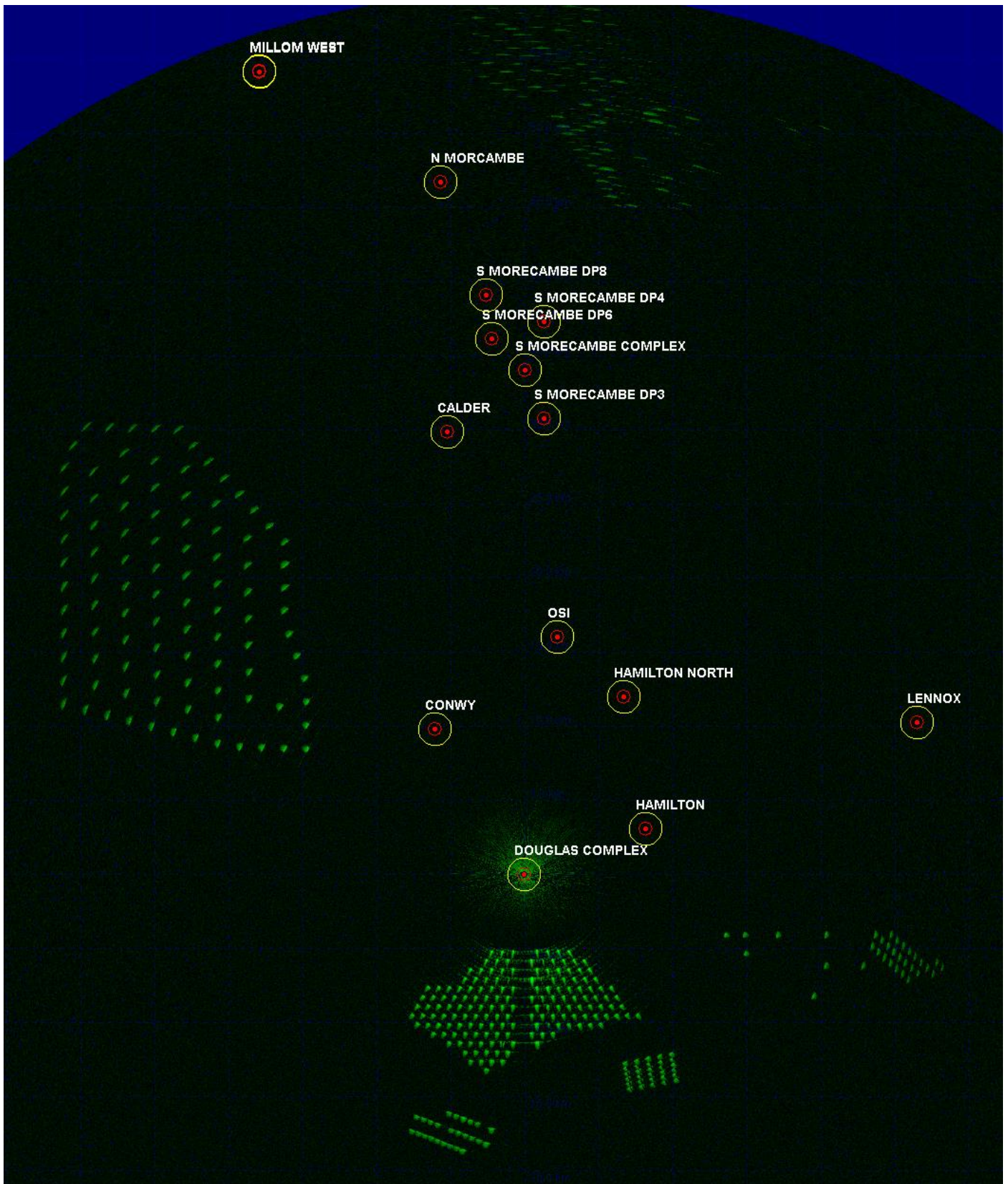


Figure 1.27: ENI Energy's Douglas platform REWS clutter map showing returns from the Mona wind turbines and sea clutter.

MONA OFFSHORE WIND PROJECT

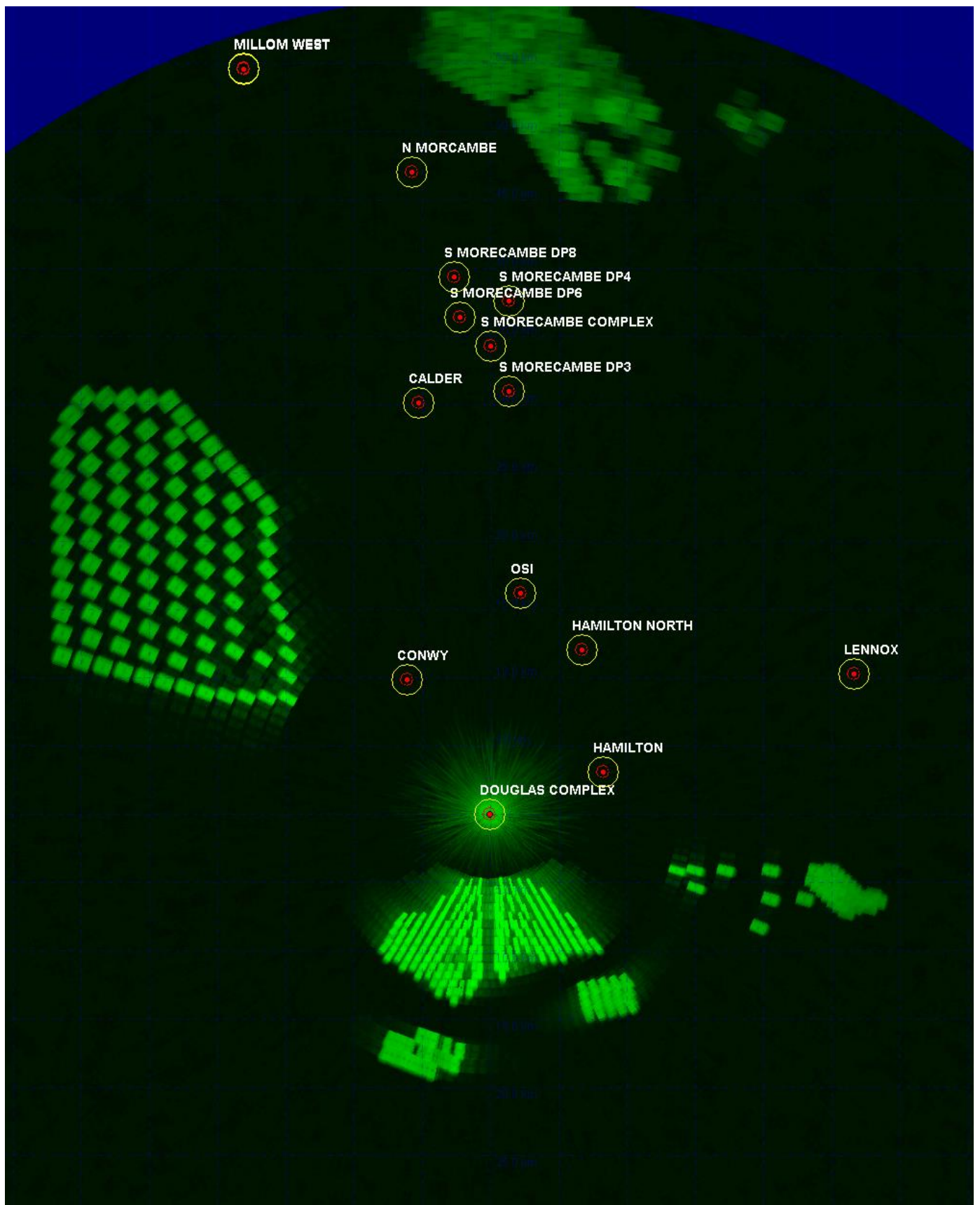


Figure 1.28: ENI Energy's Douglas platform REWS detection threshold over the Mona Array Area.

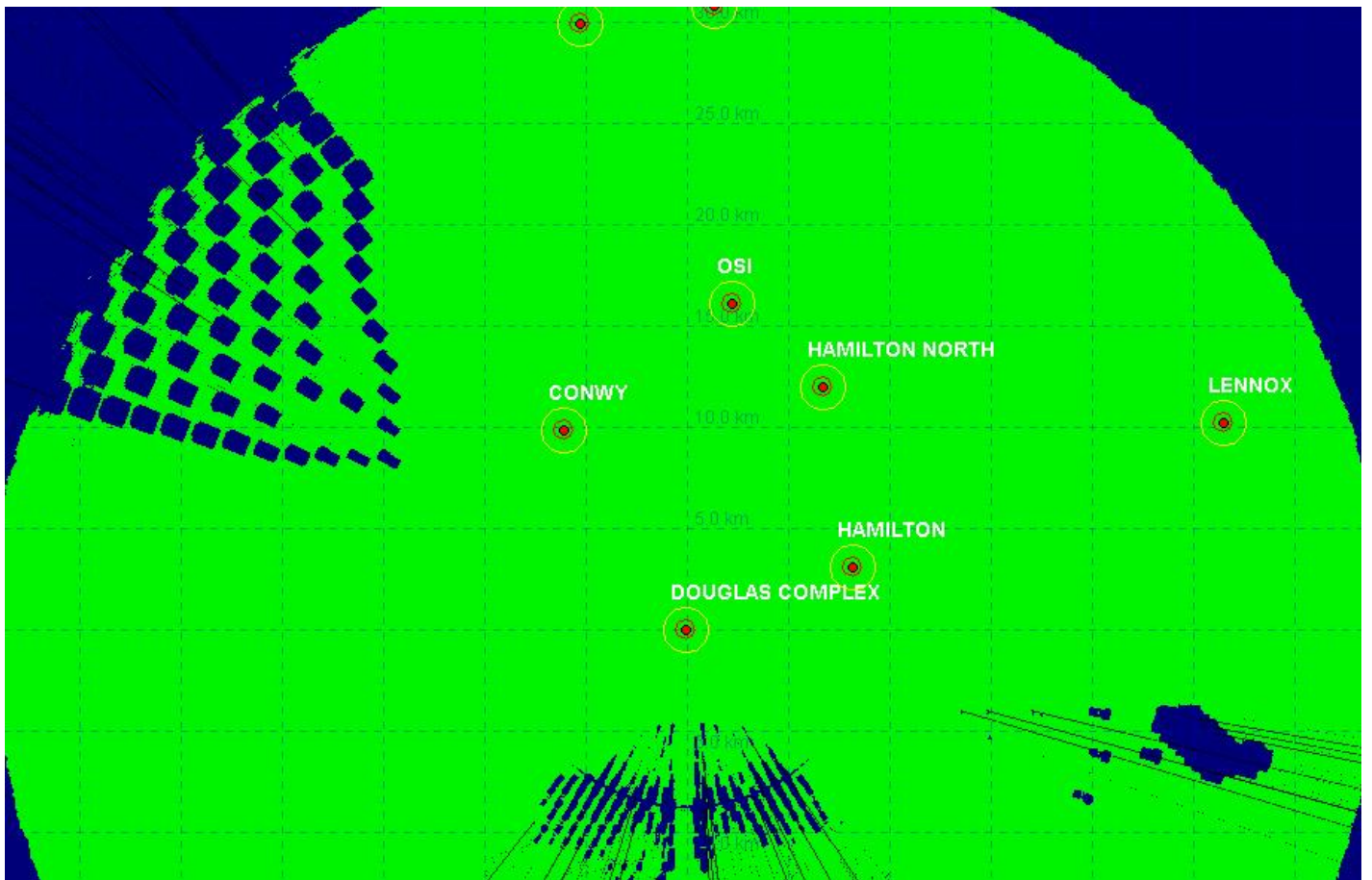


Figure 1.29: ENI Energy's Douglas platform REWS detection plot showing loss regions for a 1000 m² target.

MONA OFFSHORE WIND PROJECT

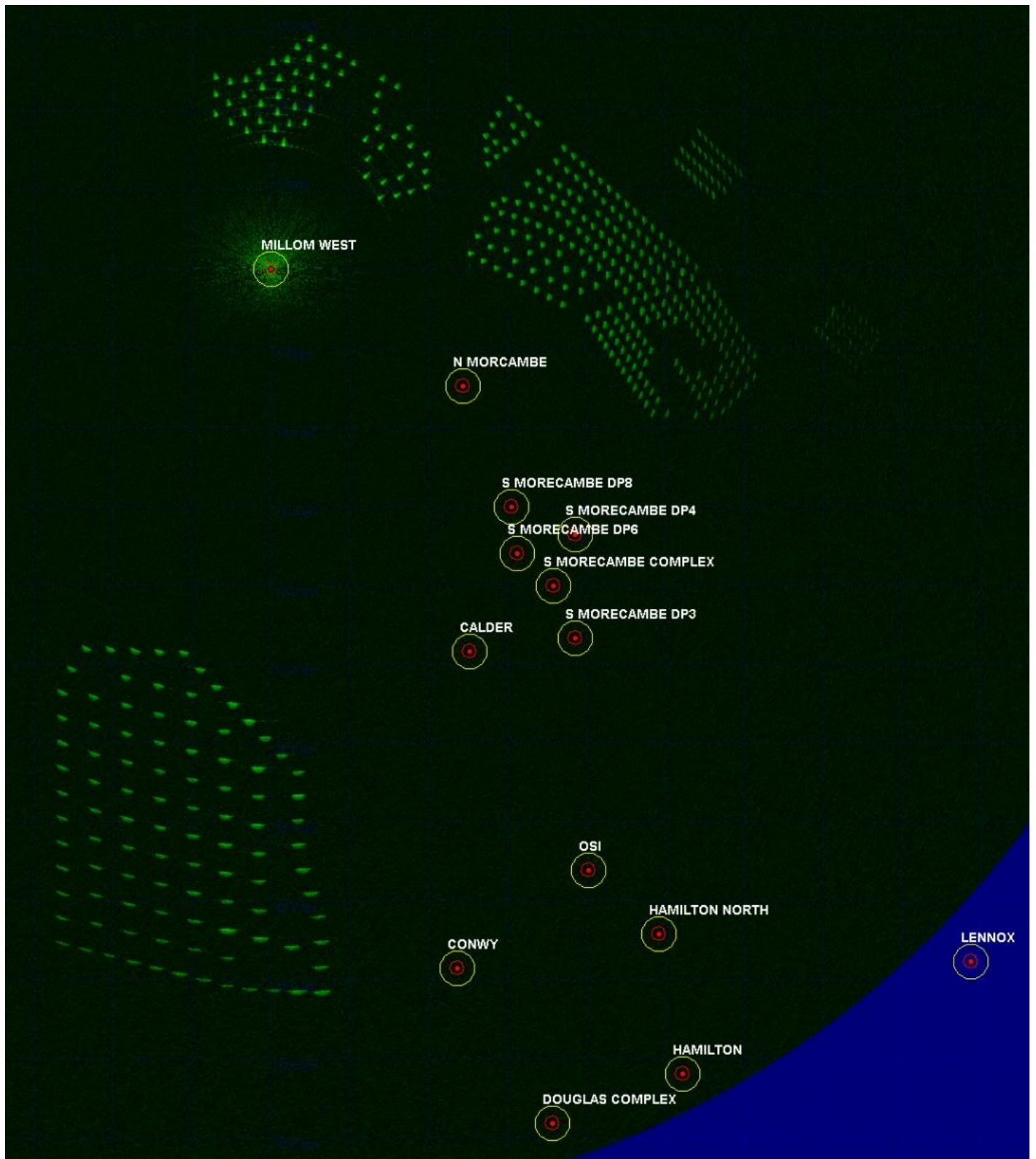


Figure 1.30: Harbour Energy’s Millom West platform REWS clutter map showing returns from the Mona wind turbines and sea clutter.

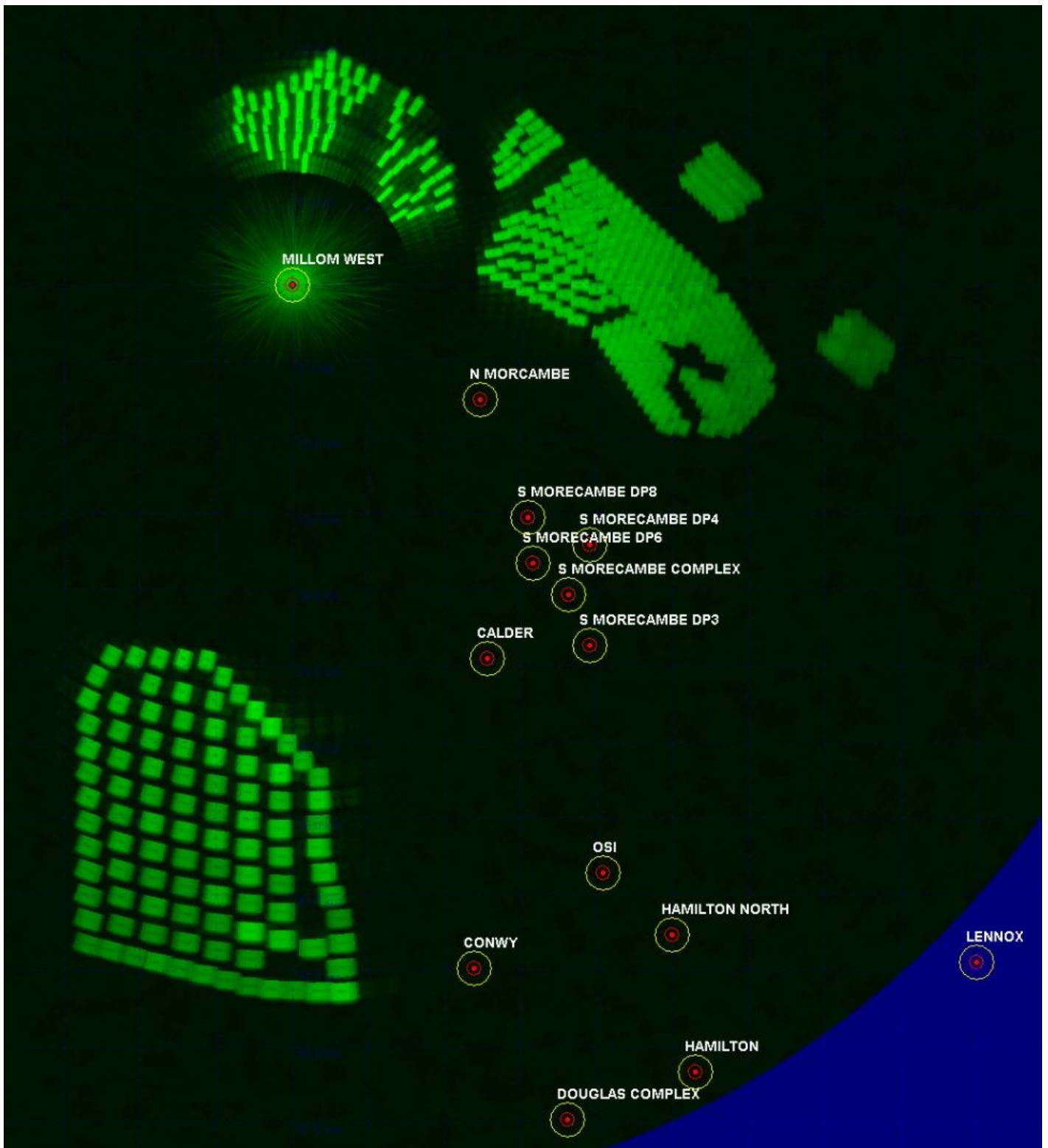


Figure 1.31: Harbour Energy’s Millom West platform REWS detection threshold over the Mona Array Area.

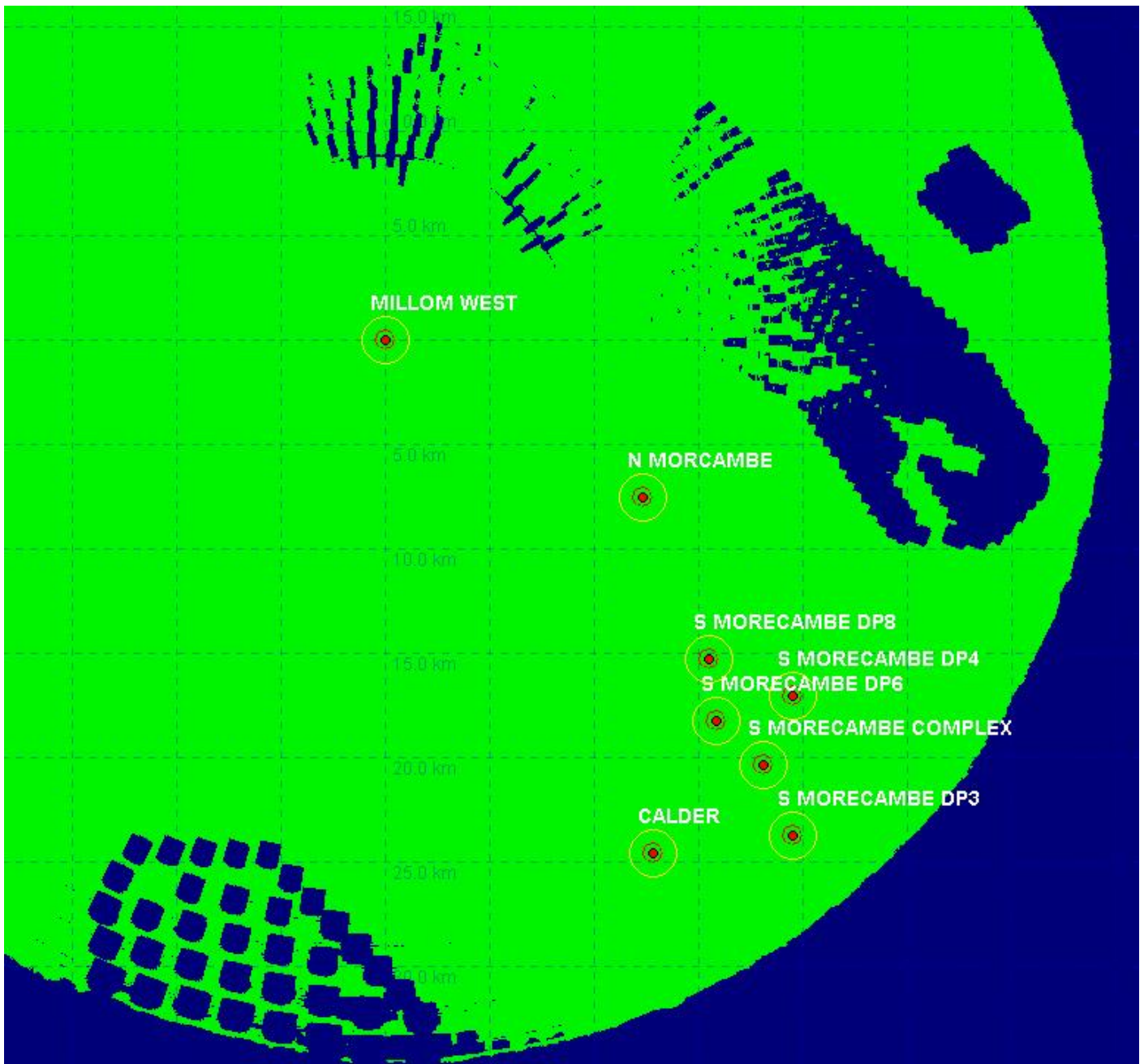


Figure 1.32: Harbour Energy’s Millom West platform REWS detection plot showing loss regions for a 1000 m² target.

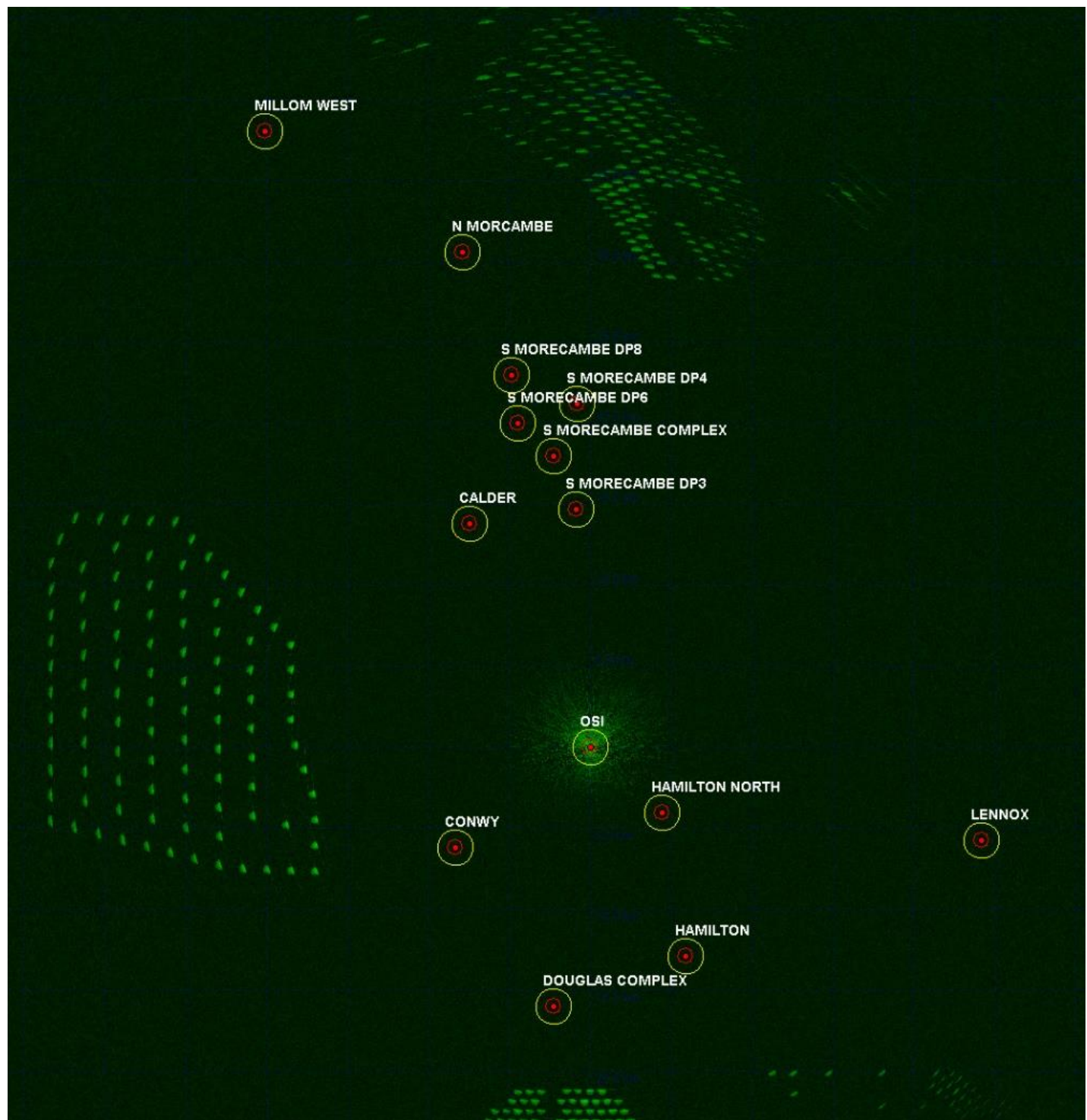


Figure 1.33: ENI Energy's OSI REWS detection clutter map showing returns from the Mona wind turbines and sea clutter.

MONA OFFSHORE WIND PROJECT

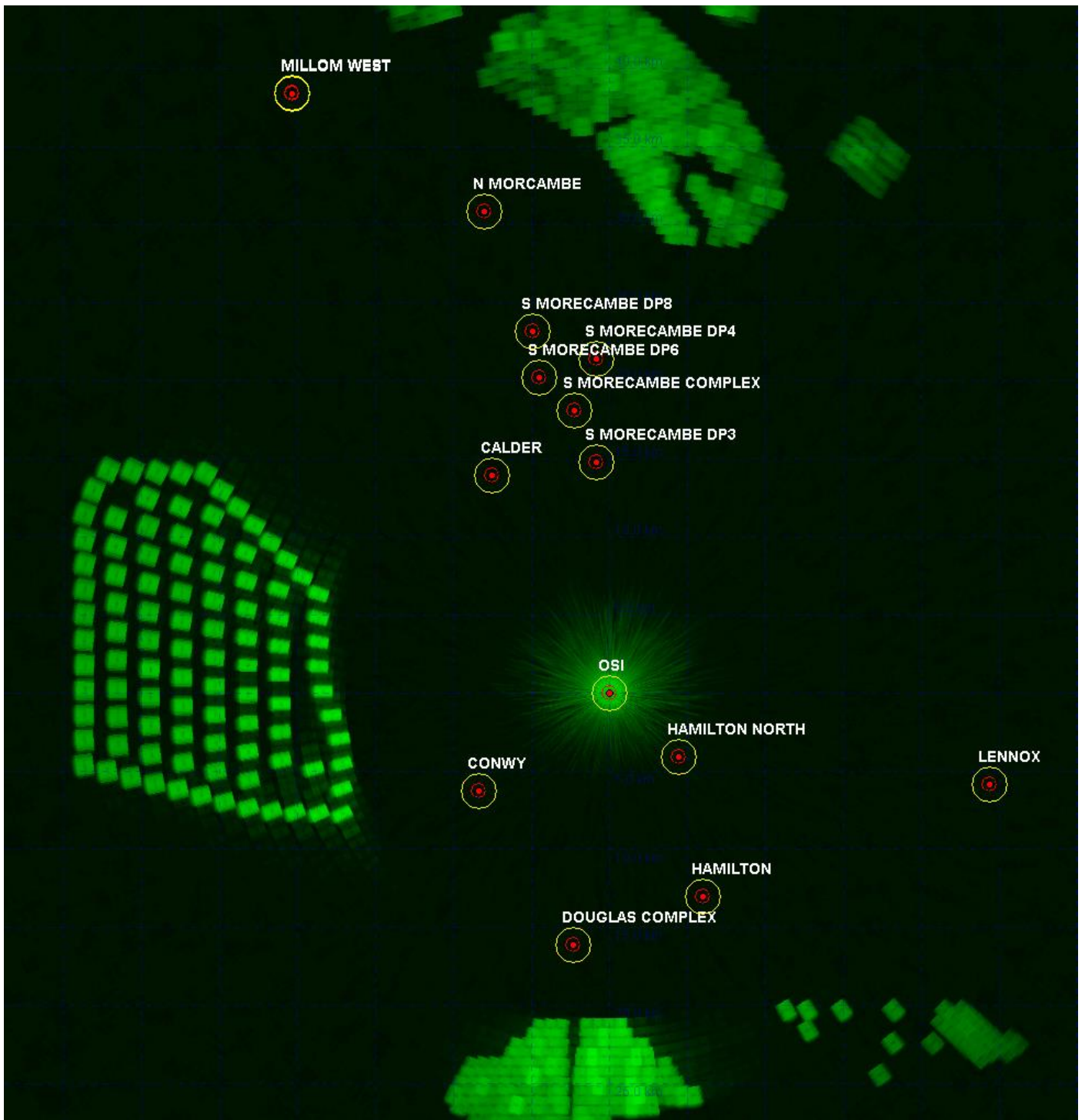


Figure 1.34: ENI Energy’s OSI REWS detection threshold over the Mona Array Area.

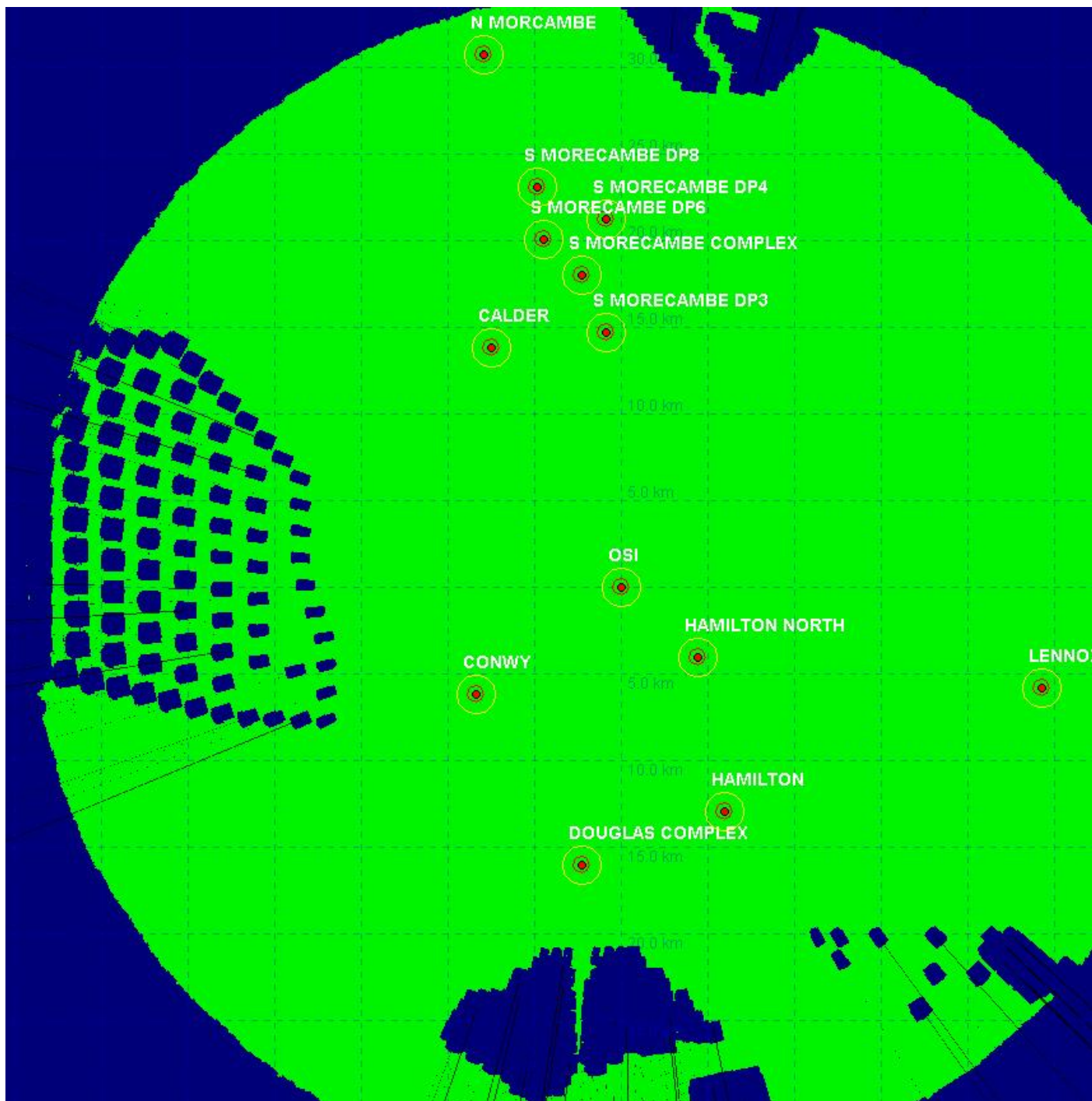


Figure 1.35: ENI Energy's OSI REWS detection plot showing loss regions for a 1000 m² target.

MONA OFFSHORE WIND PROJECT

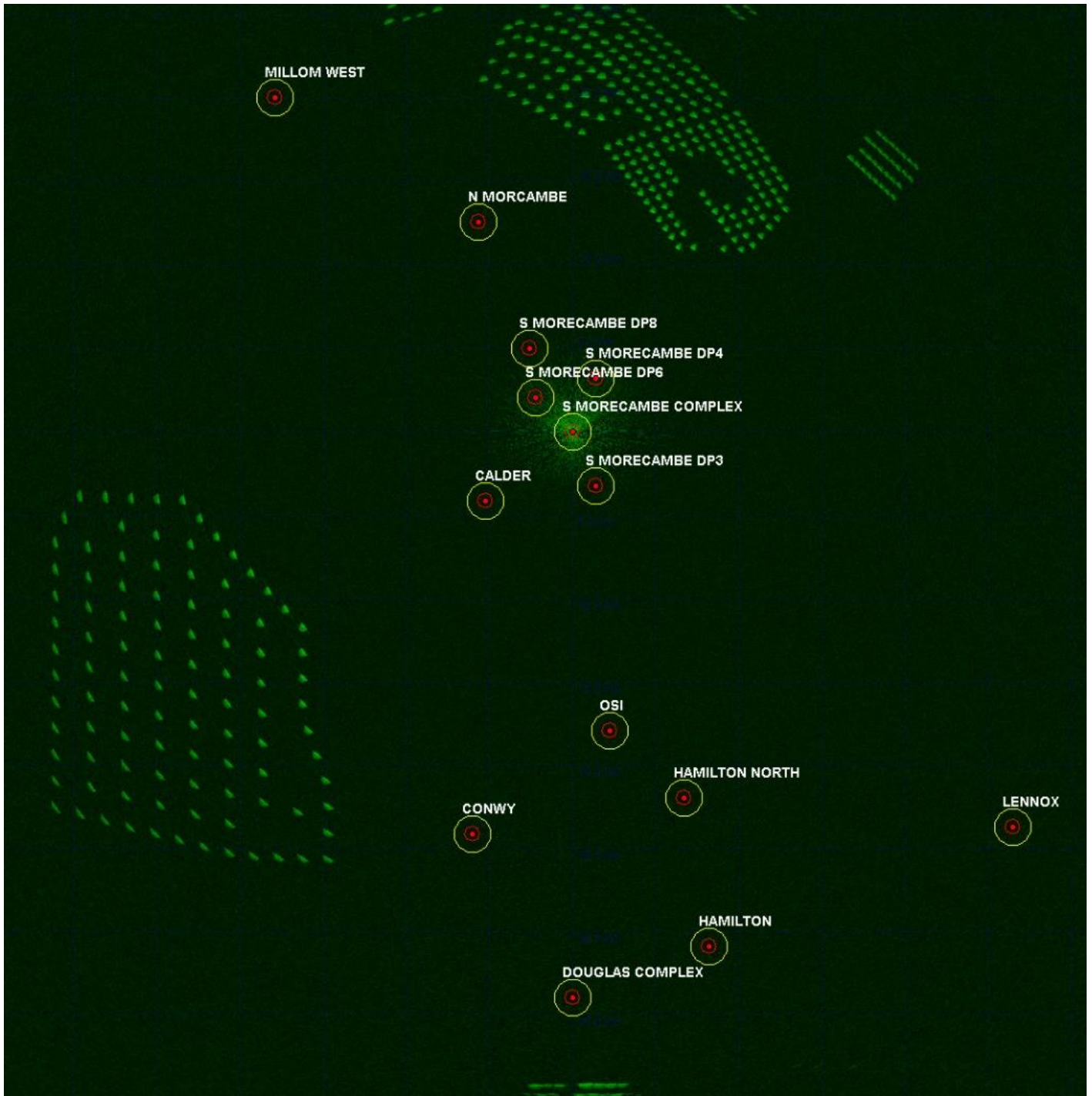


Figure 1.36: Spirit Energy’s South Morecambe AP1 platform REWS clutter map showing returns from the Mona wind turbines and sea clutter.

MONA OFFSHORE WIND PROJECT

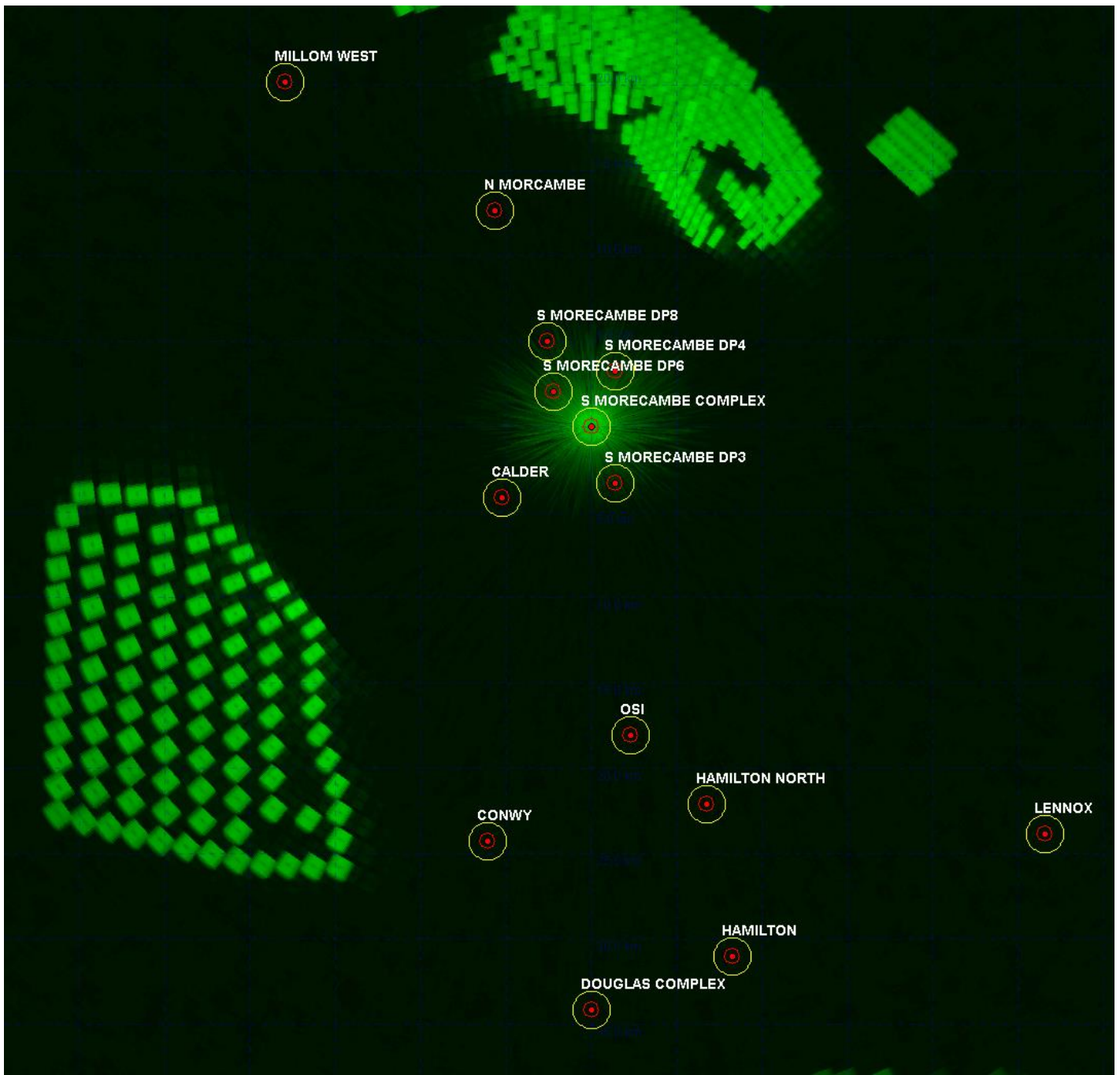


Figure 1.37: Spirit Energy's South Morecambe AP1 platform REWS detection threshold over the Mona Array Area.

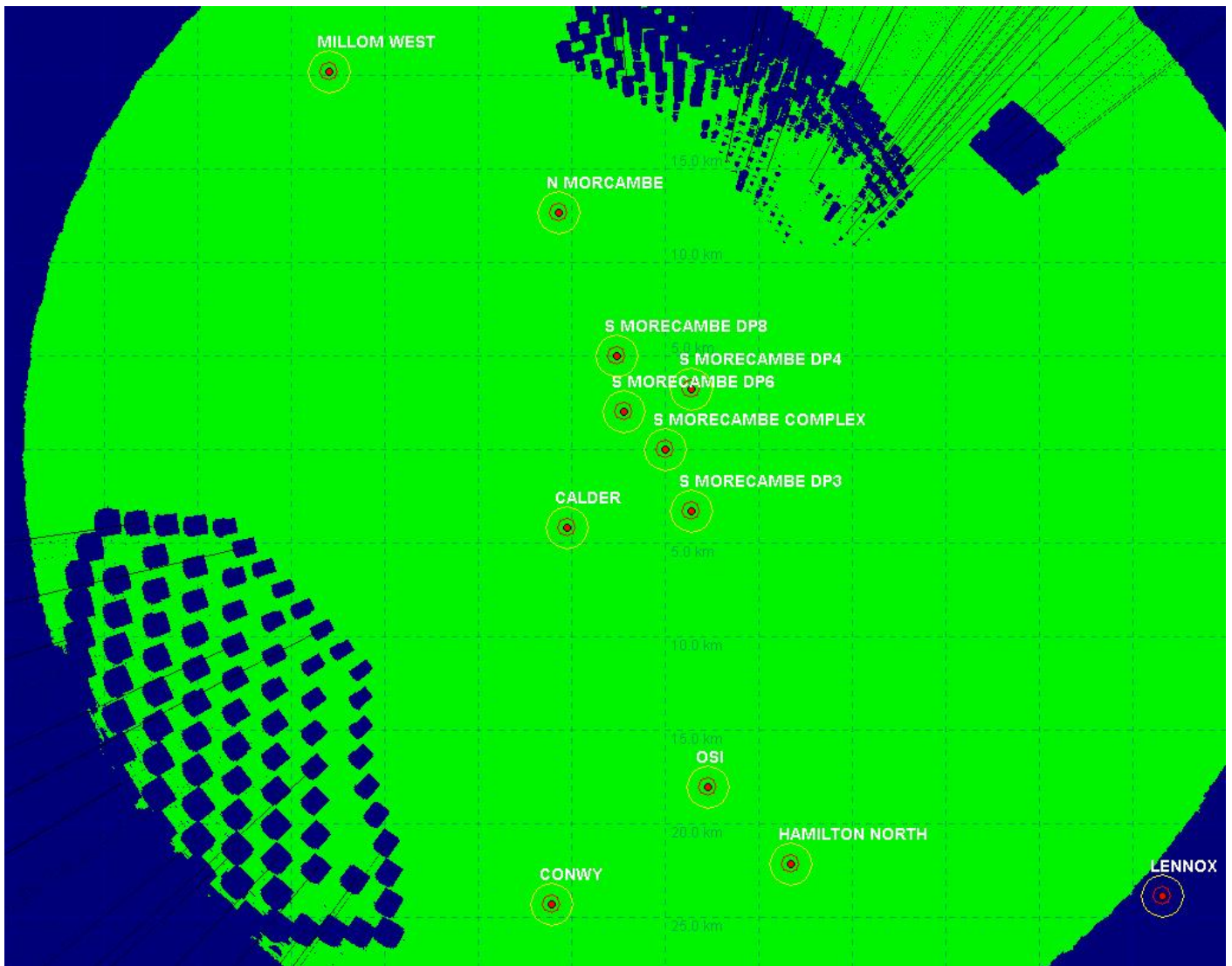


Figure 1.38: Spirit Energy’s South Morecambe AP1 platform REWS detection plot showing loss regions for a 1000 m² target.

MONA OFFSHORE WIND PROJECT

1.4.2.11 As shown in the base case modelling, the results indicate that the raw, single scan detection performance of the REWS due to the presence of the Mona Offshore Wind Project is affected adversely within the wind farm regions. Radar detection of vessels travelling within the Mona Offshore Wind Project may be lost temporarily as they move close to the modelled turbines located within the radar range. The loss of detection is mainly caused by the elevated threshold levels due to the presence of the wind turbines while a small number of losses are expected to occur due to shadowing. However, typically, in terms of tracking vessels within the wind farm, the tracker software is expected to compensate for most of the detection losses of the vessels. Additionally, the integration of AIS data with the REWS will provide an alternative source of vessel information and location which can complement the data when temporary radar losses are experienced. Therefore, the impact of the Mona Offshore Wind Project in isolation on nearby REWS installation is expected to be relatively low and manageable without the need for mitigation measures.

1.4.3 Cumulative assessment

1.4.3.1 The Mona Offshore Wind Project REWS assessment area covers a number of existing wind farms along with wind farms that are at various stages in their planning and consent process. The wind farms that are within the study area are shown in Figure 1.39.

MONA OFFSHORE WIND PROJECT

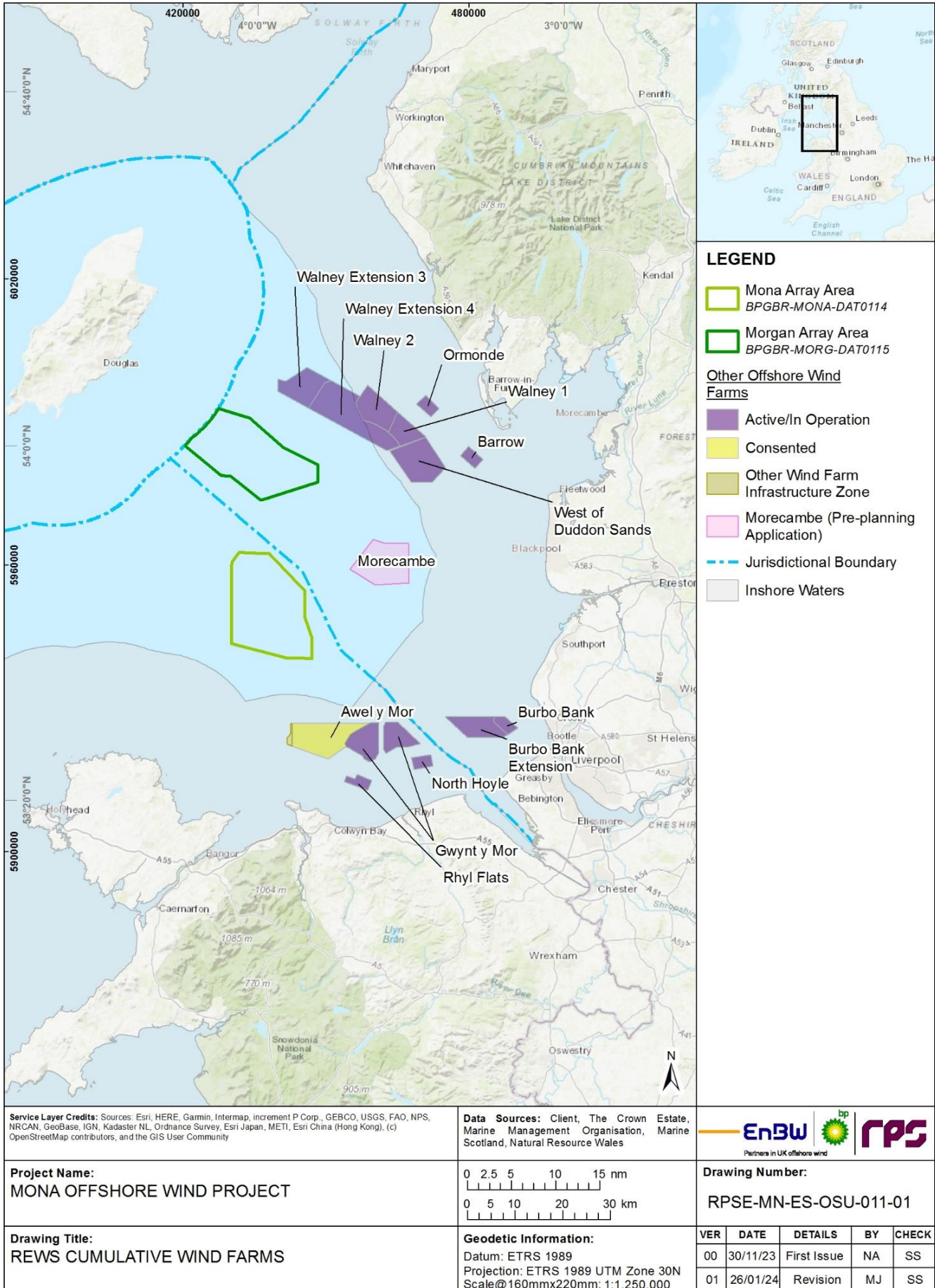


Figure 1.39: REWS cumulative wind farms.

MONA OFFSHORE WIND PROJECT

1.4.3.2 At the time of conducting the REWS assessment, the locations and layout of the turbines within the Morecambe Offshore Windfarm: Generation Assets (hereafter referred to as Morecambe Generation Assets) and the Awel y Mor Offshore Wind Farm were unavailable to the Applicant. Therefore, their potential impact in the cumulative assessment was not included in this report.

1.4.3.3 It was noted that the Awel y Mor Wind Farm is sufficiently far from the REWS installations and the Mona Offshore Wind Project and it is therefore not expected to add to the impact on the REWS. However, the impact of the Morecambe Generation Assets might be more complex due to its location and proximity to the Mona Offshore Wind Project and the REWS installations in the region. Nevertheless, the impact of the Morecambe Generation Assets and the Awel y Mor Offshore Wind Farm were not included in the study due to the lack of data. Hence, this report will present the modelling results of the combined impact on the REWS from Mona Offshore Wind Project in combination with Morgan Generation assets.

Cumulative REWS assessment of Mona Offshore Wind Project with Morgan Offshore Wind Project: Generation Assets

1.4.3.4 The location and layout of turbines within the Morgan Offshore Wind Project: Generation Assets (hereafter referred to as the Morgan Generation Assets) was available and hence was included in the cumulative assessment. Therefore, the next step in the REWS assessment is to model the impact of the Mona Offshore Wind Project and the Morgan Generation Assets cumulatively with the existing wind farms. This was done in a similar manner to the process shown in previous sections. The modelled layout is shown in Figure 1.40 while the REWS returns, expected threshold levels and the detection regions are illustrated in Figure 1.41 to Figure 1.52.

MONA OFFSHORE WIND PROJECT

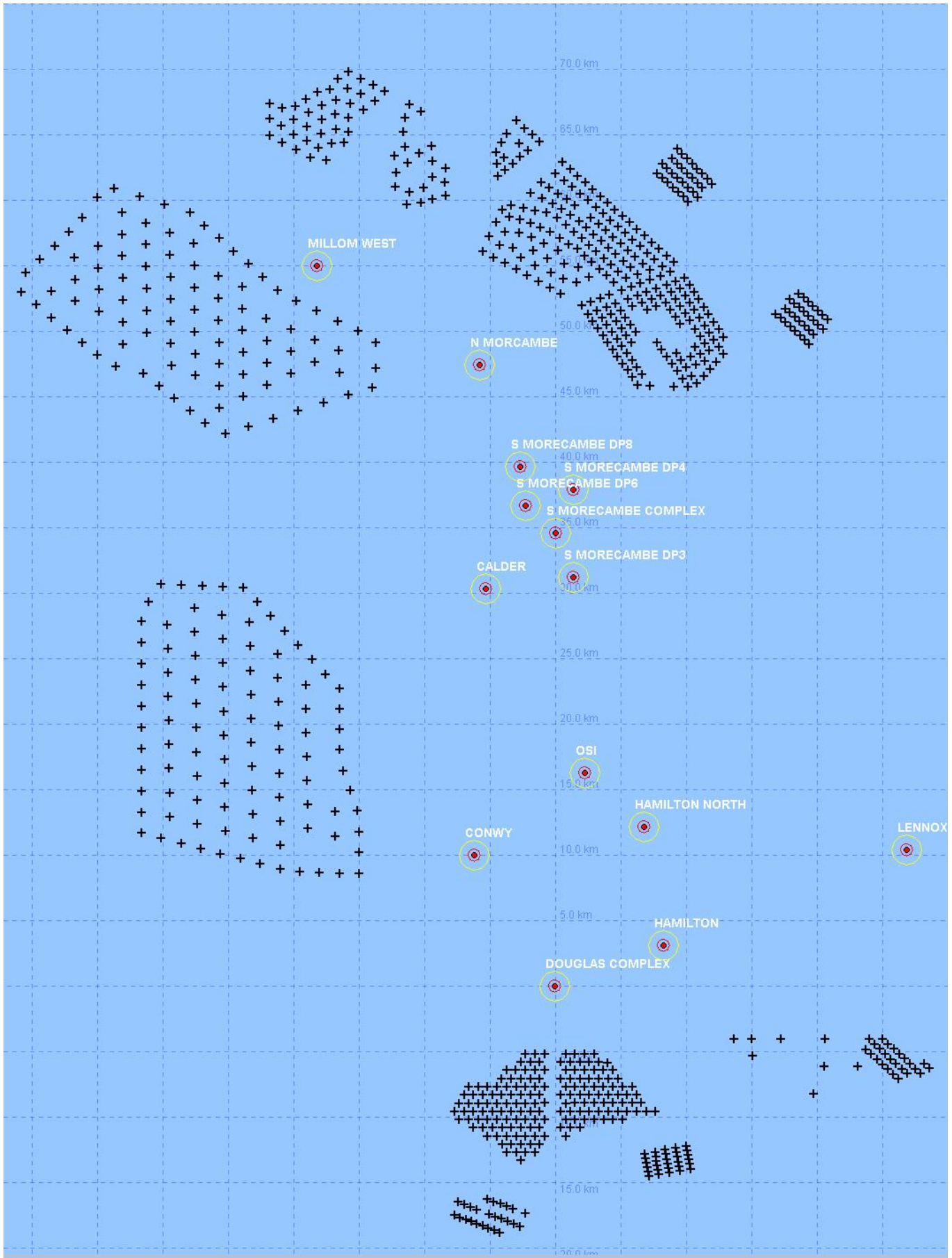


Figure 1.40: Modelled cumulative layout of the Mona Offshore Wind Project and Morgan Generation Assets showing the indicative location of the wind turbines and the location of oil and gas platforms in the region.

MONA OFFSHORE WIND PROJECT

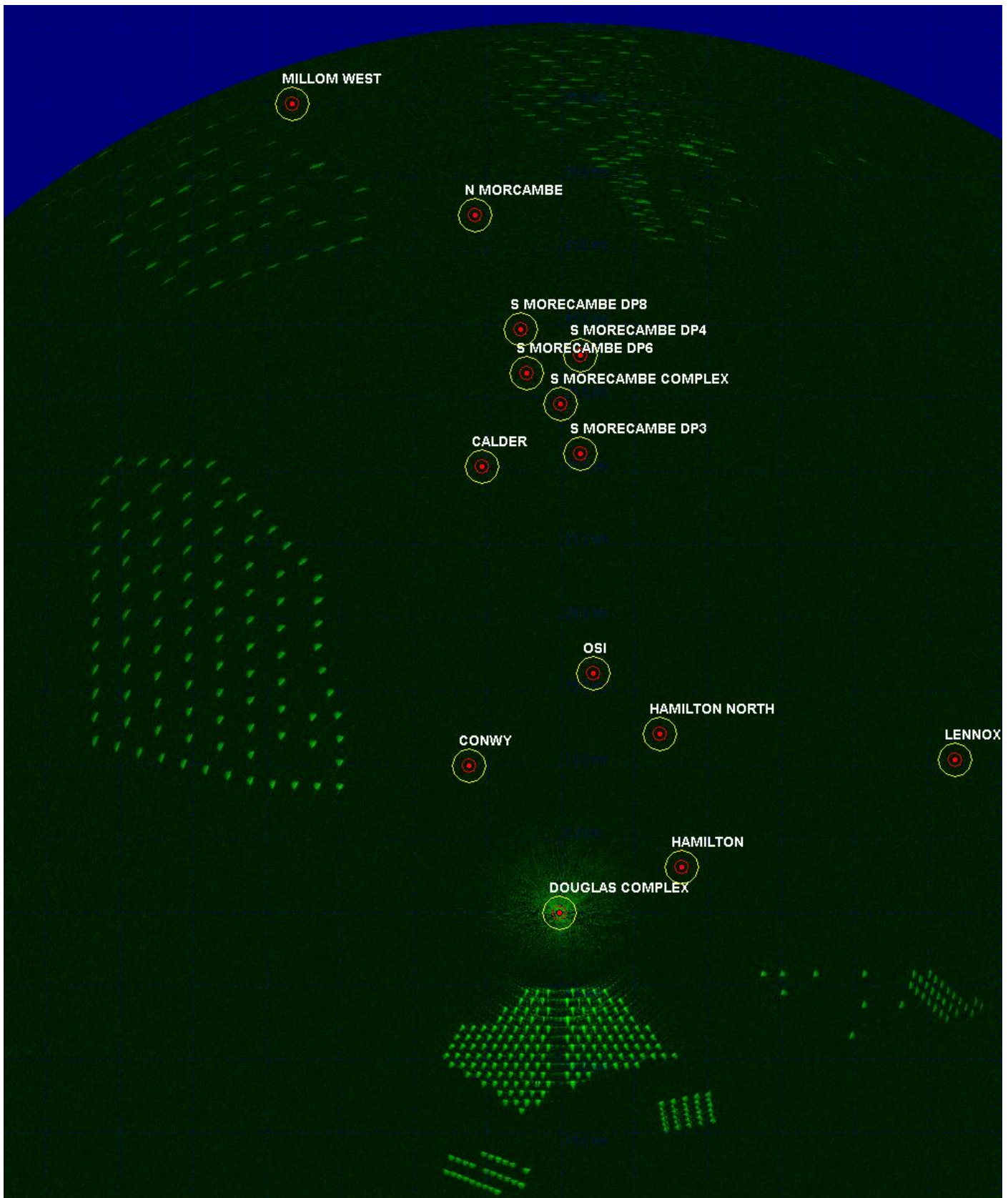


Figure 1.41: ENI Energy’s Douglas platform REWS clutter map showing returns from the wind turbines and sea clutter.

MONA OFFSHORE WIND PROJECT

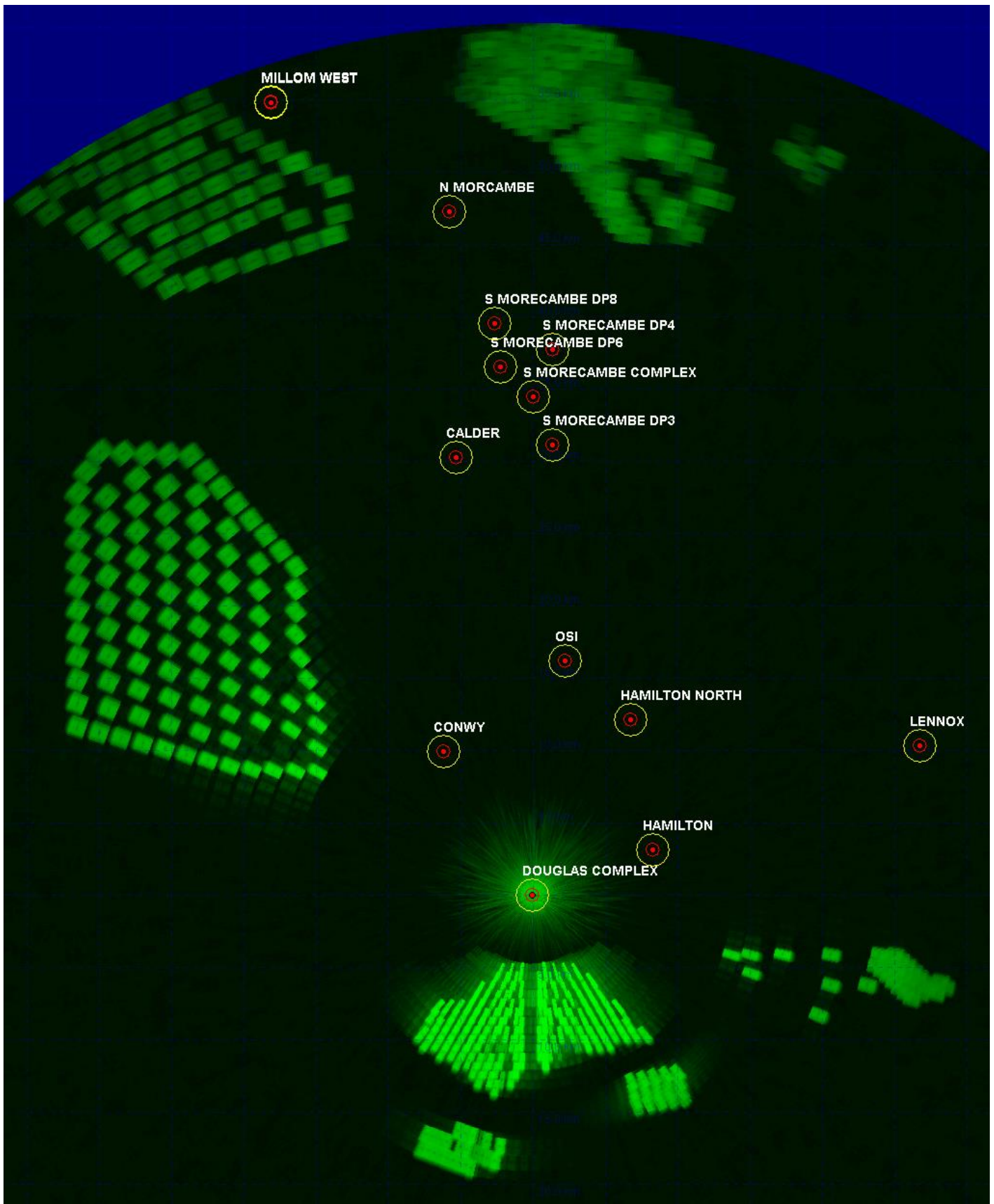


Figure 1.42: ENI Energy's Douglas platform REWS detection threshold.

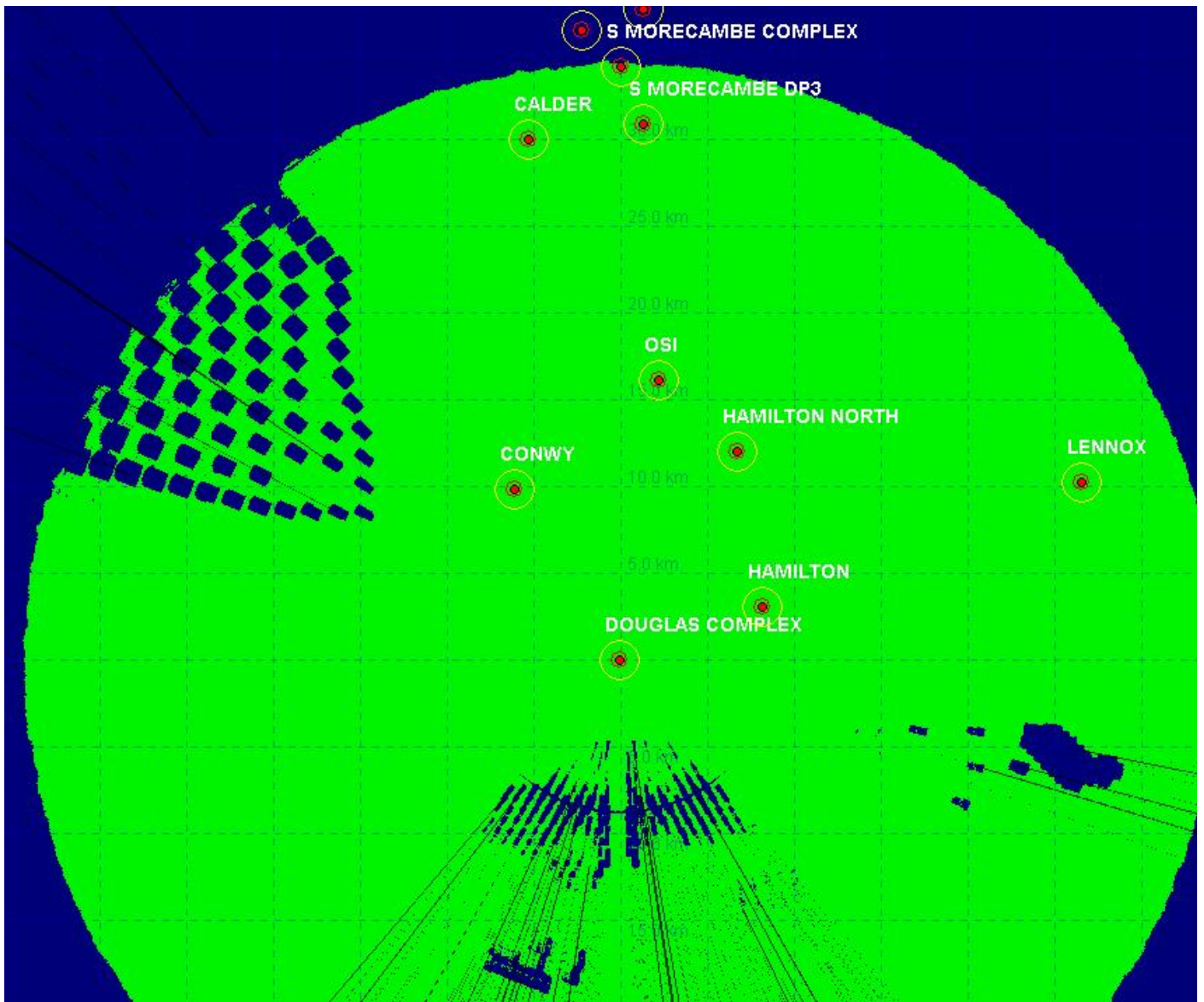


Figure 1.43: ENI Energy's Douglas platform REWS detection plot showing loss regions for a 1000 m² target.



Figure 1.44: Harbour Energy's Millom West platform REWS clutter map showing returns from the wind turbines and sea clutter.

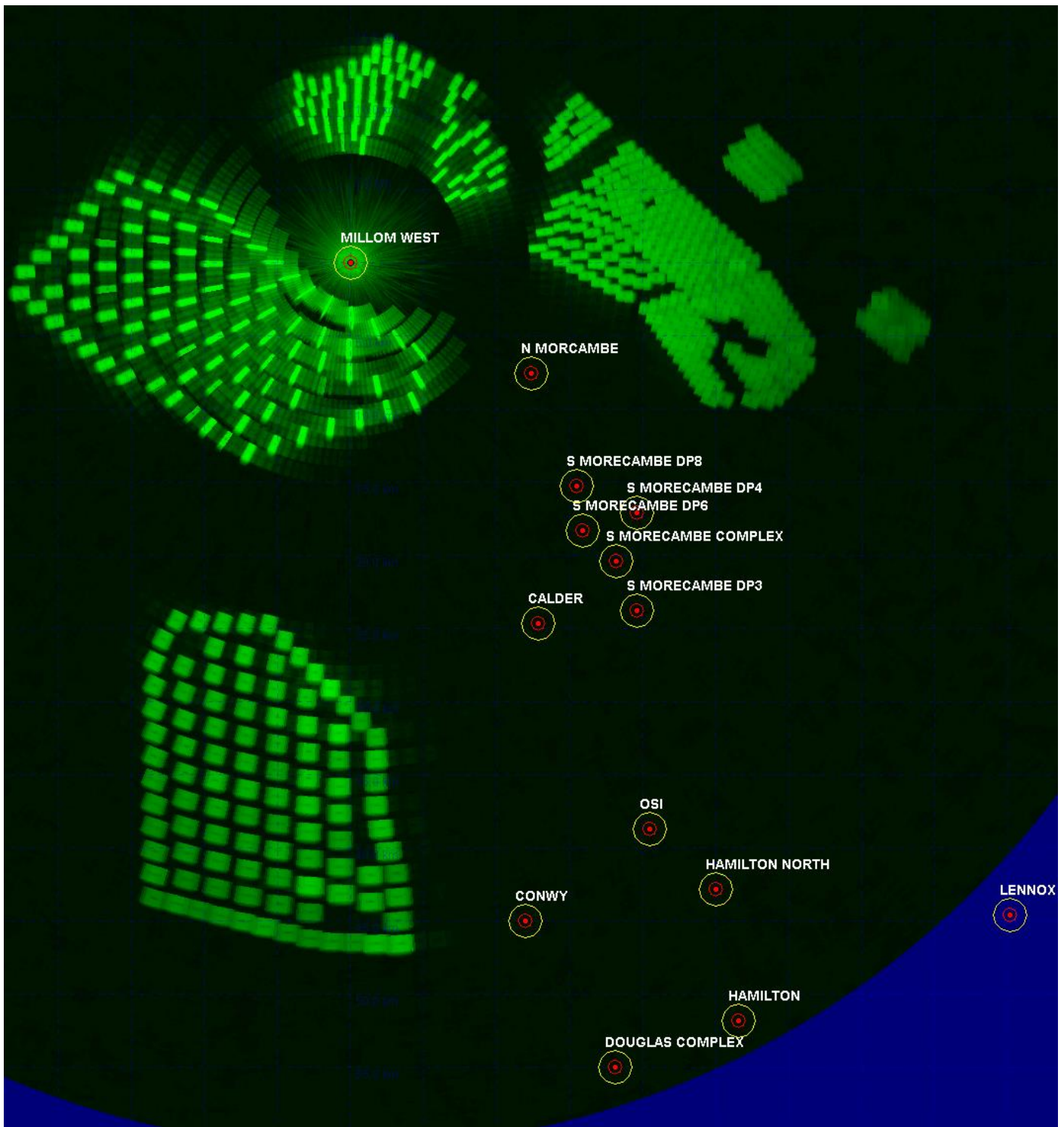


Figure 1.45: Harbour Energy’s Millom West platform REWS detection threshold.

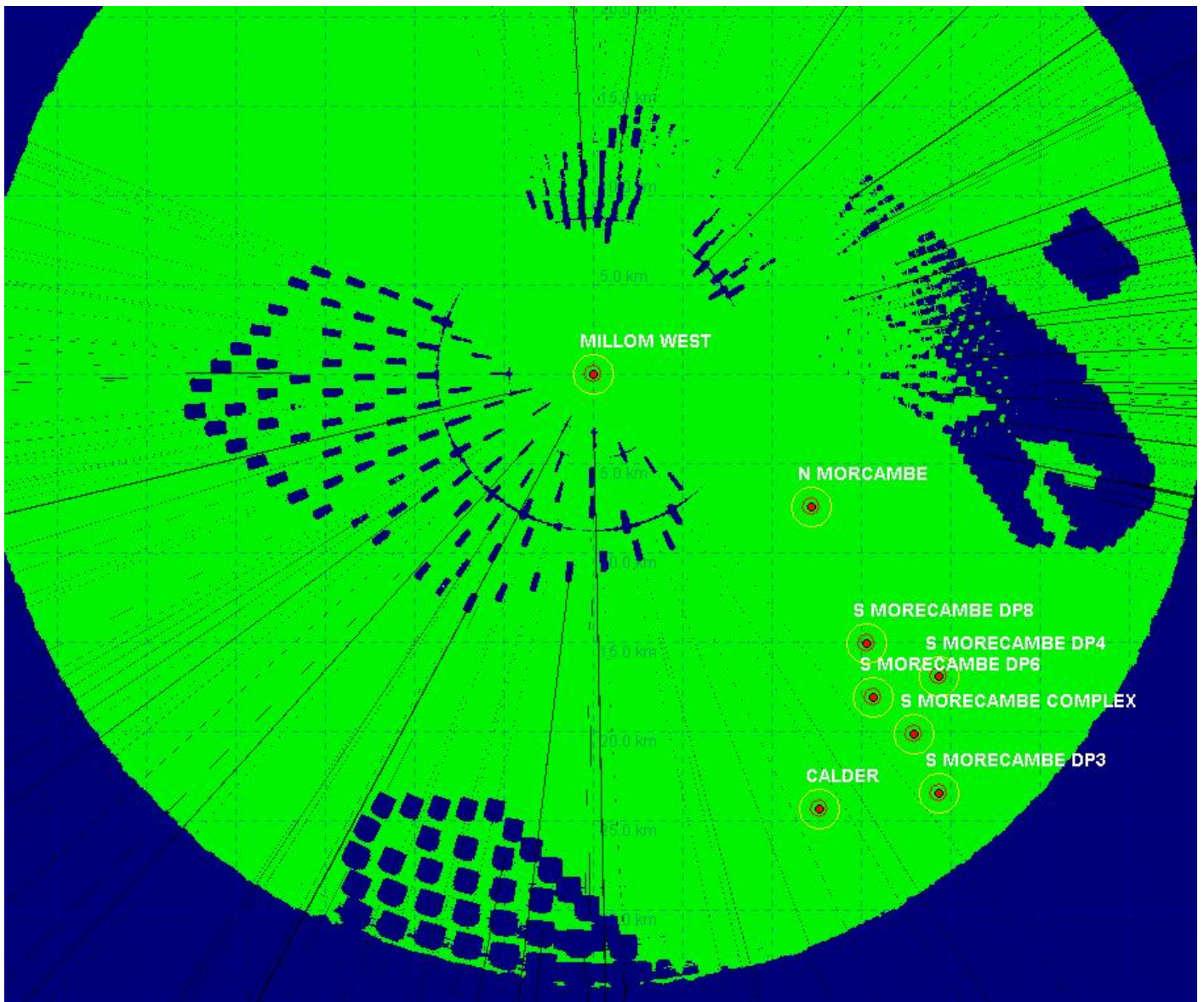


Figure 1.46: Harbour Energy’s Millom West platform REWS detection plot showing loss regions for a 1000 m² target.

MONA OFFSHORE WIND PROJECT

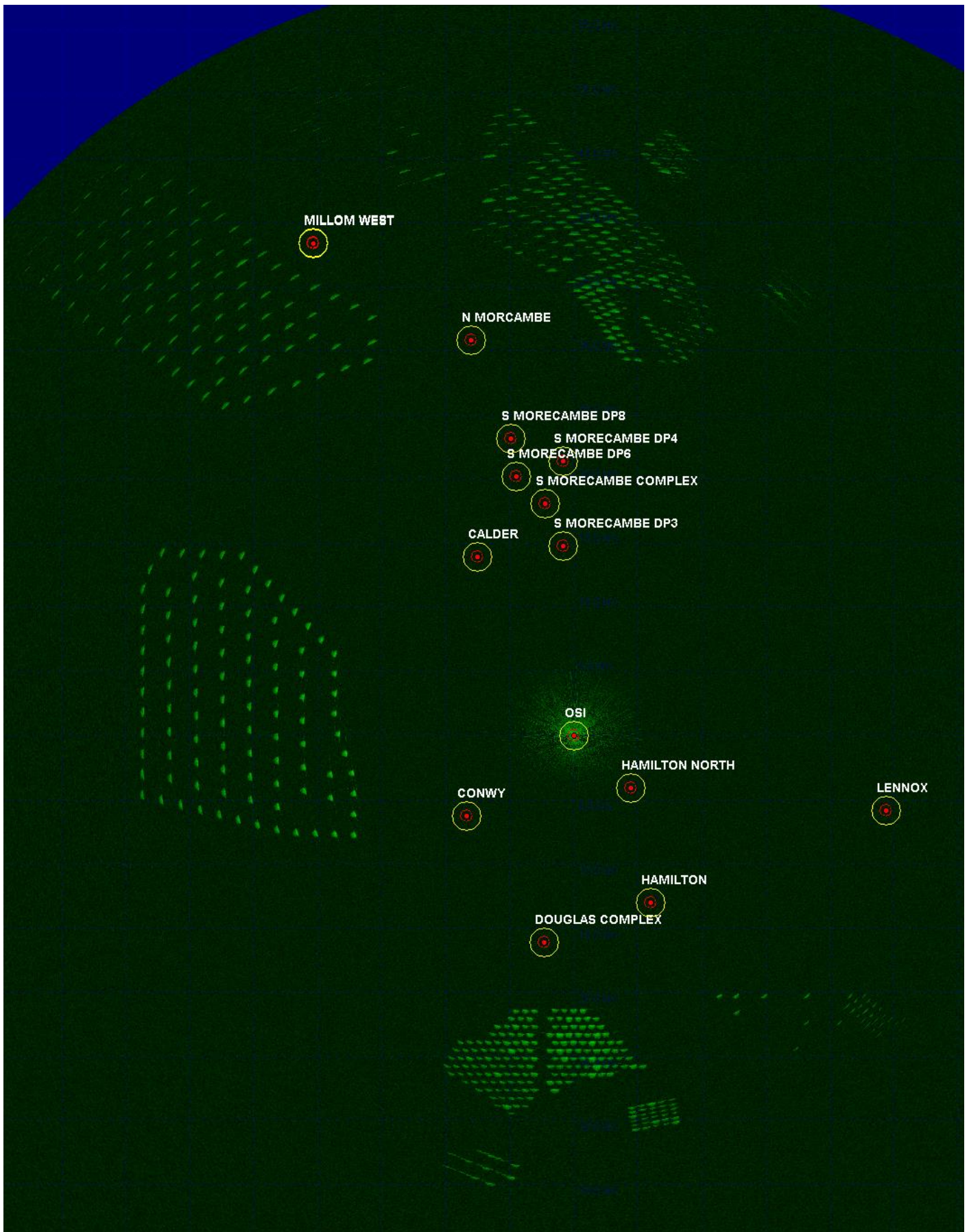


Figure 1.47: ENI Energy’s OSI REWS detection clutter map showing returns from the wind turbines and sea clutter.

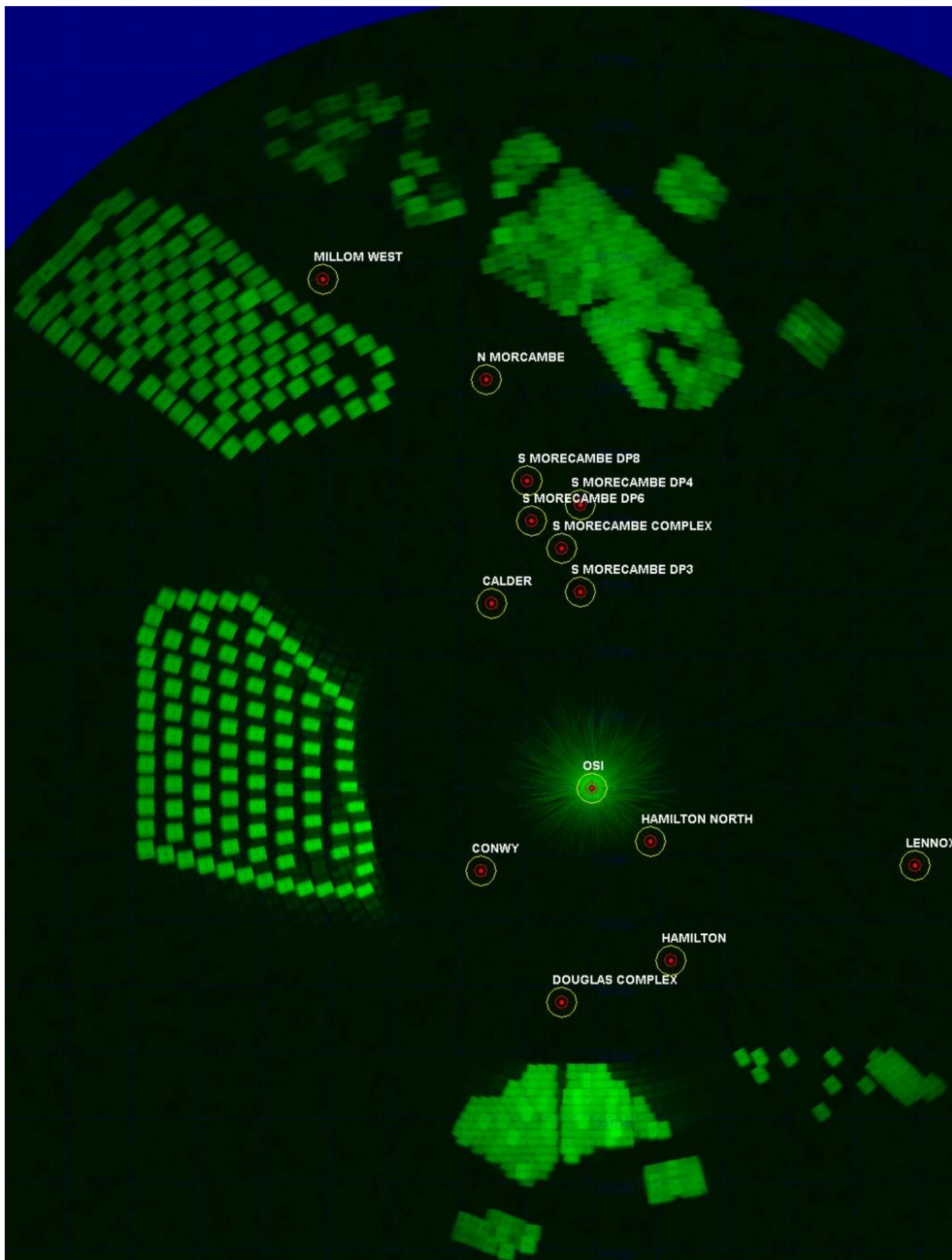


Figure 1.48: ENI Energy's OSI REWS detection threshold.

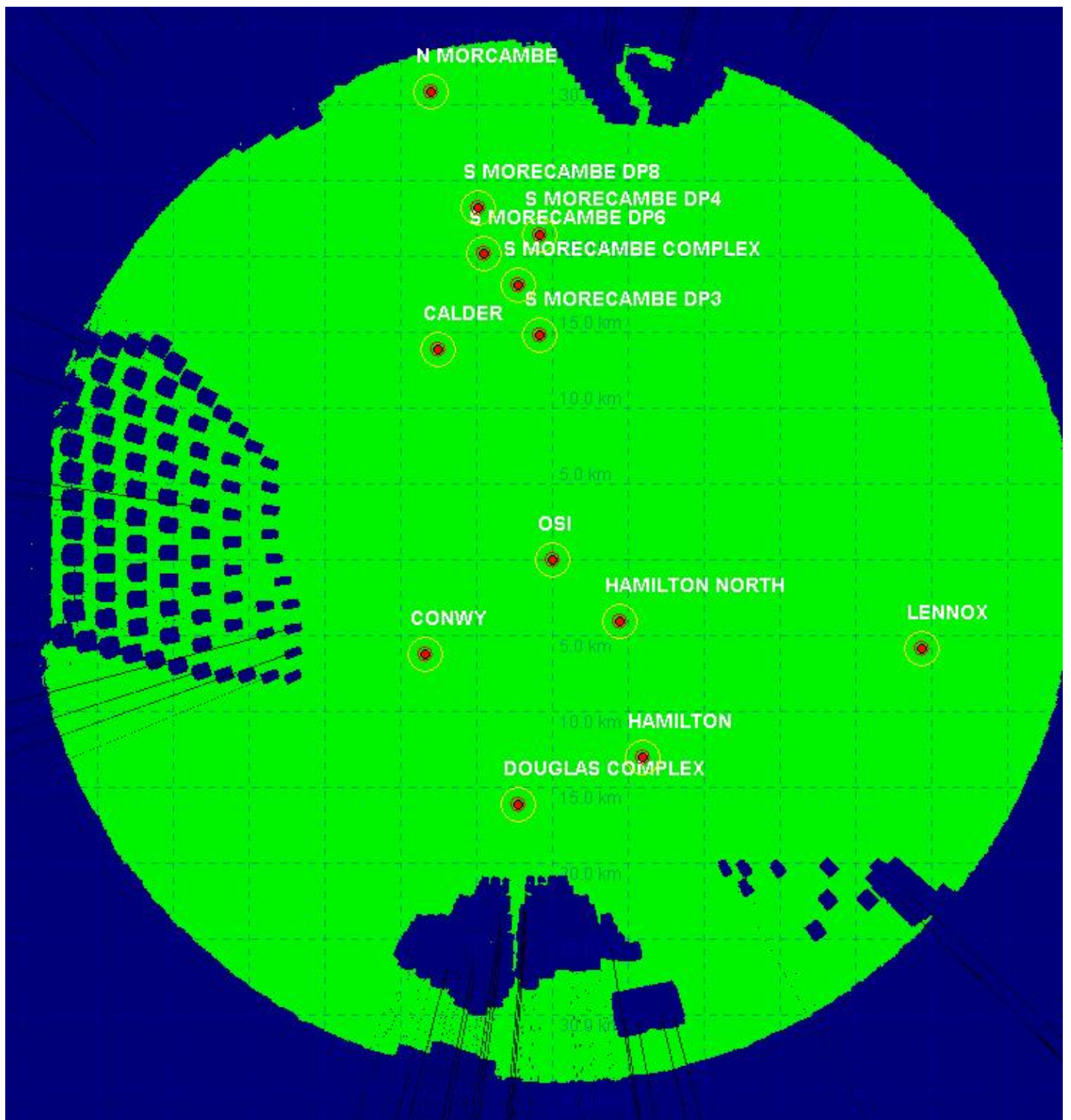


Figure 1.49: ENI Energy's OSI REWS detection plot showing loss regions for a 1000 m² target.

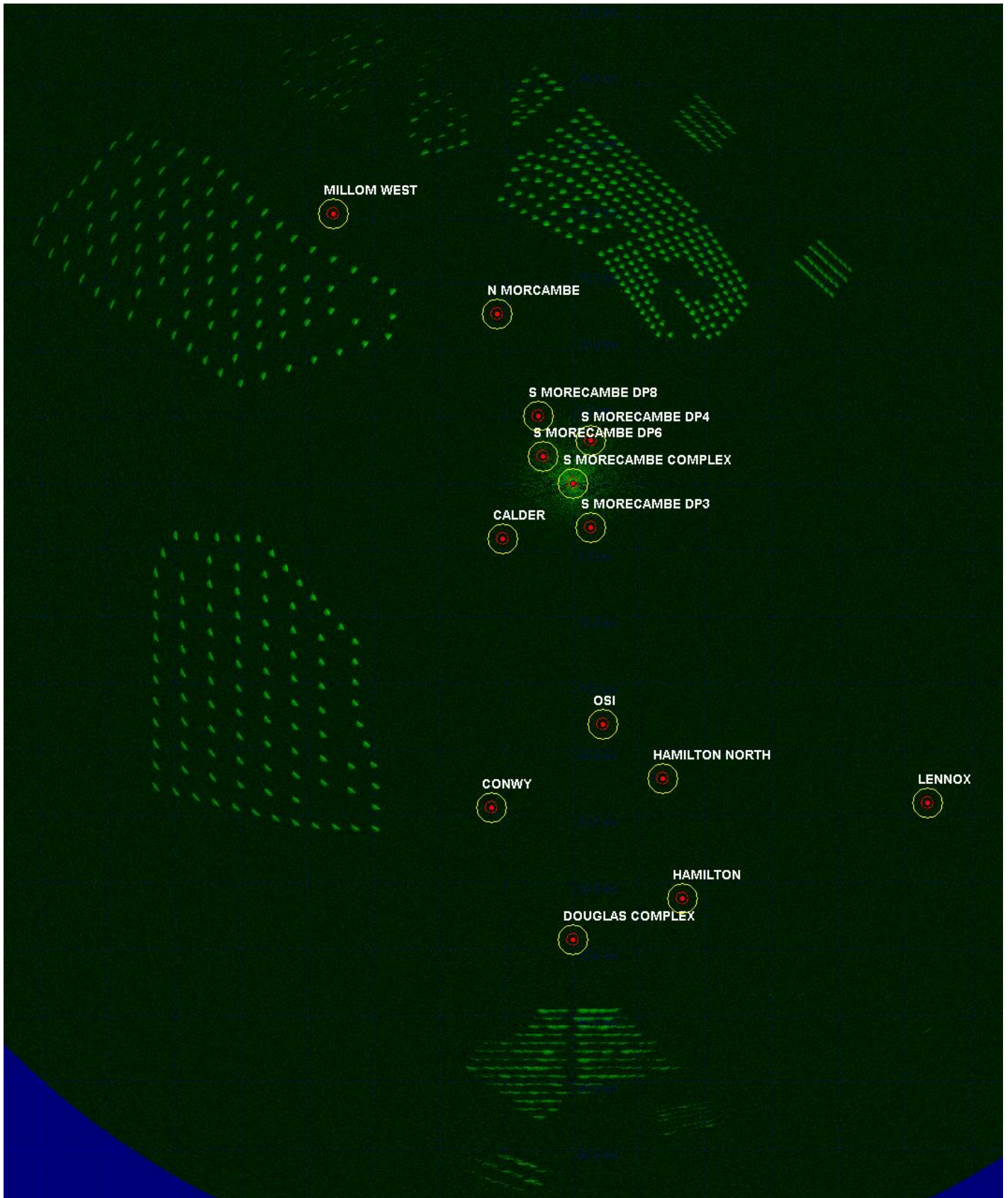


Figure 1.50: Spirit Energy's South Morecambe AP1 platform REWS clutter map showing returns from the wind turbines and sea clutter.

MONA OFFSHORE WIND PROJECT

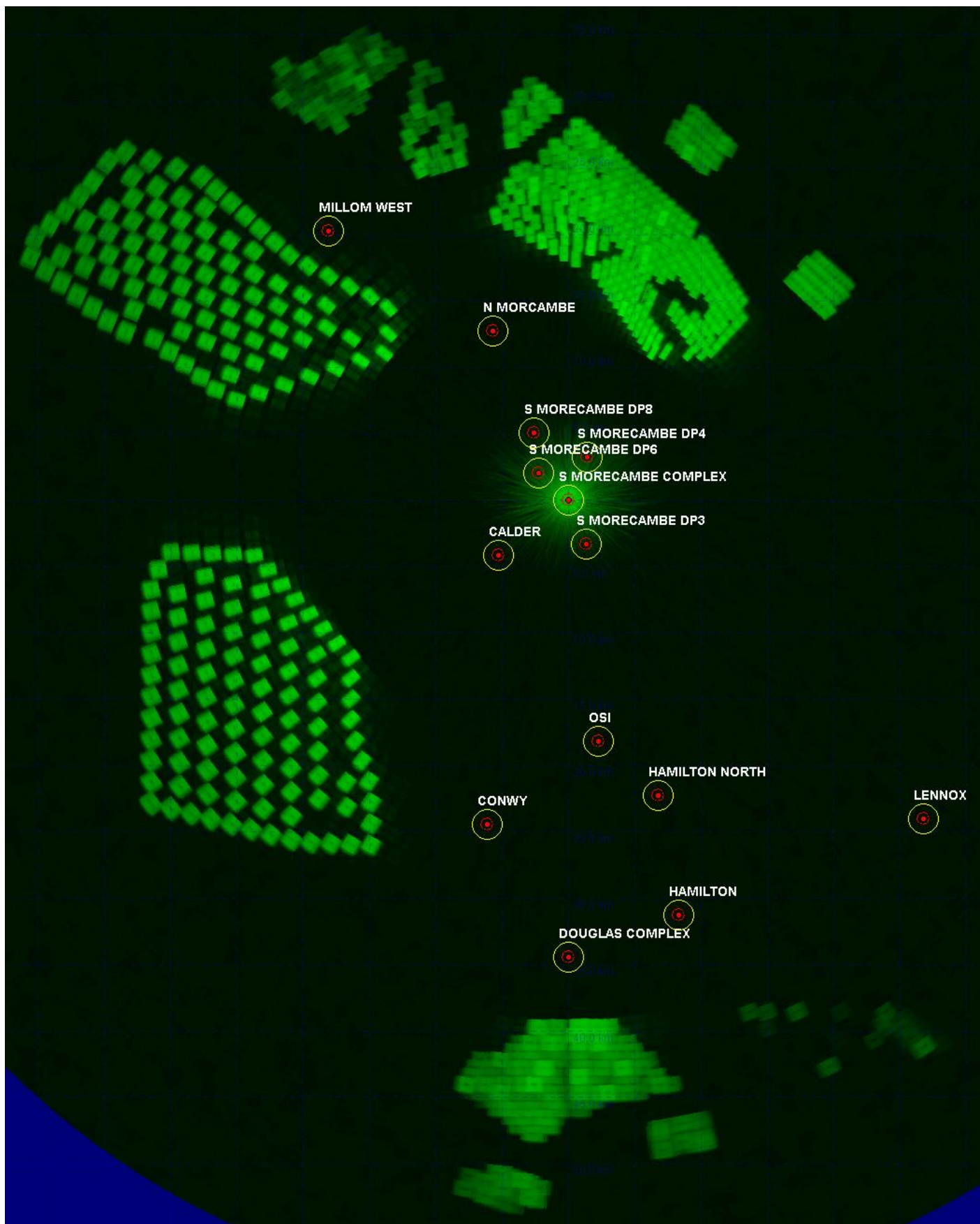


Figure 1.51: Spirit Energy's South Morecambe AP1 platform REWS detection threshold.

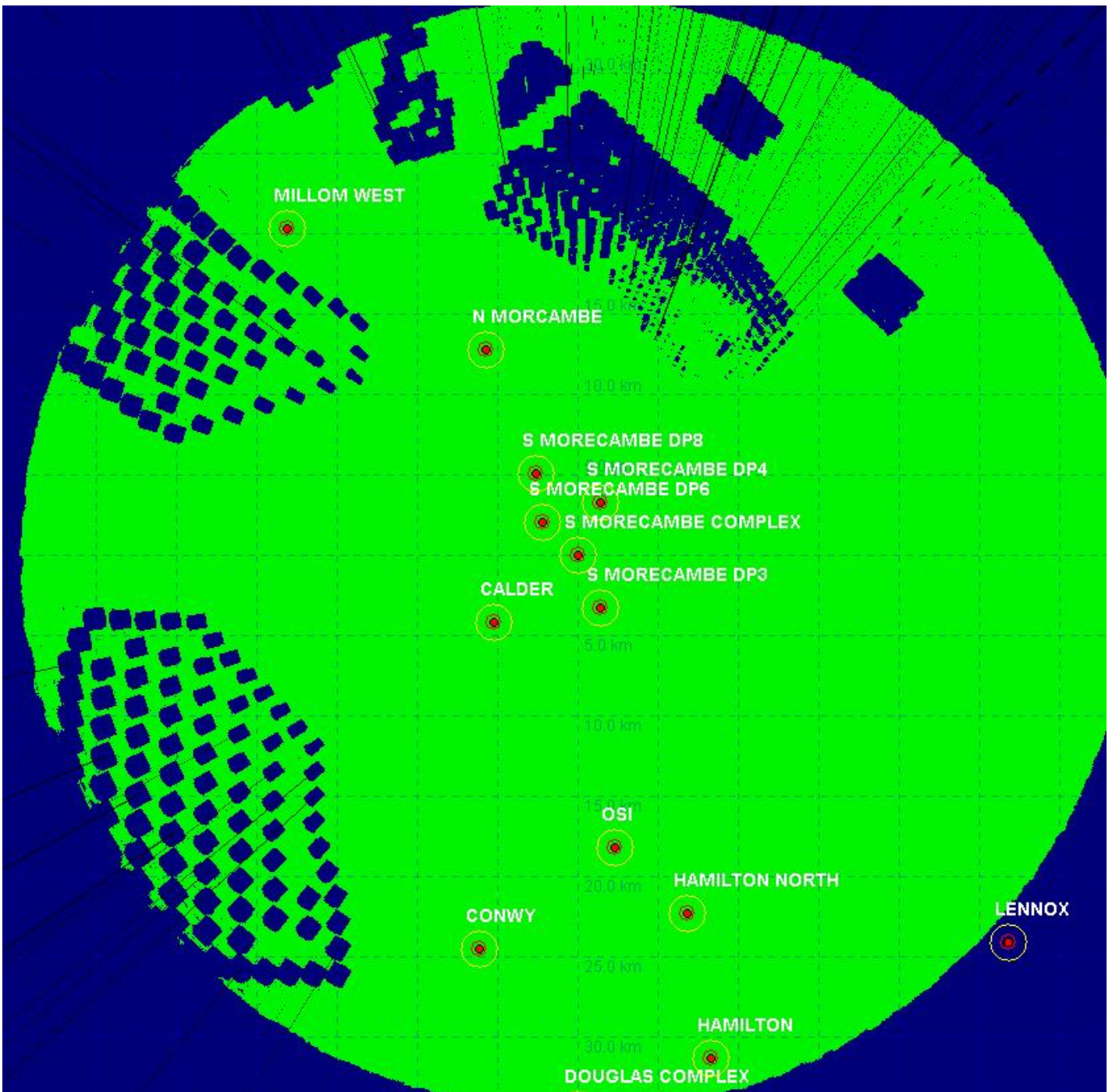


Figure 1.52: Spirit Energy's South Morecambe AP1 platform REWS detection plot showing loss regions for a 1000 m² target.

1.4.3.5

The modelling results of the cumulative assessment of the Mona Offshore Wind Project and the Morgan Generation Assets on the REWS installations on ENI Energy's Douglas platform, Harbour Energy's Millom West platform, ENI Energy's OSI and Spirit Energy's South Morecambe AP1 platform show that the raw, single scan detection performance is affected adversely within the wind farm regions. Due to the presence of the Mona Offshore Wind Project and Morgan Generation Assets, there will be small gaps in the detection map due to the elevated thresholds and shadowing effects from the wind turbines. However, as discussed previously, these effects will be largely mitigated by the advanced tracking techniques within the REWS. Additionally, the integration of the available AIS data with the REWS coverage will provide an

alternative source of vessel information and location within the zones where the REWS may lose detection. Therefore, the models show that the impact of the cumulative effect of the Mona Offshore Wind Project and the Morgan Generation Assets on detection performance of nearby REWS installation is expected to be relatively low and will be manageable without the need for further mitigation measures.

Cumulative REWS assessment of Mona Offshore Wind Project with Morgan Offshore Wind Project: Generation Assets and with other proposed wind farms in the study area

- 1.4.3.6 The impact of the Awel y Mor and the Morecambe Generation Assets wind farms could not be modelled within this study due to the lack of turbine size parameters and turbine layouts for these wind farms.
- 1.4.3.7 Although REWS installation on ENIs' Douglas platform may detect turbines with the Awel y Mor wind farm, in general Awel y Mor is not expected to create a notable cumulative impact with Mona Offshore Wind Project alone or cumulatively with the Morgan Generation Assets on REWS due to its location and distance from the REWS.
- 1.4.3.8 The Morecambe Generation Assets location is closer to the REWS installations in the region and predicted to have a more obvious impact on the REWS. The exact extent of the impact was not assessed or modelled due to the lack of turbine geometry and layouts with the farm array area. As such, the impact of the Morecambe Generation Assets was based on qualitative assessment. The quantitative impact of the Morecambe Generation Assets is expected to be complex to assess due to its location and proximity to the REWS installations in the region. It is recommended that a full assessment is carried out when the turbine parameters and layouts become available.
- 1.4.3.9 Based on the initial qualitative assessment, the REWS impact from the Morecambe Generation Assets is expected to be more significant than the impact of the Mona Offshore Wind Project. This may indicate that the potential impact on REWS might be largely attributed to the presence of Morecambe Generation Assets rather than Mona Offshore Wind Project. Cumulatively, although the presence of Mona Offshore Wind Project with Morgan Offshore Wind Project: Generation Assets and with other proposed wind farms in the study area may add to the overall impact on the REWS, it is expected that Mona Offshore Wind Projects' contribution to the impact will be relatively low and predicted to be manageable without the need for further mitigation measures.

1.5 Assessment of the rerouted traffic on REWS alarm rates

1.5.1 Overview

- 1.5.1.1 The REWS uses the radar returns to monitor and track vessels within the detection region and alert the operator when a proximity violation or an allision threat is detected. The REWS uses a defined set of rules to identify a breach of the CPA and TCPA parameters. For the assessed platforms, the alarm parameters and conditions are as outlined in paragraph 1.3.5.1.
- 1.5.1.2 Within this technical report, the effect of the rerouting of traffic on the REWS alarm rates have been modelled based on the existing traffic in the region and the predicted alterations to the traffic around the Mona Offshore Wind Project.
- 1.5.1.3 Due to the location of proposed wind farms and the predicted changes to the existing shipping traffic routes, this assessment considers the effect of rerouted shipping routes

on the existing offshore platforms (i.e. Conway, Douglas DA, Douglas DW, Hamilton, Hamilton North, Lennox, Calder, Millom West, North Morecambe DPPA, South Morecambe AP1, South Morecambe CPP1, South Morecambe DP1, South Morecambe DP6, South Morecambe DP8 and the OSI).

1.5.2 Routes and alarms modelling

- 1.5.2.1 A review of vessel movements in the region, and predicted shipping reroutes to account for the Mona Offshore Wind Project is provided in Volume 6, Annex 7.1: Navigational Risk Assessment of the Environmental Statement. This includes measured radar and AIS data for the base case and predicted data for future reroutes around the Mona Offshore Wind Project. The routes and their statistical data (including each routes' mean and standard deviation) were imported into the REWS models. The statistical data enables the REWS models to estimate the width of the shipping route and the likelihood of vessels to deviate from the central (mean) route. Accounting for possible deviations from the central line of the route in a manner which is representative to the real movements of traffic in the region provides a good indication of the overall existing and future alarm rates.
- 1.5.2.2 The route statistical data is given as a set of discrete points along key locations on the route containing the mean and the 90th percentile width of the route. Once the discrete route data were imported, the models then used linear interpolation between data points to extract the standard deviation at intermediate points. The mean and standard deviation is then used to generate 1,000 paths along each route in both the forward and reverse directions (a total of 2,000 runs per route). This was done in order to generate a large set of data that can then be used for statistical analysis. This large number of runs was then used to estimate the probability of raising TCPA or CPA alarms for each route. The probability of raising an alarm was then multiplied by the number of vessels travelling on each route per year to establish the number of alarms expected per year for each platform.
- 1.5.2.3 For each of the platforms considered in the assessment (i.e. Conway, Douglas DA, Douglas DW, Hamilton, Hamilton North, Lennox, Calder, Millom West, North Morecambe DPPA, South Morecambe AP1, South Morecambe CPP1, South Morecambe DP1, South Morecambe DP6, South Morecambe DP8 and the OSI), the assessment utilised the CPA/TCPA parameters described in paragraph 1.5.1.1 above. In order to better model the impact of moving vessels on TCPA alarms, marine traffic data collected as part of the overarching Navigation Risk Assessment process was used to estimate a speed distribution representative of routed vessels in the area of most relevance to the REWS report. This provides a good approximation of the speeds of different sizes of vessels in the region. A TCPA/CPA alarm was assumed to be raised whenever a vessel breached the alarm rules.
- 1.5.2.4 Typically, an amber TCPA alarm is triggered when a vessel is heading along a vector that would bring it within 0.6 nm from a protected platform within a specified time range (35 minutes for manned installations and 25 minutes for NUIs). If the vessel continues along its path and is 25 minutes away from a manned installations or 15 minutes from an NUI, the alarm status would escalate to a red alarm. In scenarios whereby multiple platforms are present in the region a vessel may trigger multiple TCPA alarms for different platforms along the route of the vessel. If a vessel raises a TCPA alarm, the REWS operator or the ERRV crew would attempt to establish radio contact with the vessel to make them aware of the presence of platforms along the routes. If no radio contact is established the ERRV would be deployed to intercept the vessel and issue audio and/or visual warnings to get the attention of the crew on the offending vessel.

Hence, it is assumed within this study that once an alarm triggered and addressed by the REWS operator or ERRV crew, no alarm escalation would occur and no further alarms are registered for other platforms along the route, as it is assumed that the vessel has already been communicated with and is known to be under command and aware of the platforms.

1.5.2.5 Finally, to avoid false alarms due to temporary vector breach of the TCPA while vessels are turning, the models were set to only issue a TCPA alarm if the vessel continues to breach the TCPA rules for more than 36 radar rotations (as noted in section 1.5.1 above).

1.5.3 Modelling the existing traffic (pre-development of the Mona Offshore Wind Project)

1.5.3.1 In order to be able to estimate a change in alarm rates due to the rerouting of traffic around the proposed projects array areas, a base case scenario was considered. The base case scenario utilises the existing traffic data within the region, as provided by radar and AIS data, along with extrapolated data in the regions where no data was available.

1.5.3.2 This study assessed a region of 10 nm around the proposed projects array area to provide a sufficient range to assess the TCPA alarms. The complete list of routes is shown in Table 1.3 and is illustrated in Figure 1.53 and Figure 1.54. Figure 1.55 illustrates the modelled routes output for 1,000 runs, showing the variation of route traffic around the mean line. Individual red lines/strands represent the modelled possibilities of vessels travelling along the modelled routes.

Table 1.3: Shipping routes in the region and the number of vessels travelling on each route per day.

(*) From the vessel traffic survey data, the average transits per day on this route was lower; however DFDS Seaways confirmed during consultation that the King Seaways was in dry dock during the majority of the winter survey period. Therefore, the number given above is reflective of the typical transit activity on this route.

| Route number | Average transits per year | Description (main ports, also may include alternative ports) |
|--------------|---------------------------|--|
| 1 | 1563 | Skerries TSS to Liverpool TSS (W) |
| 2 | 428 | W IoM to Liverpool TSS (E) |
| 3 | 1610 | Liverpool TSS to Skerries TSS (E) |
| 4 | 525 | Liverpool TSS to Skerries TSS |
| 5 | 17 | Inshore Anglesey to Liverpool |
| 6a | 13 | Off Skerries TSS to Barrow I |
| 6b | 10 | Off Skerries TSS to Heyshl(E) |
| 7 | 4 | Off Skerries TSS to Barrow (W) |
| 8 | 7 | Heysham to Off Skerries TSS (W) |
| 9 | 36 | Irish Sea to LiverpoolISS (E) |
| 10 | 13 | Liverpool TSS to Inshore Anglesey (W) |
| 11 | 45 | Liverpool TSS to Central Irish Sea (W) |
| 12 | 137 | Liverpool TSS to Irish Sea via Skerries TSS (W) |

MONA OFFSHORE WIND PROJECT

| Route number | Average transits per year | Description (main ports, also may include alternative ports) |
|---------------------|----------------------------------|---|
| 13 | 533 | Liverpool TSS to W IoM (W) |
| 14 | 184 | E IoM to Heysham |
| 15a | 10 | Liverpool –o E IoM - W |
| 15b | 54 | Liverpool –o E IoM - Central |
| 15c | 14 | Liverpool –o E IoM - E |
| 16 | 6 | Douglas to Heysham |
| 18 | 153 | Liverpool to W IoM |
| 19 | 9 | Douglas to Liverll TSS (E) |
| 20 | 60 | Southern Irish Sea to Solway Firth |
| 21 | 42 | Off Skerries TSS to Solway Firth |
| 22 | 8 | Douglas to Liverpool TSS |
| 23 | 66 | Liverpool to E West of Duddon Sands |
| 24 | 9 | Liverpool to Off Skerries TSS (via NE Anglesey) |
| 25 | 13 | Colwyn Bay to W IoM |
| 26 | 55 | Liverpool TSS to Northen Ireland (W) |
| 27 | 6 | Douglas to Liverpool |
| F1 | 1451 | Heysham to Douglas IoM |
| F2 | 593 | Liverpool to Douglas IoM |
| F3 | 1099 | Heysham to Carlingford Lough |
| F4 | 606 | Heysham to Dublin |
| F5 | 194 | Liverpool to Belfast E (W of Morecambe) |
| F6 | 1098 | Liverpool to Belfast W |
| F7 | 196 | Liverpool to Belfast E |
| F8 | 1094 | Heysham to East IoM |
| F9 | 226 | Liverpool to Belfast W (TSS E) |
| F10 | 166 | Liverpool to Belfast W (TSS W) |
| F11 | 294 | Liverpool to Dublin 3 |
| F12 | 1627 | Liverpool to Dublin 2 |
| F13 | 1331 | Liverpool to Dublin 1 |
| 1 | 1563 | Liverpool TSS to Slries TSS (E) |
| 2 | 428 | W IoM to Liverpool TSS (E) |
| 3 | 1610 | Skerries TSS to Liverpool TSS (W) |
| 4 | 525 | Liverpool TSS to Skerries TSS |
| 5 | 17 | Inshore Anglesey to Liverpool |
| 6a | 13 | Off Skerrl TSS to Barrow (E) |

MONA OFFSHORE WIND PROJECT

| Route number | Average transits per year | Description (main ports, also may include alternative ports) |
|--------------|---------------------------|--|
| 6b | 10 | Off Skeles TSS to Heysham (E) |
| 7 | 4 | Off Skerries TSS to Barrow (W) |
| 8 | 7 | Heysham to Off Skerries TSS (W) |
| 9 | 36 | IrlSea to Liverpool TSS (E) |
| 10 | 13 | Liverpool TSS to Inshore Anglesey (W) |
| 11 | 45 | Liverpool TSS to Central Irish Sea (W) |
| 12 | 137 | Liverpool TSS to Irish Sea via Skerries TSS (W) |

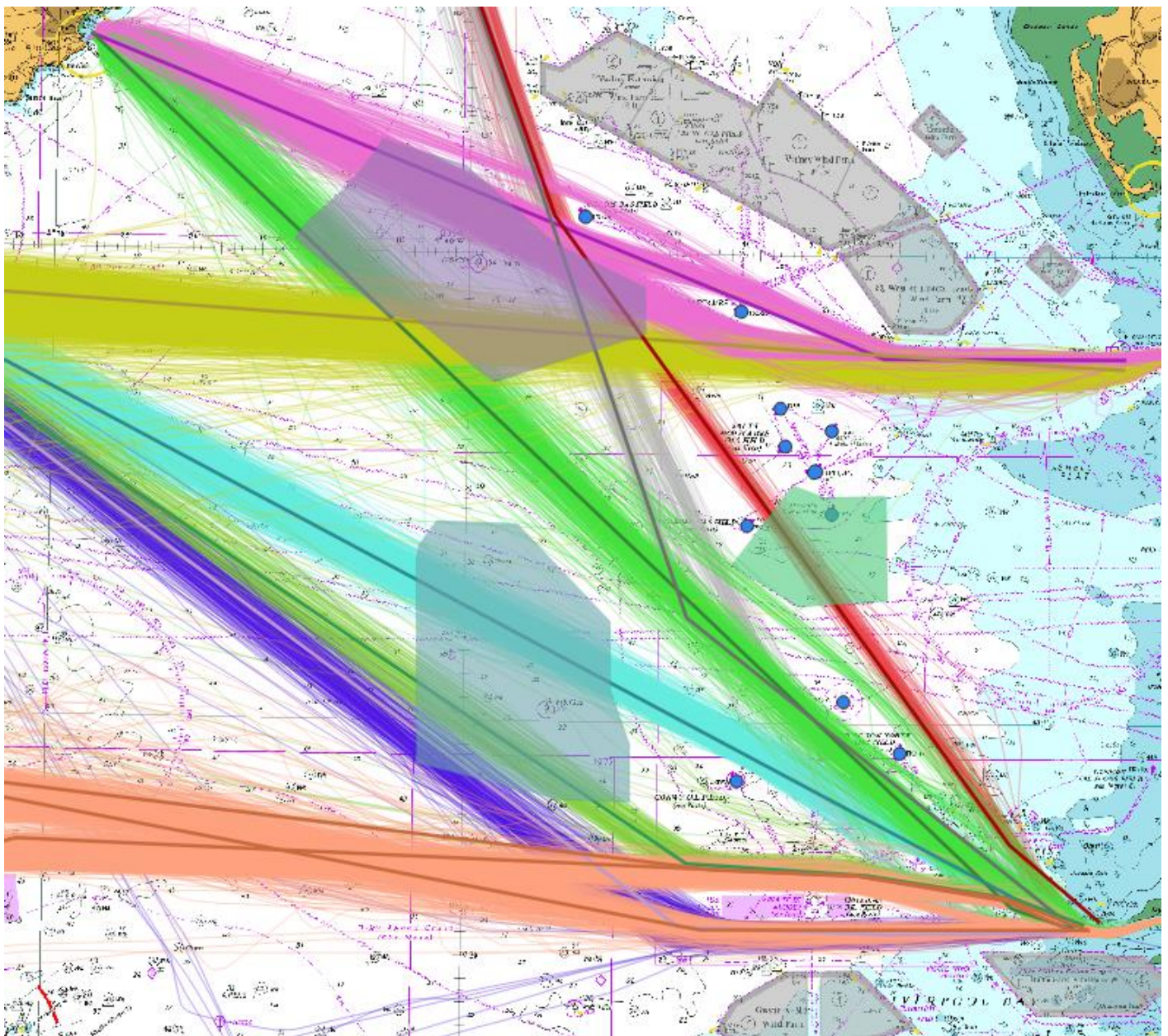


Figure 1.53: Existing ferry routes within and around the Mona Array Area.

MONA OFFSHORE WIND PROJECT

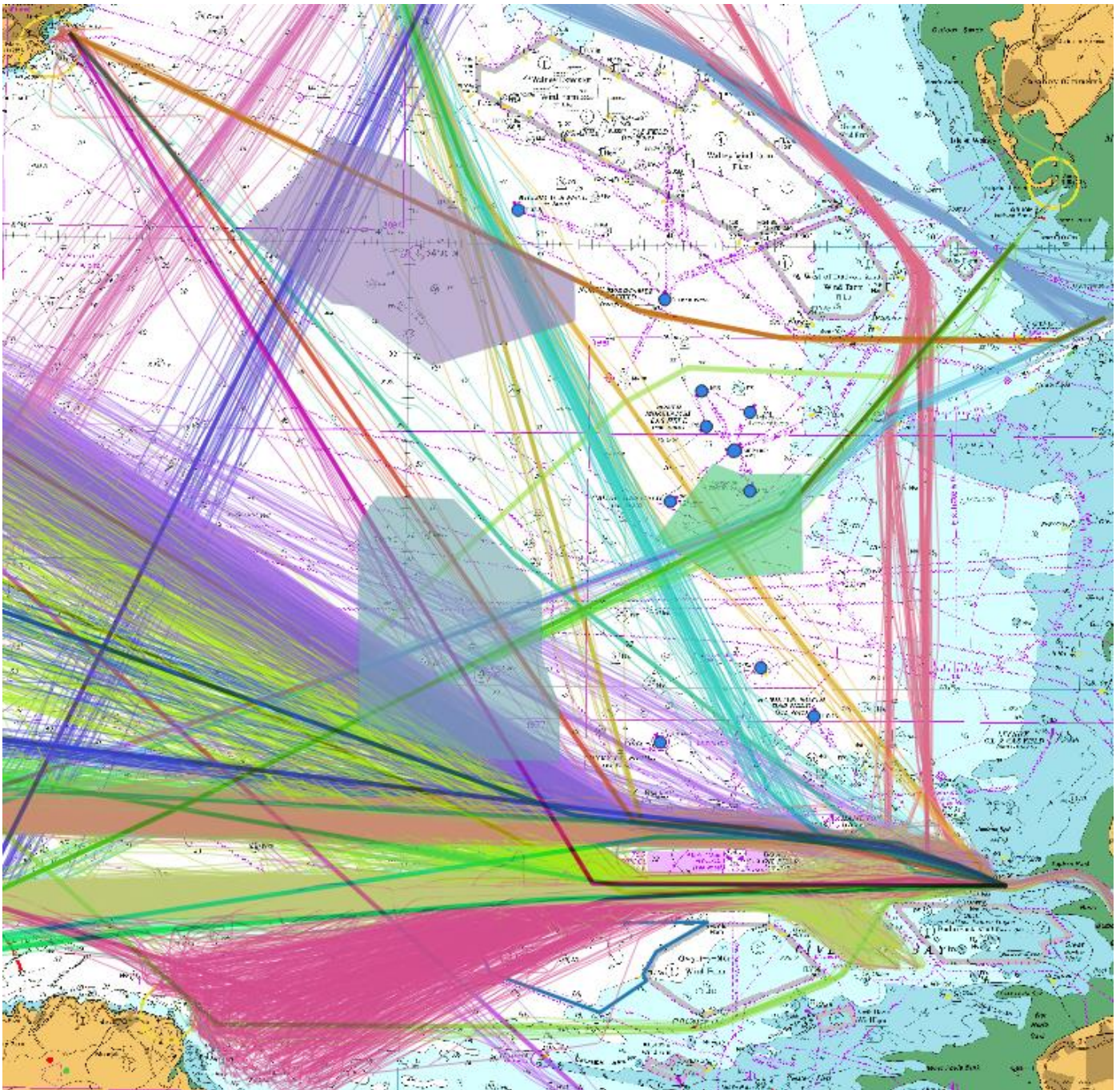


Figure 1.54: Existing commercial routes within and around the Mona Array Area.

MONA OFFSHORE WIND PROJECT

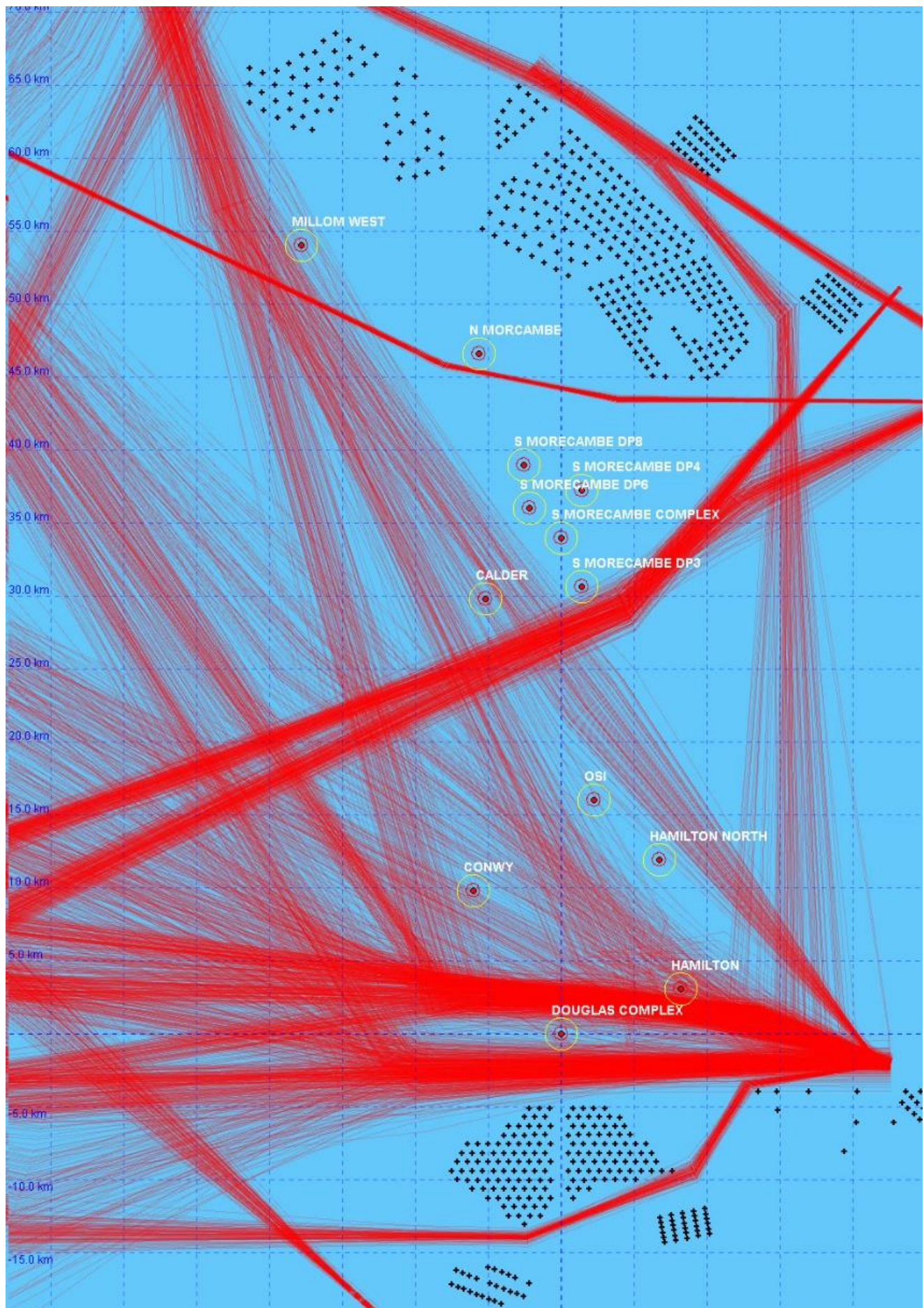


Figure 1.55: Modelled existing shipping routes (1,000 variations each route).

MONA OFFSHORE WIND PROJECT

- 1.5.3.3 The models were used to simulate each route in both directions and identify each type of alarm on every platform. Using the statistical nature of the data, a probability of alarm is calculated for each platform by taking the number of alarms triggered over the 1,000 runs and presenting this as a platform percentage. This probability is then used in conjunction with the data in Table 1.3 to estimate the number of alarms per year for each platform.
- 1.5.3.4 It is noted that in some cases within the base scenario, some routes raised no alarms while other routes show some probability of alarms in the existing (base) case. This is due to the proximity and direction of the route as well as the statistical nature/width of the route.
- 1.5.3.5 Additionally, due to simplifying assumption when representing the existing routes in the form of a mean line with a set of 90th percentile widths, the resultant modelled routes did not follow the exact behaviour of the measured routes when vessels are travelling near offshore platforms. This was identified during the modelling process but due to the lack of data it was deemed acceptable at this stage for modelling use. Therefore, although the results presented are an estimate of the existing effect of traffic on the REWS alarms, it provides a good basis from which to compare predicted future cases.

1.5.4 Modelling the predicted shipping reroutes Around the Mona Offshore Wind Project in isolation and cumulatively with other wind farms in the study area

- 1.5.4.1 In a similar manner to the base-case scenario, the vessel traffic around the Mona Offshore Wind Project (in isolation) was modelled based on the reroutes predicted and described in Volume 6, Annex 7.1: Navigational Risk Assessment of the Environmental Statement . Both the mean line for each route, along with its standard deviation, were considered in the model. This data was then used to create 1,000 runs for each route in either direction (total of 2,000 runs) to provide sufficiently large set of results to undergo statistical analysis of the data. and the modelled routes are shown in Figure 1.56. Once each route was modelled and the yearly alarm rates were obtained, the modelling results for the predicted traffic were compared against the base-case.
- 1.5.4.2 Similarly, the rerouted traffic due to the cumulative presence of the Mona Offshore Wind Project with the Morgan Generation Assets were modelled based on the predicted reroutes described in Volume 6, Annex 7.1: Navigational Risk Assessment of the Environmental Statement .The modelled routes are shown in Figure 1.57.

MONA OFFSHORE WIND PROJECT

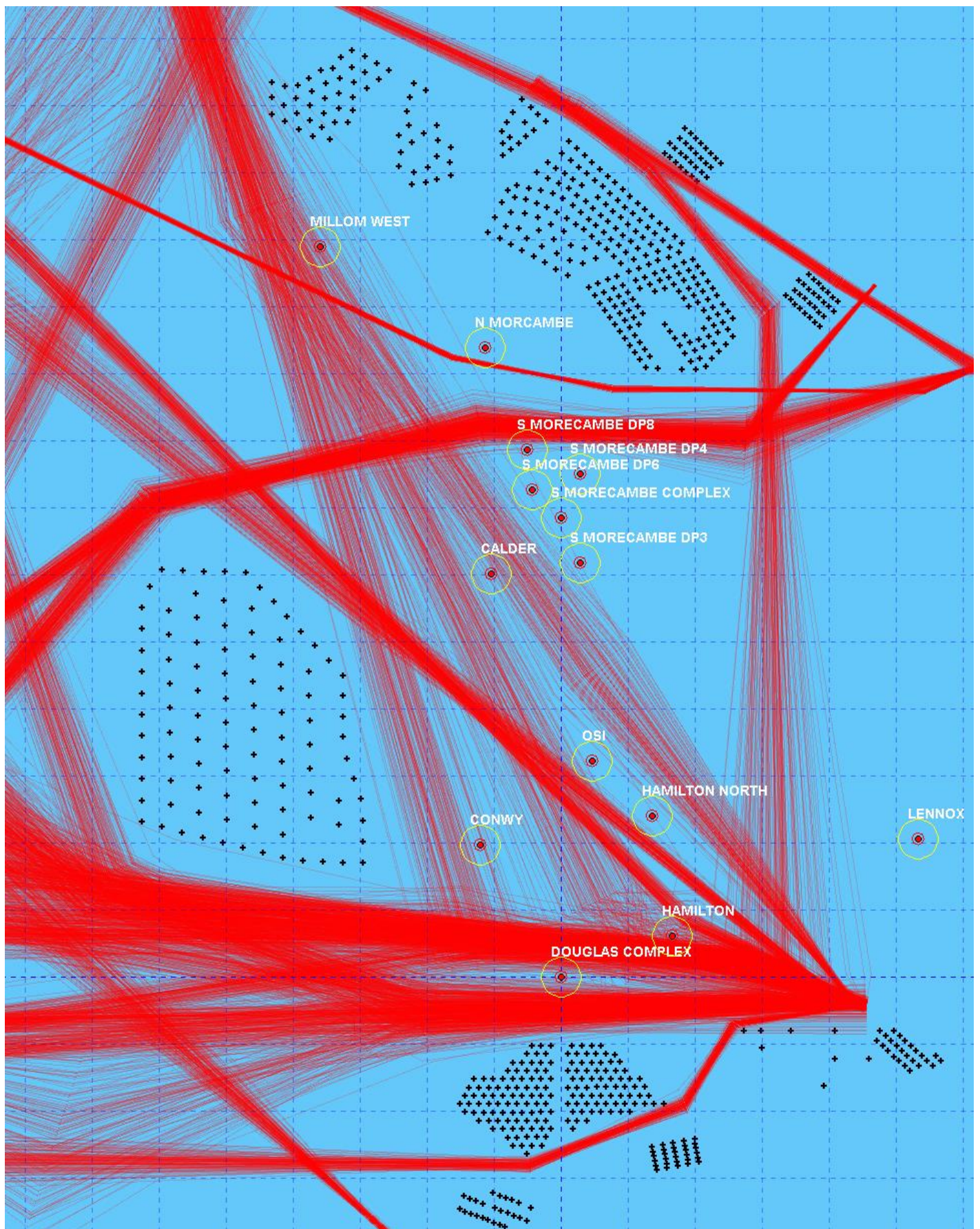


Figure 1.56: Modelled shipping routes post-construction of the Mona Offshore Wind Project.

MONA OFFSHORE WIND PROJECT

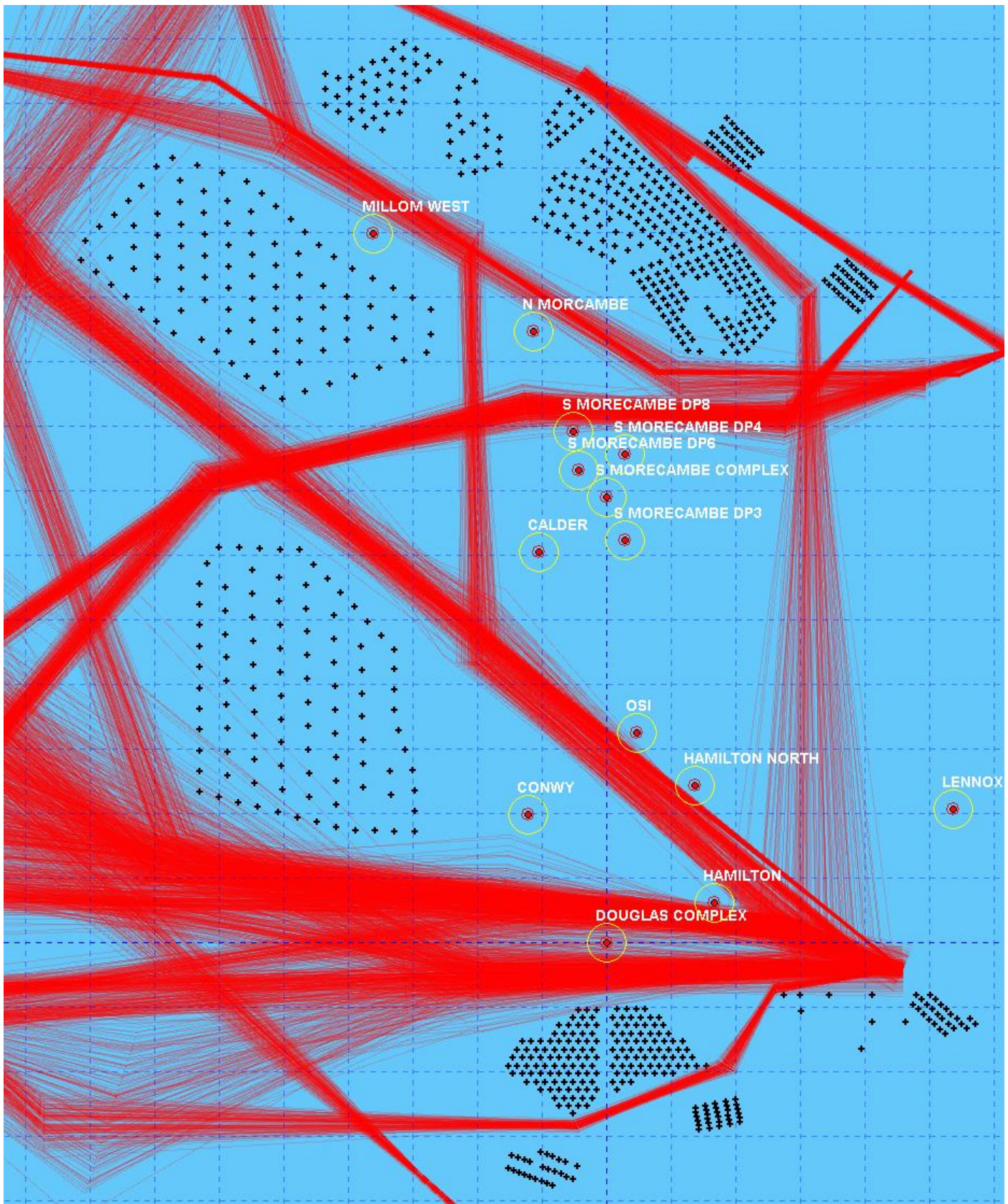


Figure 1.57: Modelled shipping routes post-construction of the Mona and Morgan Generation Assets cumulatively.

1.5.5 Modelling results and comparison of the base case and the predicted shipping reroutes around the Mona Offshore Wind Project in isolation and around Mona Offshore Wind Project and Morgan Generation Assets cumulatively.

1.5.5.1 To understand the potential impact of proposed projects on the alarm rates, the modelled data from the existing base case was compared against the post construction modelling results. The comparison looks at the number of alarms each platform is expected to have in a one-year period. The data compares both Amber and Red TCPA alarms for the base case, Mona Offshore Wind Project in isolation and Mona Offshore Wind Project alongside Morgan Generation Assets cumulatively. The annual alarm rates modelling results for each platform are shown in Figure 1.58 to Figure 1.71.

1.5.5.2 To simplify the comparison, Table 1.4 shows the estimated difference in alarm rates between the base case and the three other considered scenarios (i.e. Mona Offshore Wind Project in isolation and the cumulative case Morgan Generation Assets).

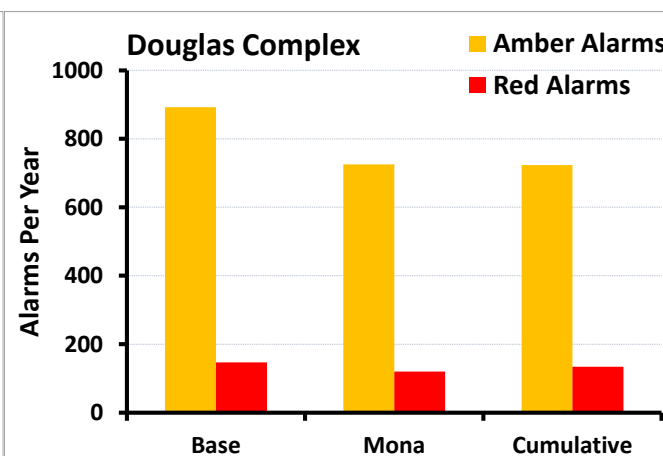
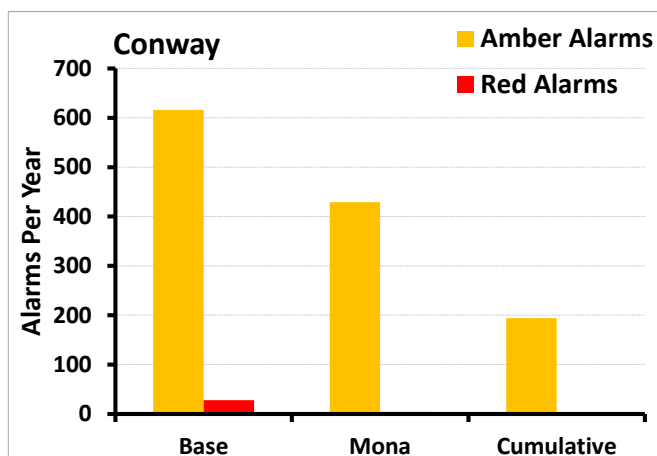


Figure 1.58: Modelled yearly alarm rates for the Conway platform.

Figure 1.59: Modelled yearly alarm rates for the Douglas Complex.

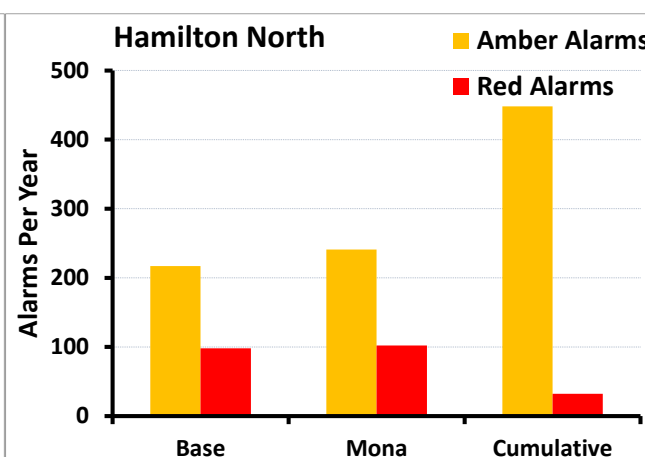
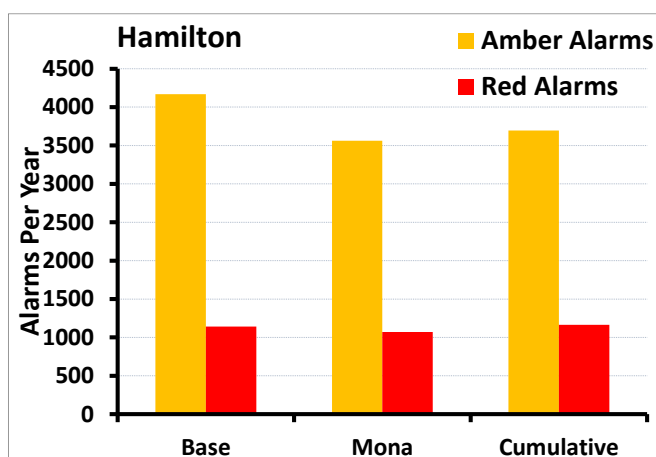


Figure 1.60: Modelled yearly alarm rates for the Hamilton platform.

Figure 1.61: Modelled yearly alarm rates for the Hamilton North platform.

MONA OFFSHORE WIND PROJECT

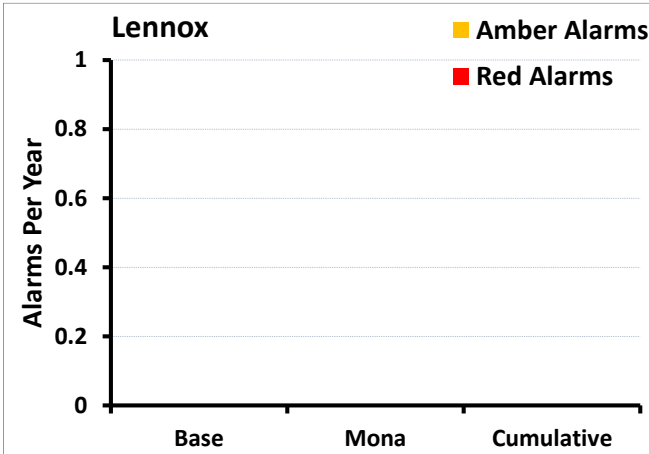


Figure 1.62: Modelled yearly alarm rates for the Lennox platform.

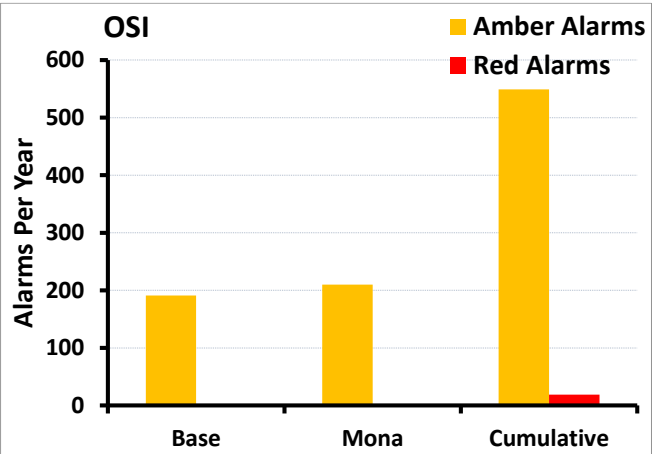


Figure 1.63: Modelled yearly alarm rates for the OSI.

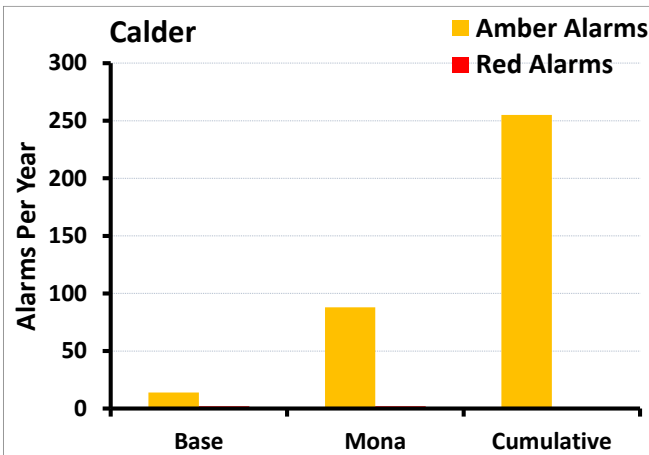


Figure 1.64: Modelled yearly alarm rates for the Calder platform.

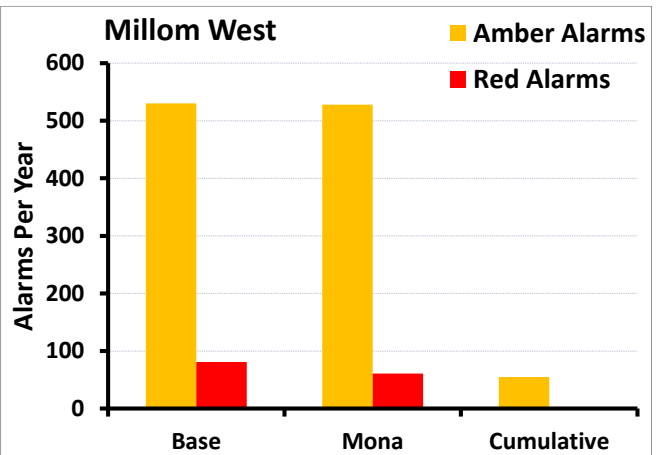


Figure 1.65: Modelled yearly alarm rates for the Millom West platform.

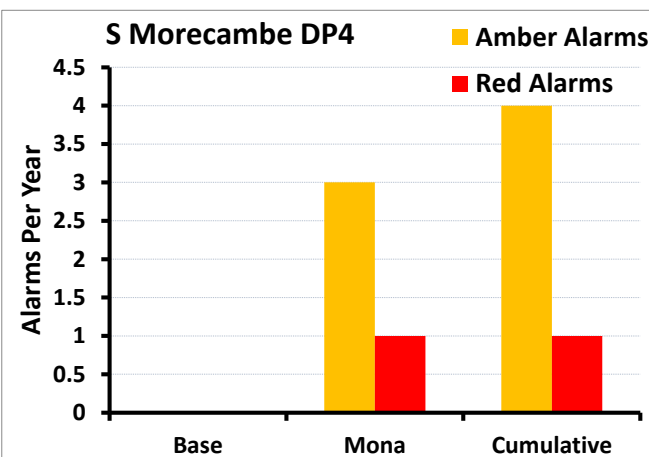


Figure 1.66: Modelled yearly alarm rates for the South Morecambe DP4 platform.

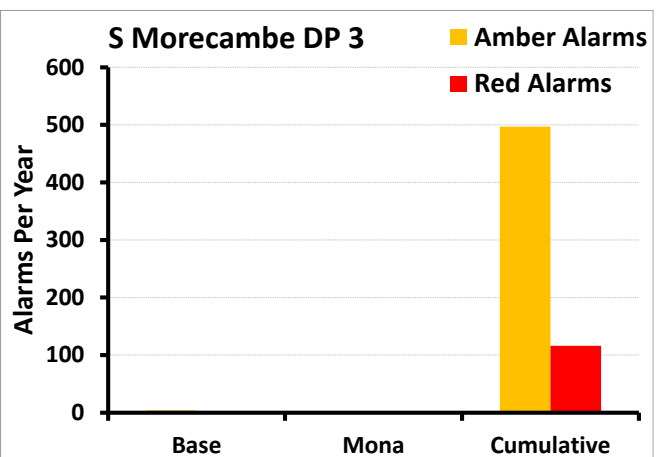


Figure 1.67: Modelled yearly alarm rates for the South Morecambe DP3 platform.

MONA OFFSHORE WIND PROJECT

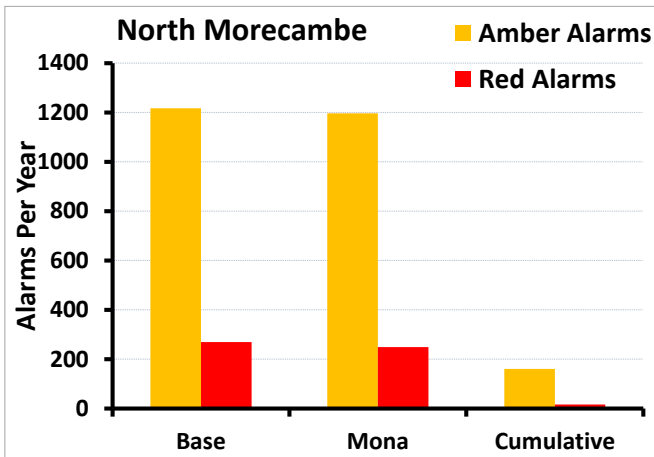


Figure 1.68: Modelled yearly alarm rates for the North Morecambe platform.

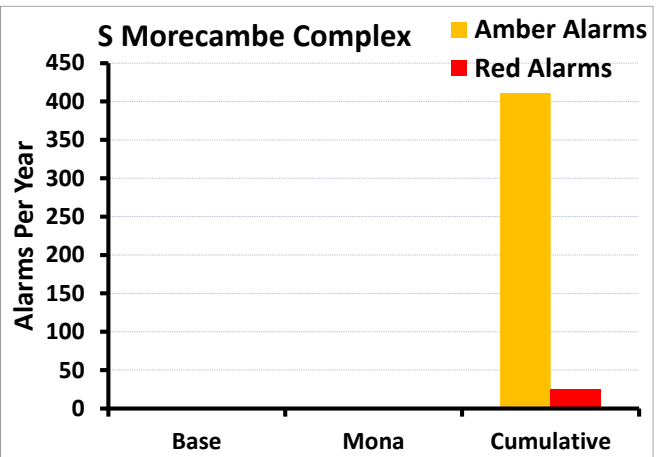


Figure 1.69: Modelled yearly alarm rates for the South Morecambe AP1 platform.

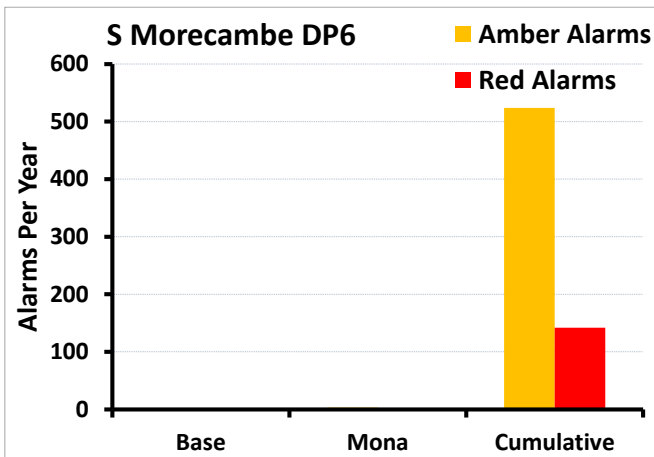


Figure 1.70: Modelled yearly alarm rates for the South Morecambe DP6 platform.

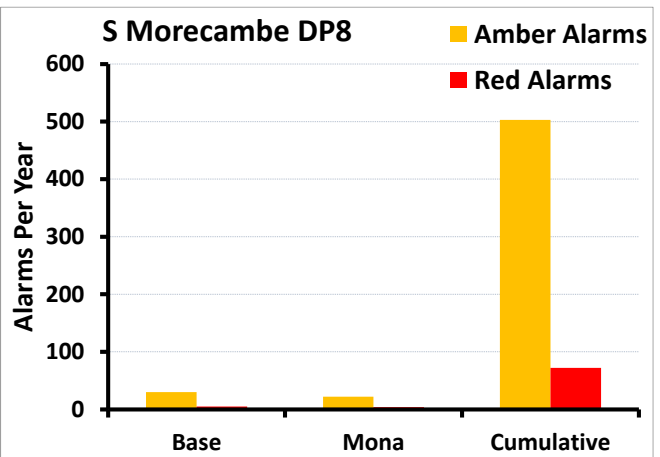


Figure 1.71: Modelled yearly alarm rates for the South Morecambe DP8 platform.

MONA OFFSHORE WIND PROJECT

Table 1.4: The estimated change in yearly alarm rates against the base case (green = reduced alarms / no change, white = small alarm increase, orange = elevated alarm increase).

(*) The models use statistical data to generate a large number of paths along a given route (adhering to a Normal Distribution specified by the provided route data). The results are expected to vary slightly (by approximately $\pm 1\%$) between each run due to the nature of the Normal Distribution of the generated paths.

| Platform | Change* in yearly alarm rates considering Mona in isolation | | Change* in yearly alarm rates considering the cumulative effect with Morgan Generation Assets | |
|---------------------|---|-------------|---|-------------|
| | Orange | Red | Orange | Red |
| Conwy | -187 | -24 | -422 | -27 |
| Douglas Complex | -167 | -27 | -169 | -13 |
| Hamilton | -607 | -70 | -473 | 22 |
| Hamilton North | 24 | 4 | 231 | -66 |
| Lennox | 0 | 0 | 0 | 0 |
| Osi | 19 | 1 | 358 | 18 |
| Calder | 74 | 0 | 241 | -2 |
| S Morecambe Dp4 | 3 | 1 | 4 | 1 |
| Millom West | -2 | -21 | -478 | -81 |
| S Morecambe Dp3 | -4 | -1 | 493 | 115 |
| N Morecambe | -20 | -20 | -1057 | -253 |
| S Morecambe Complex | 1 | 0 | 411 | 25 |
| S Morecambe Dp6 | 3 | 1 | 524 | 142 |
| S Morecambe Dp8 | -8 | -1 | 473 | 67 |
| Total Change | -873 | -177 | -339 | -132 |

1.5.6 Remarks on the TCPA/CPA alarm modelling results

1.5.6.1 The existing base case sees regular traffic in the proposed Mona Array Area and surrounding region (Figure 1.55). For this reason, Spirit has deployed a REWS installation on South Morecambe AP1 to protect and manage their offshore platforms in the regions. A large set of measured data of the vessels operating in the region is available to inform the base case scenario. The measured data was captured using AIS data and radar data of vessels travelling around the proposed projects array area. However, to assess the effects of the base case scenario on the REWS alarm rates, certain simplifying assumptions were made. These assumptions would allow the models to generate a large statistical dataset to calculate the average alarm rates per platform per year. Hence, the measured data were represented based on their statistical behaviour at a number of waypoints along the route. The routes were given as a set of discrete points along key locations on the route containing the mean and the 90th percentile width of the route. However, upon closer inspection of the measured data and the resultant modelled routes, it was noted that the measured data showed that the vessel operators actively avoided being too close to the offshore oil and gas

installations. This can be observed to examining Figure 1.53 and Figure 1.54 around the vicinity of the Calder, Conway, Hamilton platforms as well as the OSI. This active avoidance act by the vessels operators was not modelled within the assessment as it was not included within the statistical representation of the data. This can be noted in Figure 1.55 around the abovementioned installations. This phenomenon would cause the models to produce more alarm rates than what is experienced by the REWS operators in the existing base case. Hence, the reduction in alarm rates observed post the construction of the proposed projects should be considered with a degree of conservatism. If the statistical representation of the measured data should include the active avoidance of the offshore installations, the models can be modified to include them in future assessments if needed.

1.5.6.2 It is also worth noting that the models generate a large number of vessel paths within each route by generating the way points in a random manner (based on the mean and standard deviation of each route). Therefore, the results of the statistical analysis may vary slightly depending on the normal distribution around the mean line of each route. Therefore, some of the small changes in the alarm rates observed (less than 1%) can be assumed to fall within the error margins of the predicted data and the statistical approach used within the models.

1.5.7 Assessment of the TCPA/CPA alarm modelling results

1.5.7.1 The modelling results indicate that while some platforms will not experience a change in yearly alarm rates, other platforms will see an increase of alarm rates due to the displacement of traffic around the proposed projects array areas. This was noted to be the case for Spirit Energy's Morecambe platforms. The re-routed lanes alter the direction and heading of the routes making them more likely to trigger TCPA alarms. Also, as some routes are pushed closer to some platforms, the increased density of traffic along with the closer proximity will result in an increase in both CPA and TCPA alarms. Further analysis and discussion of the results are given in section 1.5.6.

1.5.7.2 When drawing conclusions from the results of the models there are two aspects that need to be considered; the number of alarms the REWS operator have to deal with, and the system's ability to respond to potential risks of allision.

1.5.7.3 The results show that some REWS operators may experience higher alarm rates due to the rerouted traffic. Although, in some cases this might need manual intervention and this may add to the work-load of the REWS operator, overall, this is considered to be largely acceptable. It is expected that most alarms will be generated by vessels that frequently use the same routes and are known by the REWS operator and are easily contactable. Upon identification and radio contact, the REWS operator may resolve the warning and temporarily switch off the alarm for that particular vessel.

1.5.7.4 It is also noted that the proposed project will have an impact on the rerouted traffic in the region and some vessels will travel closer to the platforms due to the location of the wind farms and the corridors formed between the proposed project and the existing wind farms. The number of alarms and the risk of allision can become a more significant issue during adverse weather conditions. The findings of Volume 6, Annex 7.1: Navigational Risk Assessment of the Environmental Statement suggests that during adverse weather conditions, there is an increased risk of allision. Although the REWS is expected to continue to detect, track and issue alarms in a timely manner, the pressure on the REWS operators in such conditions will be elevated due to the increased risk of allisions. Hence, during adverse weather conditions alarms TCPA and CPA alarms need to be attended to more carefully. Therefore, the potential impact of the proposed project on REWS under adverse weather conditions is considered to

be elevated beyond those for regular conditions. It is considered that operators will be able to manage any related potential increased impact on REWS through implementation of their existing adverse weather operational procedures.

1.6 Microwave communication links assessment

1.6.1 Overview

1.6.1.1 Offshore oil and gas platforms often utilise microwave communications links to transmit operational data and communicate status and other critical information regarding the operation and maintenance of these platforms. The presence of large structures close to line-of-sight communication links may interfere with the performance of the link and may reduce the effectiveness and efficiency of communication protocol. Interference can also be caused by scattering from large structures that aren't in the way of the link. However, offshore wind farms may be located within the same regions of the oil and gas platforms.

1.6.1.2 This assessment considers the potential impact of the proposed Mona Offshore Wind Project on the existing microwave communications links onboard the ENI Energy platforms and the Spirit Energy Platforms operating in the Irish Sea.

1.6.1.3 The following ENI Energy installations were identified to have microwave communication links:

- Douglas
- Conway
- Hamilton
- Hamilton North
- Lennox
- The OSI.

1.6.1.4 The following Spirit Energy installations were identified to have microwave communication links:

- North Morecambe DPPA
- South Morecambe AP1
- Barrow North (onshore).

1.6.1.5 Figure 1.72 shows the layout of the platforms and the considered links. It is worth noting that during the consultation process, only the platforms with the communication links were provided. The exact network of hops was not defined and hence not all possibilities were to be considered. The models were instead used to consider the closest turbine to the abovementioned platforms and assess the potential impact on any link operated by the platforms.

MONA OFFSHORE WIND PROJECT

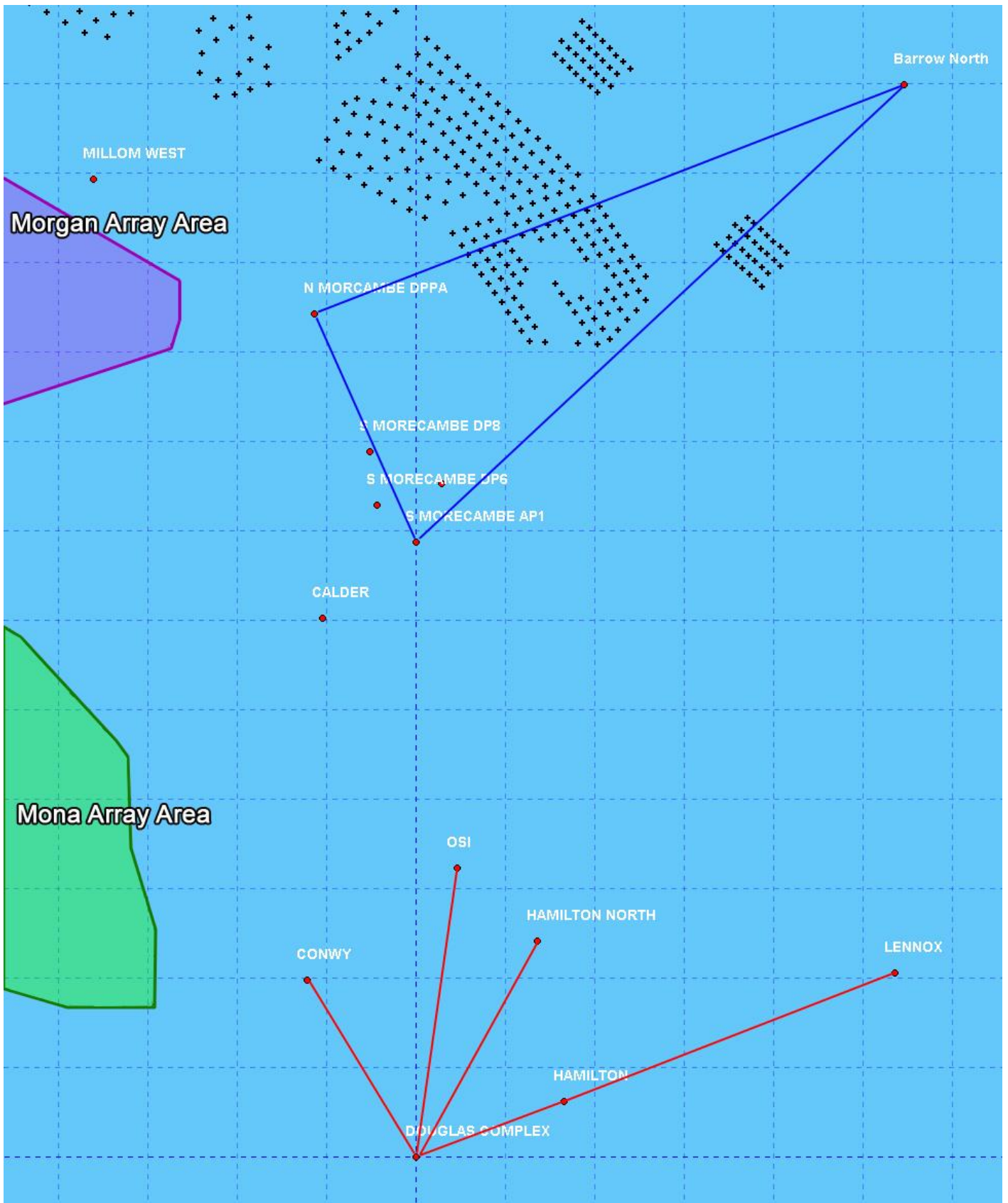


Figure 1.72: Layout of the modelled platforms and the communication links considered.

1.6.2 Modelling parameters

1.6.2.1 The interaction between wind turbines and communications links can be complex in nature and will depend on a number of parameters related to the communication link, the wind turbines and the local environment. In this assessment, the modelling process considered the specifications of the communication links and has also undertaken detailed modelling of the wind turbine scattering to establish the exclusion zones recommended by Ofcom. These exclusion zones to ensure that the integrity and efficiency of the communication links are maintained.

Communication link parameters

Hop length

1.6.2.2 The performance of communication link depends on a number of key parameters. Arguably, the most important is the hop length, which refers to the distance between the two communicating sites. The hop length is obtained by comparing the coordinates of the communicating platforms and deriving the line-of-site distance between the two antennas.

Gain and antenna radiation pattern

1.6.2.3 Antenna pattern was modelled in accordance with the ITU-R F.699-4 recommendation, which details a methodology to model the radiation pattern for line-of-sight microwave communications links. This approach is also used by Ofcom for their recommended procedure for modelling the impact of wind farms on communication links (Bacon, 2002).

1.6.2.4 The maximum gain of the antenna is calculated using the frequency and physical size of the antenna. These parameters are discussed below.

Antenna size and operational frequency

1.6.2.5 The size of the communications antenna and the operational frequency will determine the gain of the antenna. This in turn will impact the quality of the signal transmission and reception. Within this assessment the links are modelled to operate at 7.5 GHz, which is the common frequency, which offshore oil and gas platforms use for their line-of-site communications.

1.6.2.6 The size of the antenna was not available at the time of modelling and therefore was assumed to be 1.2 m. This size of antenna is commonly used within offshore communications links and is expected to increase the size of the exclusion zone around the sites. This would result in more pessimistic interference patterns and would then result in a more conservative approach to the siting analysis.

Wind turbine parameters

1.6.2.7 A summary of the MDS parameters for the communication link interface modelling is presented in Table 1.1. As discussed previously in the REWS assessment (section 1.2) the RCS models used the MDS geometry of the proposed turbines to model the bistatic scattering around the wind turbine at different angles and ranges. This is a critical step in the calculation of the exclusion zones, and it is often stated in other studies as an assumption that may limit the validity of these studies. The geometry of

MONA OFFSHORE WIND PROJECT

the bistatic RCS modelling is shown in Figure 1.73 while the results of the bistatic RCS modelling of the wind turbine are shown in Figure 1.74.

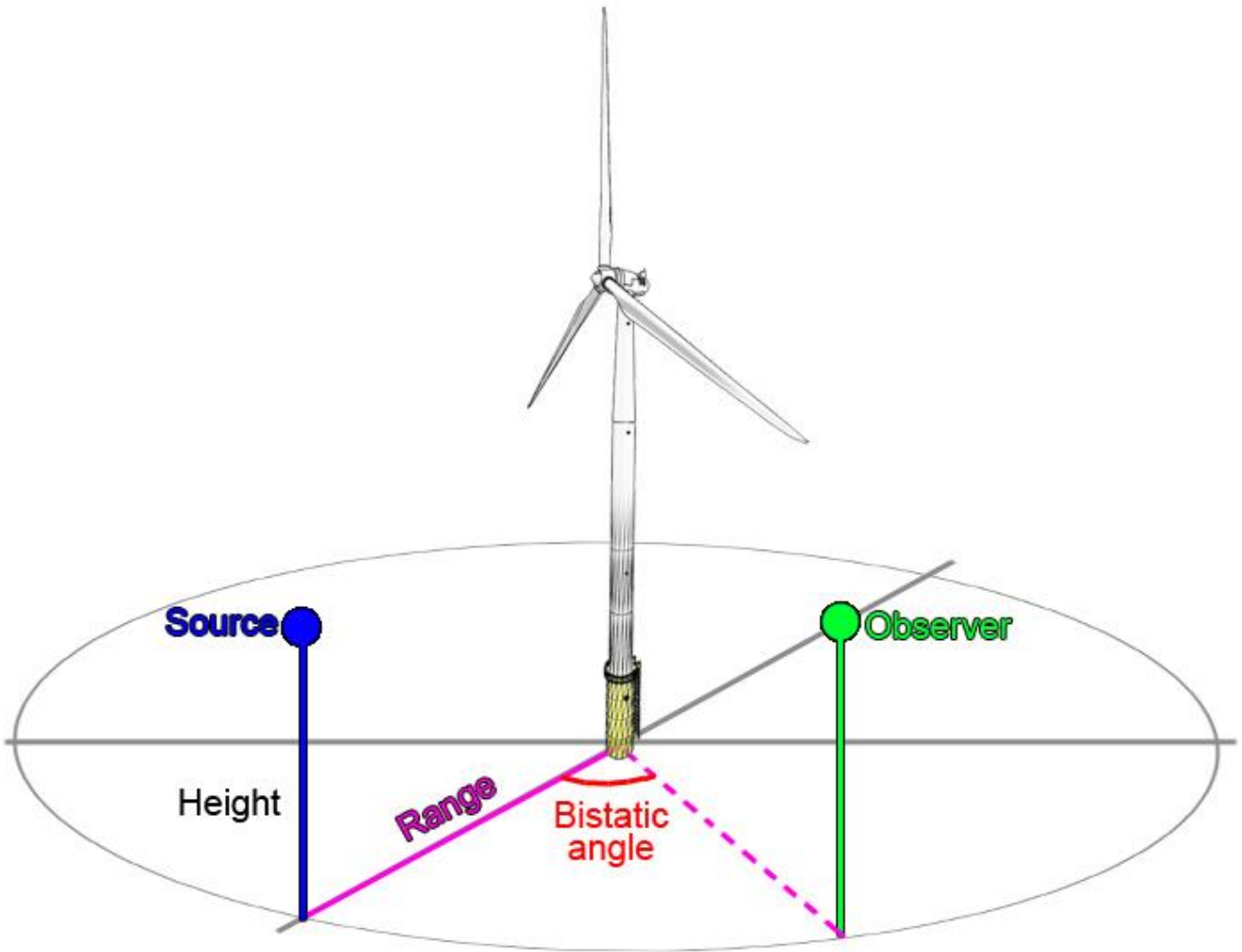


Figure 1.73: Geometry and parameters used in the wind turbine bistatic RCS modelling.

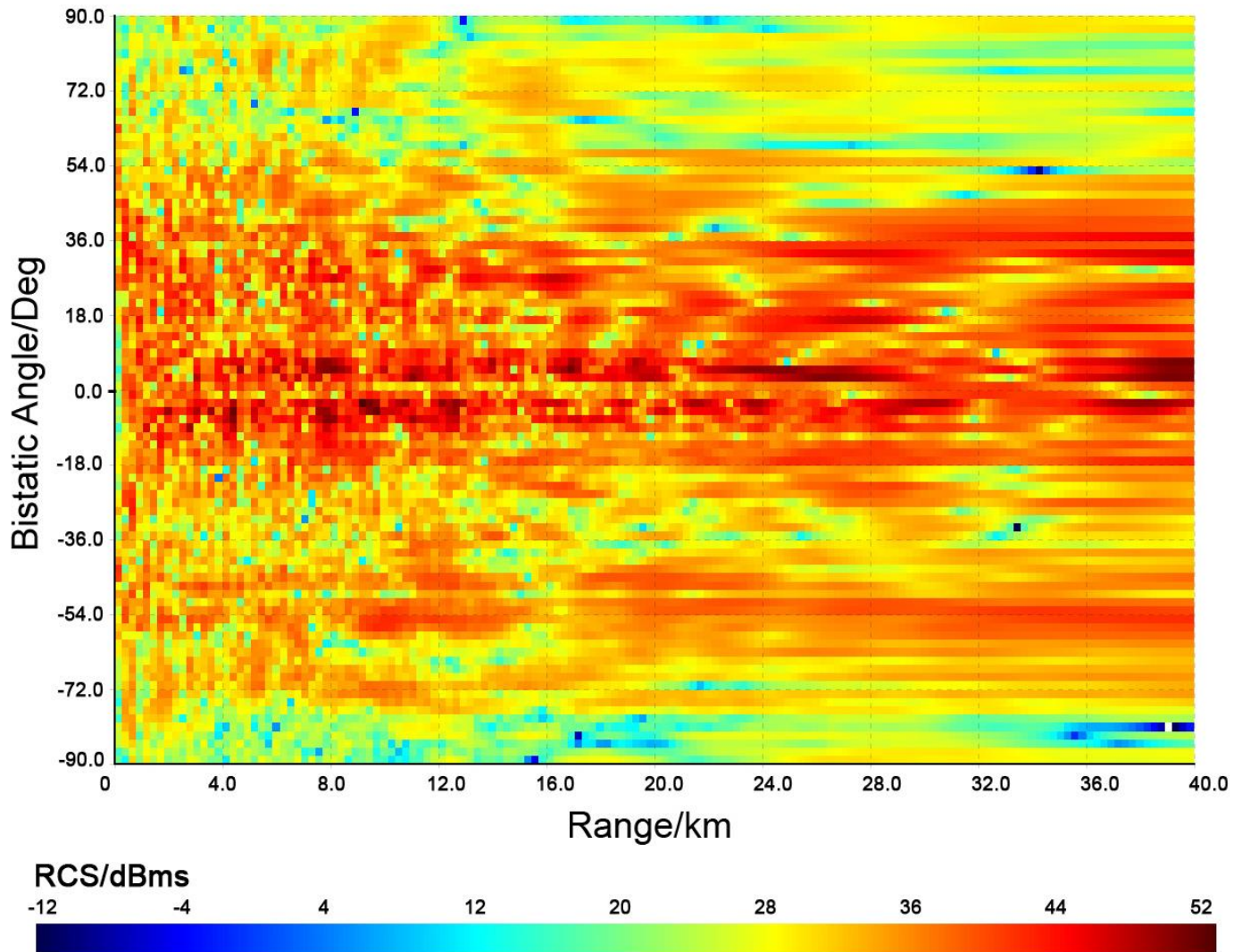


Figure 1.74: Bistatic RCS modelling results of the proposed MDS wind turbine.

Exclusion zones modelling

- 1.6.2.8 The modelling work presented within this assessment follows the recommended Ofcom methodology to calculate the safe distances between wind turbines and microwave communications links to avoid negative effects (Bacon, 2002).
- 1.6.2.9 It is noted that the impact of wind turbines might occur due to three phenomena. The interaction of the wind turbine with nearfield of the antenna radiation region, the diffraction of the communication signals around the wind turbines within the Fresnel zone and the reflection of the signal off nearby turbines.
- 1.6.2.10 This section will explain the modelling methodology of each interference mechanism and the required exclusion zone needed to avoid such interactions. This section will use the microwave communication link between Douglas and Hamilton as an example to illustrate the exclusion zones considered within this study. The results of other communication links in the region are summarised in Table 1.5 and Table 1.6.

Nearfield calculations

- 1.6.2.11 The nearfield is a region around the antenna whereby the radiation characteristics of the antenna is still forming. The presence of obstacles and/or reflecting objects within this region may interfere with the antennas' radiation pattern and can change the power transmission efficiency within the communication link. Therefore, wind turbines should be excluded from the near-field of any microwave antennas since it is not possible to accurately predict the effect they will have on the performance of the antenna.
- 1.6.2.12 The nearfield distance ends where the far-field region begin. The distance to the far-field region can be approximated by considering the dimensions of the antenna as well as the operational frequency. As mentioned previously in the antenna parameter modelling, it was assumed that all the communication links are operating at 7.5 GHz and has an antenna diameter of 1.2 m. This would result in a near-field exclusion zone with a radius of 72 m around each antenna. This is illustrated as circular region around the sites as shown in Figure 1.75 as the amber region. This is generally quite a small area and is unlikely to be a significant factor in the placement of wind turbines.

Diffraction region calculations

- 1.6.2.13 Diffraction of electromagnetic waves occur when an object is in the path of an advancing wavefront. Diffraction can detrimentally modify the wavefront if the object obstructs part of the waves path of travel. It should be noted that the object does not need to be a good reflector for this to happen. Diffraction effects can also occur when the obstructing object is totally absorbing. Avoidance of diffraction effects can be guaranteed by requiring obstructing structures to be outside a specified Fresnel zone of a radio link.
- 1.6.2.14 When considering the impact of wind turbines on communication links, it is recommended that turbines be excluded from an elliptical area equivalent to the area bounded by the 2nd Fresnel zone. The diffraction exclusion zone is as illustrated as the red ellipse in Figure 1.75. The diffraction exclusion zone will have a maximum width at the midpoint between the two sites. To simplify the results of the study, this report will only present the maximum width of the diffraction exclusion zone for each of the considered links.

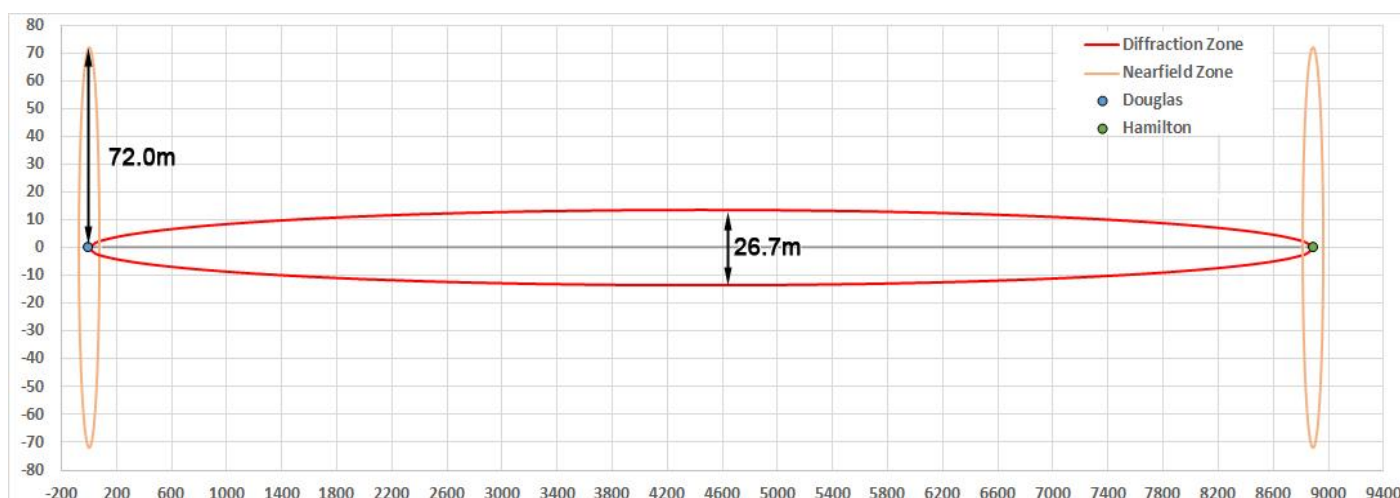


Figure 1.75: Illustration of the nearfield and diffraction exclusion zones.

Reflection region calculations

- 1.6.2.15 When electromagnetic waves illuminate an object some of the incident energy is re-radiated in various directions. Wind turbines will reflect a large portion of the incident wave in all directions. This is because at microwave frequencies, many surfaces are either curved or rough in comparison with the wavelength. The re-radiated energy may be somewhat concentrated in a specular direction, but a significant proportion often exists in other directions.
- 1.6.2.16 Therefore, if a microwave communications link transmitter illuminates a wind turbine and some of the scattered wave enters the receiver, the result is a multipath situation. Unless the level of the scattered signal is negligible compared to the direct signal, the combination of the signals and the time differences between their modulation may cause performance degradation.
- 1.6.2.17 This is calculated such that any scattered signal from the wind turbine outside the zone will arrive at the receiver with an amplitude sufficiently smaller than the direct signal such that its effect, even allowing for the delayed arrival, will be negligible. This calculation is based on the concept of carrier-to-interference ratio (C/I), usually expressed in dB. A fixed radio link is often designed to operate under different values of C/I.
- 1.6.2.18 The choice of C/I ratios will depend on the modulation and coding schemes of the link and the required performance. For the radio link to function with minimal degradation, a minimum value of C/I must be achieved and for the purposes of this study we have chosen a target C/I of 33 dB which is the figure quoted by Ofcom for design of a 28 MHz/32QAM radio link. Note that this would provide sufficient protection for reflections from the wind turbines located close to the edge of the exclusion zone.
- 1.6.2.19 This study used the modelled bistatic RCS of the proposed MDS turbines shown in Figure 1.74. The RCS value fluctuates significantly with respect to the range and bistatic angle. At ranges between 5 km and 25 km a conservative average of 44 dBm² is considered to be suitable for the purposes of this study.
- 1.6.2.20 The modelling results of the C/I for the Douglas – Hamilton communication link is shown in Figure 1.76. For the purpose of this assessment only values that are under 33 dB are considered to form the exclusion zone. Figure 1.77 shows the exclusion zone with C/I ratio under the 33 dB limit.

MONA OFFSHORE WIND PROJECT

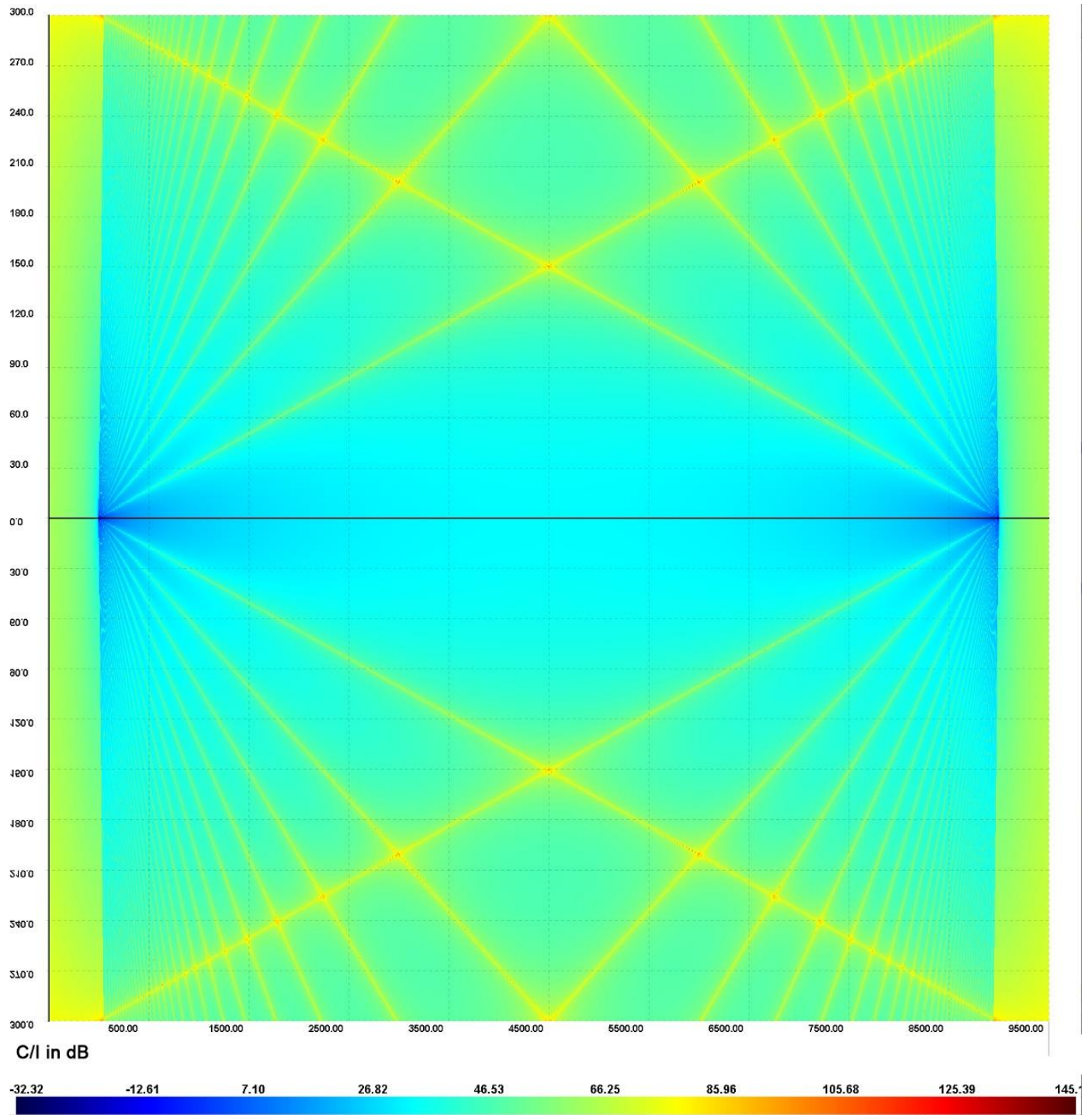


Figure 1.76: The signal to noise ratio around the Douglas – Hamilton link.

MONA OFFSHORE WIND PROJECT

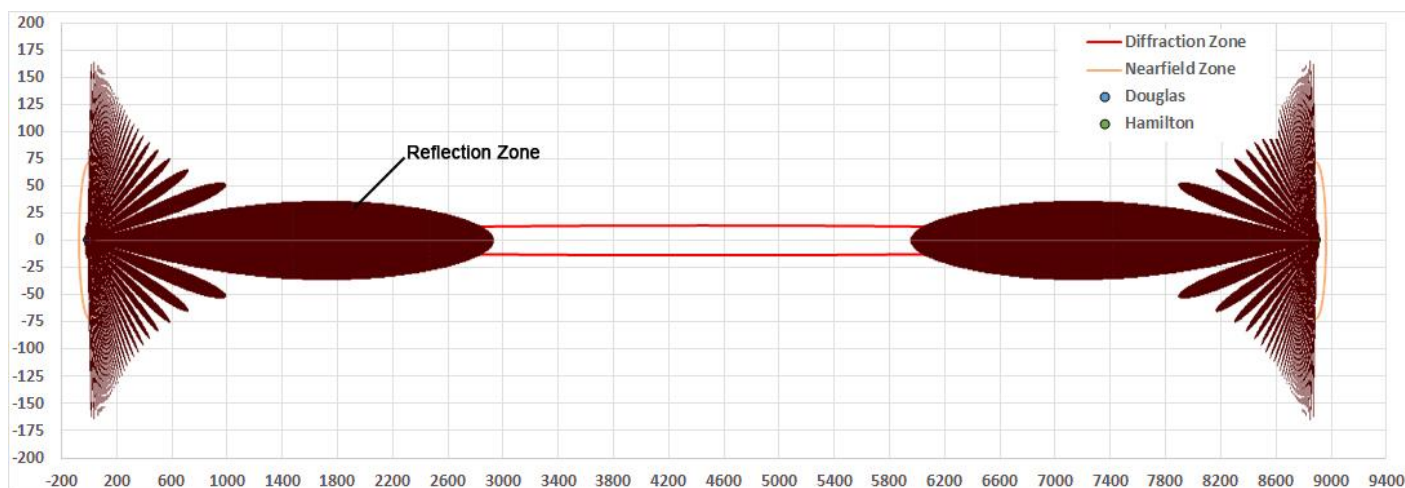


Figure 1.77: Illustration of the refraction exclusion zone resulting in C/I less than 33 dB.

- 1.6.2.21 It can be noted that the exclusion zone is closely related to the radiation pattern of the antenna. Therefore, to simplify the results further, only the maximum length and maximum width of the exclusion zones are considered. This is illustrated in Figure 1.78 whereby the reflection is represented as a rectangle, while the refraction and nearfield regions are represented as ellipses.
- 1.6.2.22 It should be noted that the reflection interference is only significant within a few km of each end of the link – outside that area the exclusion zone is dominated by diffraction effects where the exclusion zone is defined by the 2nd Fresnel zone.

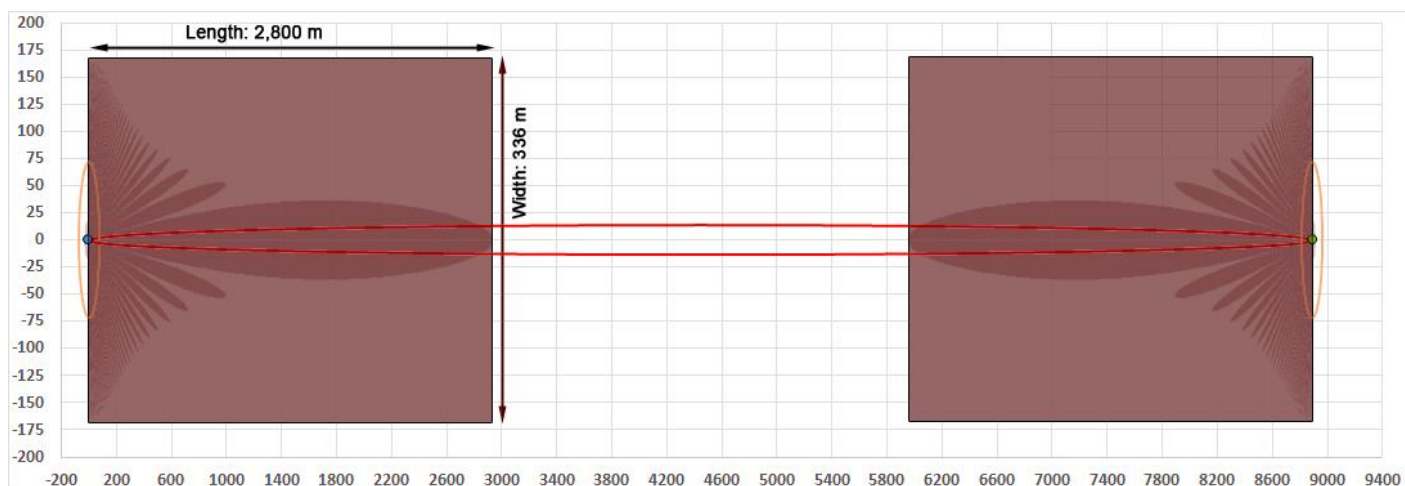


Figure 1.78: Simplified illustration of all exclusion zones around the Douglas – Hamilton link.

1.6.3 Exclusion zone modelling results

- 1.6.3.1 Using the methodology outlined above the exclusion zones for each link are summarised in Table 1.6 for the Spirit Energy assets and in Table 1.7 for the ENI Energy assets. Also, the distance between the nearest turbine and the communication link is included in the last column.

MONA OFFSHORE WIND PROJECT
Table 1.5: Exclusion zones around the Spirit Energy microwave communication links.

| Site one | Site two | Hop length (km) | Reflection zone length (km) | Reflection zone width (km) | Diffraction zone max width (m) | Nearest turbine (km) |
|----------------------|----------------------|-----------------|-----------------------------|----------------------------|--------------------------------|----------------------|
| Barrow North | North Morecambe DPPA | 35.4 | 2.220 | 0.362 | 53.2 | Mona 12.9 |
| North Morecambe DPPA | South Morecambe AP1 | 14.0 | 2.475 | 0.359 | 33.4 | Mona 10.7 |
| South Morecambe AP1 | Barrow North | 37.4 | 2.152 | 0.390 | 54.7 | Mona 11.7 |

Table 1.6: Exclusion zones around the ENI Energy microwave communication links.

| Site one | Site two | Hop length (km) | Reflection zone length (km) | Reflection zone width (km) | Diffraction zone max width (m) | Nearest turbine (km) |
|----------------|----------|-----------------|-----------------------------|----------------------------|--------------------------------|----------------------|
| Conway | Douglas | 11.6 | 2.560 | 0.342 | 30.5 | Mona 4.1 |
| Hamilton | Douglas | 8.9 | 2.800 | 0.336 | 26.7 | Mona 8.5 |
| Hamilton North | Douglas | 13.9 | 2.475 | 0.360 | 33.3 | Mona 8.5 |
| Lennox | Douglas | 28.7 | 2.200 | 0.390 | 45.9 | Mona 8.5 |
| OSI | Douglas | 16.3 | 2.390 | 0.370 | 36.2 | Mona 8.8 |
| Conway | Lennox | 32.8 | 2.695 | 0.400 | 51.3 | Mona 4.1 |

1.6.4 Remarks on the microwave communication links modelling

- 1.6.4.1 The modelling results show that the Mona Offshore Wind Project Array Area is located sufficiently far from the considered microwave communications links onboard ENI Energy and Spirit Energy platforms.
- 1.6.4.2 Based on the modelled parameters for the communications links and turbines, this study concludes that there will be no negative impact from Mona Offshore Wind Project. Hence, no mitigation measures will be needed.

1.7 Summary and final remarks

1.7.1 General REWS returns modelling summary

- 1.7.1.1 This assessment was undertaken for the MDS based on the available project parameters. The presence of wind turbines is expected to affect the REWS by introducing shadow regions and increasing the detection threshold around the wind turbines which may reduce the REWS' ability to detect and track targets within the affected area.
- 1.7.1.2 The RCS profile will depend on the size and the geometry of the wind turbines ultimately built within the Mona Offshore Wind Project Array Area, along with other external factors such as blade bending and tower vibration.
- 1.7.1.3 An existing, generic 5 MW wind turbine geometry was used and scaled up to provide a 3-dimensional representation of the MDS turbine geometry. Towers with monopile transition pieces were modelled, providing a worst case scenario for the RCS that exceeds the MDS scenario for RCS.
- 1.7.1.4 Optical shadowing was used to approximate the shadowing effects produced by the wind turbine towers. This assumes no diffraction around the tower and hence extended shadow lengths.
- 1.7.1.5 The shadows from the towers are assumed to generate detection nulls for point targets. The modelling results show that the width of the nulls varies between 4 and 15 m. For larger vessels over 1,000 GT (which are the main concern for the oil and gas platforms), the dimensions of the vessel may exceed the width of the shadowing null. This can cause a portion of the radar signal to be reflected back to the radar. Depending on the levels of the reflected energy, it may be possible to detect the vessel while moving behind the wind turbines.
- 1.7.1.6 Some of the assumptions considered within the wind turbine RCS and shadow modelling are expected to overestimate the effects of wind turbines on REWS. Measurements show that the radar shadows from turbines diminish gradually with range due to the diffraction effects. Additionally, turbine materials, exact geometry, manufacturing tolerances, and external effects such as blade and tower bending due to wind loading are expected to effect and reduce the RCS of the wind turbines. This report is set to consider the worst-case scenario using the MDS parameters for the Mona Offshore Wind Project.
- 1.7.1.7 REWS often use proprietary thresholding algorithms which are dependent on the system configuration and the operating environment. CA CFAR is applied over the clutter map to provide a constant 10^{-5} probability of false alarm. The CA-CFAR within this study uses two range cells on both sides of the cell under test as the guard region while the averaging considers six range cells on both sides of the guard region. In Azimuth the modelled CA-CFAR uses one guard cell and two averaging cells on both sides in azimuth.
- 1.7.1.8 The test vessel parameters were chosen based on the information provided by the REWS operators and comply with the IALA VTS modelling standards.
- 1.7.1.9 In conclusion, the REWS returns modelling results of the Mona Offshore Wind Project in isolation and cumulative assessment of the Mona Offshore Wind Project and the Morgan Generation Assets on the REWS installations (on ENI Energy's Douglas platform, Harbour Energy's Millom West platform, ENI Energy's OSI, Spirit Energy's South Morecambe AP1 platform) show that due to the presence of the turbines there will be small gaps in the detection map due to the elevated thresholds and shadowing

effects from the wind turbines. However, these effects will be largely mitigated by the advanced tracking techniques within the REWS. Additionally, the integration of the available AIS data with the REWS coverage will provide an alternative source of vessel information and location within the zones where the REWS may lose detection.

- 1.7.1.10 Therefore, the models show that the impact of the Mona Offshore Wind Project in isolation and cumulative impact of the Mona Offshore Wind Project and the Morgan Generation Assets on detection performance of nearby REWS installation is expected to be low and will be manageable without the need for further mitigation measures.

1.7.2 General TCPA/CPA modelling summary

- 1.7.2.1 The shipping routes and reroutes were modelled based on the available data provided by NASH (see Volume 6, Annex 7.1: Navigational Risk Assessment of the Environmental Statement), which included measured radar and AIS data for the base case and predicted data for future reroutes around Mona Offshore Wind Project in isolation and cumulatively with Morgan Generation Assets. The data included route widths based on their 90th percentiles. This was then used to derive the mean central line and the standard deviation values along each assessed route and reroute.
- 1.7.2.2 The modelled routes and reroutes were chosen based on their general direction and proximity to the existing oil and gas platforms operating near the projects array areas. The routes were chosen for their proximity for CPA alarms assessment and for their general heading vectors for TCPA alarms assessment.
- 1.7.2.3 Once the proposed project is constructed, some routes may remain unchanged relative to the assessed platforms while others might result in closer or further proximity to the platforms. However, within this assessment, all the provided routes were modelled to establish the base case alarm rates which are present prior to the introduction of Mona Offshore Wind Project and Mona Offshore Wind Project cumulatively with Morgan Generation Assets.
- 1.7.2.4 One thousand vessel paths were generated along each route in both the forward and reverse directions (a total of 2,000 runs per route). This was used to estimate the probability of raising a TCPA and/or CPA alarm for each route on each of the assessed platforms. The number of expected alarms per year was derived from the frequency of vessels travelling along each route.
- 1.7.2.5 The models were set to only issue a TCPA alarm if the vessel continues to breach the TCPA rules for more than 36 radar rotations. This was implemented to avoid false alarms due to temporary vector breach of the TCPA while vessels are turning.
- 1.7.2.6 The results show that some platforms may experience higher alarm rates, in particular orange alarms, due to the rerouted traffic around the proposed wind farm. However, the majority of installations may experience fewer red alarms and a number of platforms may experience overall reduced alarm volumes.
- 1.7.2.7 It is also noted that the proposed project will have an impact on the rerouted traffic in the region and some vessels will travel closer to the platforms due to the location of the wind farms and the corridors formed between the proposed project and the existing wind farms.
- 1.7.2.8 In the case of increased alarm rates, it is expected that most alarms will be generated by vessels that frequently use the same routes and are known by the REWS operator and are easily contactable via radio. Upon identification and radio contact, the REWS operator may resolve the warning and temporarily switch off the alarm for that

particular vessel. This may add to the work-load of the REWS operator, but overall, this is considered to be largely acceptable without the need for further mitigation measures.

- 1.7.2.9 The number of alarms and the risk of allision can become a more significant issue during adverse weather conditions. The findings of Volume 6, Annex 7.1: Navigational Risk Assessment of the Environmental Statement suggests that during adverse weather conditions, there is an increased risk of allision. Hence, under such conditions TCPA and CPA alarms may need to be attended to more carefully. Therefore, the potential impact of the proposed project on REWS under adverse weather conditions is considered to be elevated beyond those for regular conditions. It is considered that operators will be able to manage any related potential increased impact on REWS through implementation of their existing adverse weather operational procedures.

1.7.3 Further considerations

- 1.7.3.1 The variation of returns in range cells due to rotation of the blades may cause the tracker to initiate false tracks. In order for the false track to raise a TCPA alarm the generated track needs to maintain its vector for a set number of radar rotations (typically 5 to 10). This is deemed to be very unlikely and has not been previously reported; however, the effect of this cannot be quantified due to not having access to the supplier's proprietary algorithms used within the system.
- 1.7.3.2 The study of the shadowing and masking depends on the indicative layout of the proposed projects array areas and was based on the indicative layout within the design envelope. Should the final turbine positions change significantly, the details of the shadowing and masking analysis may be affected and may need checking. Slight changes within tens of metres due to seabed conditions are not expected to change the shadowing effects significantly. It is also worth noting that if a reduction in the number of wind turbines is expected; this will reduce the effects on the REWS.
- 1.7.3.3 The introduction of wind turbines to the radar coverage area will increase the number of target detections. Depending on the tracker configuration, turbine detections may be included in the track-table. The track-table is transmitted to ERRV's via a low bandwidth UHF telemetry link. Using non-acquire zones and configuring the tracker to include only moving targets in the track-table may reduce the load on the UHF links. However, the effect of the track-table size and the UHF links are not considered within the scope of this study as it falls within the effects on wireless UHF communications rather than radar or microwave communication links.
- 1.7.3.4 The REWS uses a tracking algorithm to predict the vessels movement and compensate for momentary loss of detection. Such tracking algorithms are proprietary to the manufacturer. In general, such tracking may allow improved performance in the projects array areas vicinity to compensate for temporary losses due to raised threshold levels or shadowing effects. However, typically a track will be established within 5 to 10 rotations of the radar antenna (for antenna with 24 RPM, this is equivalent to 12.5 – 25 seconds).
- 1.7.3.5 Large (time varying) returns from turbines might cause the processed tracks from vessels to be seduced into the large turbine returns causing errors in tracking. This will be corrected after a number of radar rotations and the correct track will be resolved eventually. However, this is dependent on the tracking algorithm and post signal processing, which may be mitigated by using narrow non-acquire zones around each wind turbine.

MONA OFFSHORE WIND PROJECT

- 1.7.3.6 Improvements to the CFAR performance might be achieved by using more sophisticated CFAR algorithms with different weighting on the averaging cells in order to improve the radar performance within the wind farm. Also, modification to the way that the CFAR calculations compute the threshold average over the wind farm might be modified to minimise the blind regions.
- 1.7.3.7 In the event of adverse weather, it is considered that operators will be able to manage any potential increased impact on REWS through implementation of their existing adverse weather operational procedures.

1.8 References

Bacon, D.F. (2022) A proposed method for establishing an exclusion zone around a terrestrial fixed radio link outside of which a wind turbine will cause negligible degradation of the radio link performance, Version 1.1, 28th October 2002.

Baker, R. (2007) Investigation of Technical and Operational Effects on Marine Radar Close to Kentish Flats Offshore Wind Farm. MARICO 2007, BWEA Report.

Butler, M.M. and Johnson, D.A. (2003) Feasibility of Mitigating the Effects of Wind farms on Primary Radar. AMS Ltd, ETSU W/14/00623/REP.

Danoon, L. and Brown, A. K. (2014) Modelling the radar shadowing effects of the Burbo Bank Wind Farm Extension on the BHP Billiton Radar Early Warning System. The University of Manchester, 2014.

Greenwell, K. (2016) Mitigation Strategies for the Effects of Offshore Wind farms on ULTRA Radar Early Warning Systems. Ultra ES, 2016.

Jago, P. and Taylor, N. (2002) Wind Turbines and Aviation Interests - European Experience and Practice. ETSU W/14/00624/REP, DTI PUB URN No. 03/515, 2002.

Love, S. (2014) Report on the Predicted Impact of the Burbo Bank Wind Farm Extension on the BHP Billiton Radar Early Warning System. Ultra ESS, 2014.

Poupart, G.J. (2003) Wind Farms Impact on Radar Aviation Interests. BWEA Radar Aviation Interests Report. DTI report number W/14/00614/00/REP, September 2003.

QinetiQ (2005) An assessment of the impact of the proposed Gwynt y Môr wind farm on marine radio navigation and communications systems.

Terma (2021) Wind turbine RCS assessment from radar data recorded at Hornsea One, Document No. 1739964-RA, 2021.

Wind Energy, Defence & Civil Aviation Interests Working Group (2002) Wind Energy and Aviation Interests – Interim Guidelines. ETSU W/14/00626/REP, October 2002.